Tether Transportation System Study

M.E. Bangham
The Boeing Company, Huntsville, Alabama

E. Lorenzini
Smithsonian Astrophysical Observatory, Cambridge, Massachusetts

L. Vestal
Marshall Space Flight Center, Marshall Space Flight Center, Alabama

Acknowledgments

Many thanks go out to the following individuals for their hard work and dedication in the preparation of this report:

Available from:

CONTENTS

CONTENTS (continued)

CONTENTS (continued)

LIST OF FIGURES

LIST OF FIGURES (continued)

LIST OF TABLES

LIST OF ACRONYMS

ADCS	Attitude Determination and Control System
AMTEC	Alkali Metal Thermal to Electric Converter
BASE	beta-alumina-sodium-electrolyte
BOL	beginning-of -life
BOLAS	Bistatic Observation with Low Altitude Satellites
C&DH	Command and Data Handling
CM	center of mass
COM	Cost of Money
COTS	Commercial off-the-shelf
DDT&E	Design, development, test and evaluation
EOL	end-of-life
IUS	inertial upper stages
FOV	Field of View
GEO	geosynchronous earth orbit
GLOW	Gross Lift Off Weight
GPS	Global Positioning System
GTO	GEO transfer orbit
GNC	Guidance Navigation and Control
ISS	International Space Station
LH	local horizontal
LEO	low earth orbit
LRU	Line Replaceable Units
LV	local vertical
LV-LH	local vertical-local horizontal
MEO	medium earth orbit
NASCOM	NASA COst Model
PAV	Payload Adapter Vehicle
PLAA	payload adapter assembly
PLCRA	Payload Capture and Release Assembly
PV	Photovoltaic
R & C	Rendezvous and Capture
RF	Radio Frequency
RLV	Reusable Launch Vehicle
STOTS	Spinning Tether Orbit Transfer System
SSM	Second Surface Mirror
STK	Satellite Tool Kit
TDRSS	Telemetry Data Relay Satellite System
TO	Transfer Orbit
TR	Technology Readiness

Section 1

INTRODUCTION

1.1 PURPOSE

This report presents the results of a study of an in-space system of tether facilities to transfer payloads from low earth orbit (LEO) to geosynchronous earth orbit (GEO).

1.2 BACKGROUND

The fundamental rationale for this study is to reduce the cost of transporting payloads to GEO. The projected traffic to GEO is expected to increase over the next few decades and the cost of delivering payloads from the earth's surface to LEO is projected to decrease thanks to the introduction of the Reusable Launch Vehicle (RLV). A comparable reduction in the cost of delivering payloads from LEO to GEO should take place. Consequently, studies of alternative means of transportation from LEO to GEO have been carried out. The use of in-space tethers, eliminating the requirement for traditional chemical upper stages and thereby reducing the launch mass, has been identified as such an alternative.

Tethers are possible candidates to deliver payloads from LEO to GEO because spinning tethers are excellent storage devices for kinetic energy capable of providing very large delta V's to the payload attached to the tether tip. The TSS-1R mission demonstrated, though inadvertently, this capability. A single-stage system (i.e., consisting of a single in-space tether facility) for transferring payloads from LEO to GEO was proposed some years ago by Bekey [1]. The present study is the first detailed analysis of that original proposal, its extension to a two-stage system, and the likely implementation of the operational system.

1.3 SCOPE

The report presents the results of a mission analysis that addressed the feasibility of the concept from the standpoint of orbital mechanics and other principles of physics. The report then presents the results of an engineering analysis to define the system, major elements and subsystems, and to assess the feasibility (i.e., the readiness of technology) of designing and developing the system. The report then presents an assessment of the tether system performance and an estimate of the cost of the system. The report concludes with a summary of conclusions and recommendations.

Section 2

MISSION ANALYSIS

2.1 CONCEPT OVERVIEW

Spinning tethers are used to impart the desired ΔV (or ΔVs) to the payload to be transferred. Each spinning facility has a counter platform on the opposite side of the tether. The spinning facility acts as a giant momentum wheel, i.e., for each ΔV imparted to the payload there is a ΔV, proportional to the payload/platform mass ratio, imparted to the platform. After release, the payload is injected into a higher orbit and the platform is injected into a lower orbit which depends on the payload/platform mass ratio.

The transfer from LEO to GEO transfer orbit (GTO) can be accomplished through a single ΔV of about 2.4 km/s (from a 300-km circular orbit) provided by a single stage tether system or through two smaller ΔVs provided by a two-stage tether system. This latter configuration is preferable with present day tether technology (as explained later on). A two-stage tether system involves two facilities permanently in orbit: a spinning facility in LEO and another one in medium Earth orbit (MEO) with a perigee close to the LEO facility. The payload is first boosted to MEO by the LEO facility; subsequently, it is captured (with zero relative velocity) at perigee by the MEO facility and later injected into GTO. In this study, the circularization ΔV from GTO to GEO will be provided by an element of the overall tether transportation system attached to the payload.

After payload delivery the two orbital platforms are reboosted. The masses of the payloads to be handled by the tether transportation system are assumed in the range 907 kg - 4082 kg (2000 lb - 9000 lb) which according to present projections will constitute almost 80% of the traffic to GEO in the future. A time for platform reboosting of 30 days is assumed which, consequently, determines the frequency of payload transfer to 12 launches per year.

2.2 ORBITAL TRANSFERS WITH SPINNING TETHERS

Tethers can provide ΔVs to the vehicles attached to their tips. If we refer the system dynamics to a local vertical - local horizontal (LV-LH) reference frame attached to the system CM, then tethers can be classified according to their motion with respect to LV-LH as hanging, swinging or spinning in much the same way as a pendulum in a gravity field (a tether system in orbit is in fact a gravity-gradient pendulum). Clearly, for a given tether length, spinning tethers can impart the highest ΔV to the payload. If we call ΔH the separation between the two tip masses half an orbit after release and L the tether length, the following simple rules apply (see Figure 2-1):

$\Delta H \approx 7L$ Hanging tethers

$7L < \Delta H < 14L$ Swinging tethers   (1)

$\Delta H > 14L$ Spinning tethers

Given the fact that the required ΔHs (or alternatively ΔVs) are very high for a transfer from LEO to GTO, spinning tethers are the only practical solution for achieving the desired goal with tethers of moderate lengths.
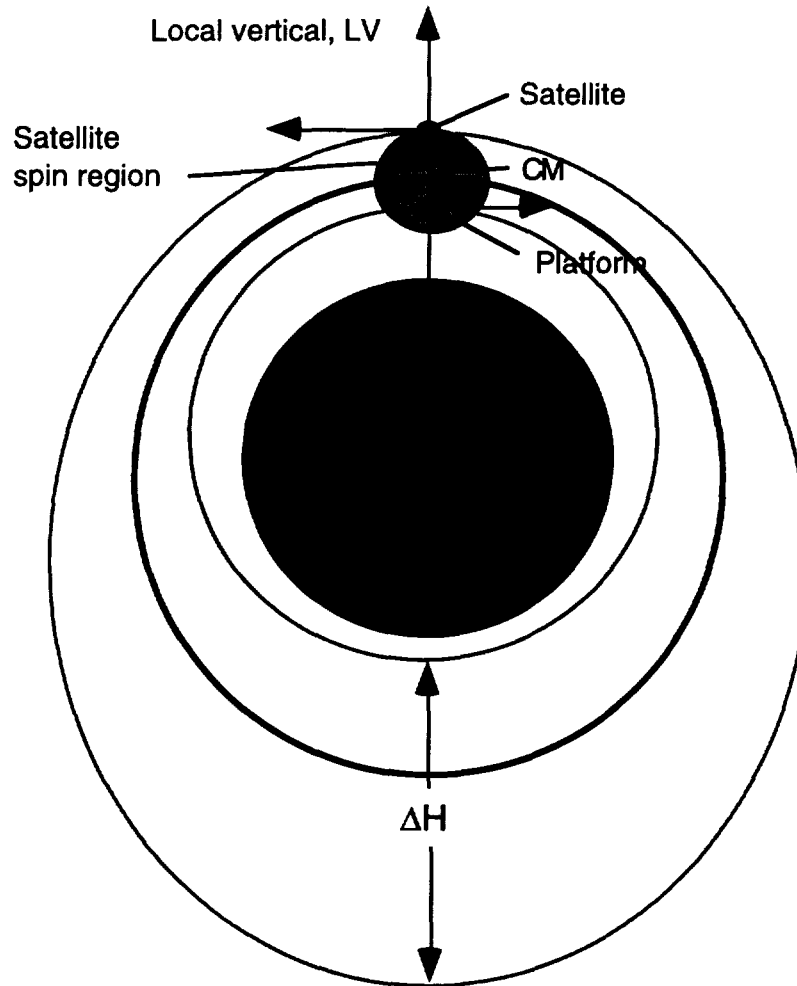
FIGURE 2-1. ORBITS AFTER CUT AT LV OF A SPINNING TETHER

2.2.1 Tether types

Tethers can have a constant cross section (cylindrical tethers) or a varying cross section (tapered tethers). The maximum velocity that a cylindrical spinning tether can sustain (the critical velocity), without any payload attached to its end, is limited by its material properties and can be written as:

$$Vc = \sqrt{\frac{2\sigma}{\rho}} \qquad\qquad (2)$$

where σ is the ultimate strength of the tether material and ρ is its mass density. A more realistic approach is to adopt a ratio $\sigma^* = \sigma / f$ where $f > 1$ is the stress safety factor. The ΔV that a cylindrical tether can provide, therefore, is bounded. For example Spectra 2000 has a Vc = 2.6 km/s ($\sigma = 3.25 \times 109$ N/m2 and $\rho = 970$ kg/m^3) with a safety factor of 1 (no safety margin) and Vc = 1.96 km/s with a safety factor of 1.75 (see later on in this report).

Since the maximum stress is at the hub of a spinning tether, the tether can be tapered thus saving tether mass and removing the limitation on the maximum sustainable ΔV. The mass of an optimally (i.e., with a constant stress distribution) tapered tether can be written as a function of the tip mass (payload) m_{PL} follows:

$$M_{tether} = M_{PL} \sqrt{\pi} \frac{V}{V_c} \exp\left(\frac{V^2}{V_c^2}\right) erf\left(\frac{V}{V_c}\right) \tag{3}$$

where V is the tip velocity and erf() is the error function [3-4]. Figure 2-2 shows the tether/payload mass ratio for a cylindrical and a tapered tether of the same material (Spectra 2000) and a safety factor equal to 1.75.

In conclusion, a tapered tether is lighter than a cylindrical tether especially for ΔV > 1 km/s and more importantly the ΔV that a tapered tether can impart is not bounded by the strength to density ratio of the material.

2.2.2 Tether vs. Rockets

A spinning tether can be compared to a rocket by comparing the tether mass needed to provide the desired ΔV to a payload and the propellant mass required to accomplish the same task. We first introduce a performance index that relates the critical velocity of the tether to the ejection velocity of the propellant from the rocket nozzle, i.e., n = Vc/(Isp g) where Isp is the specific impulse and g is the gravity acceleration on the Earth's surface (for a hydrazine system and several solid propellants, the product Ispg is ≈3 km/s). The ratio $Mprop/M_{PL}$ where Mprop is the propellant needed for the transfer is

$$M_{prop} = M_{PL}\left[\exp\left(\frac{V^2}{I_{sp}g}\right) - 1\right] = M_{PL}\left[\exp\left(n\frac{V}{V_c}\right) - 1\right] \tag{4}$$

As shown in Figure 2-3 and 2-4 for different values of the tether material safety factor, the ratios $Mtether/M_{PL}$ and $Mprop/M_{PL}$ determine the relative mass of the tether vs. the propellant mass of an equivalent chemical system. Clearly, many other considerations apply to comparing a tether system vs. chemical propulsion among which the most important one is that a tether system is reusable while a chemical system is not. Nevertheless, the plot of Figure 2-4 gives a good indication of the ΔV range in which a spinning tether transportation system should operate with present day materials.
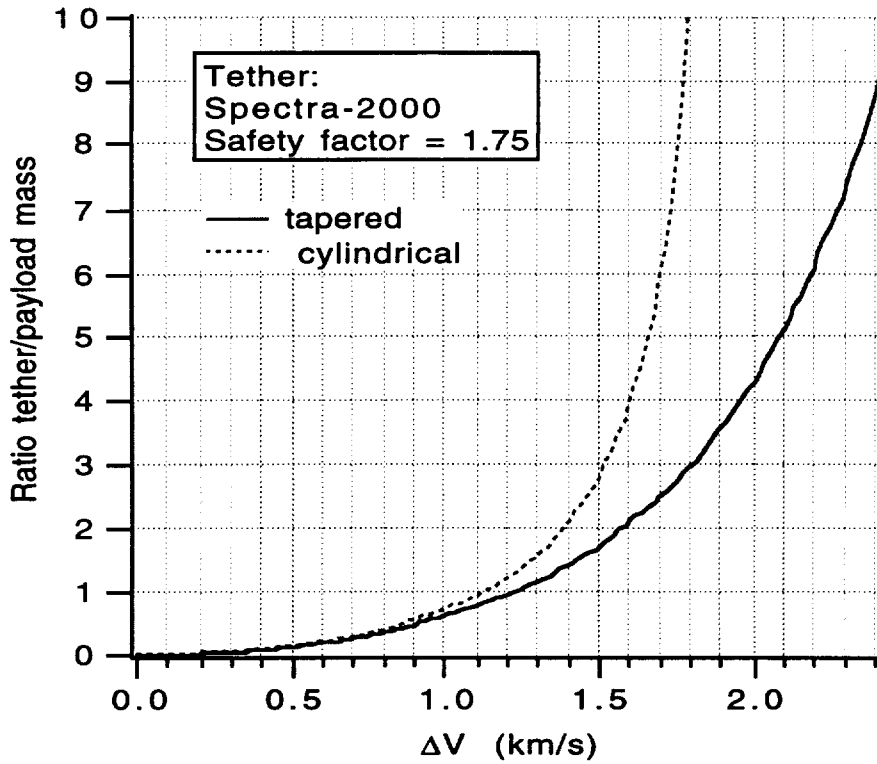
FIGURE 2-2. TETHER/PAYLOAD MASS RATIO FOR CYLINDRICAL AND TAPERED TETHERS.
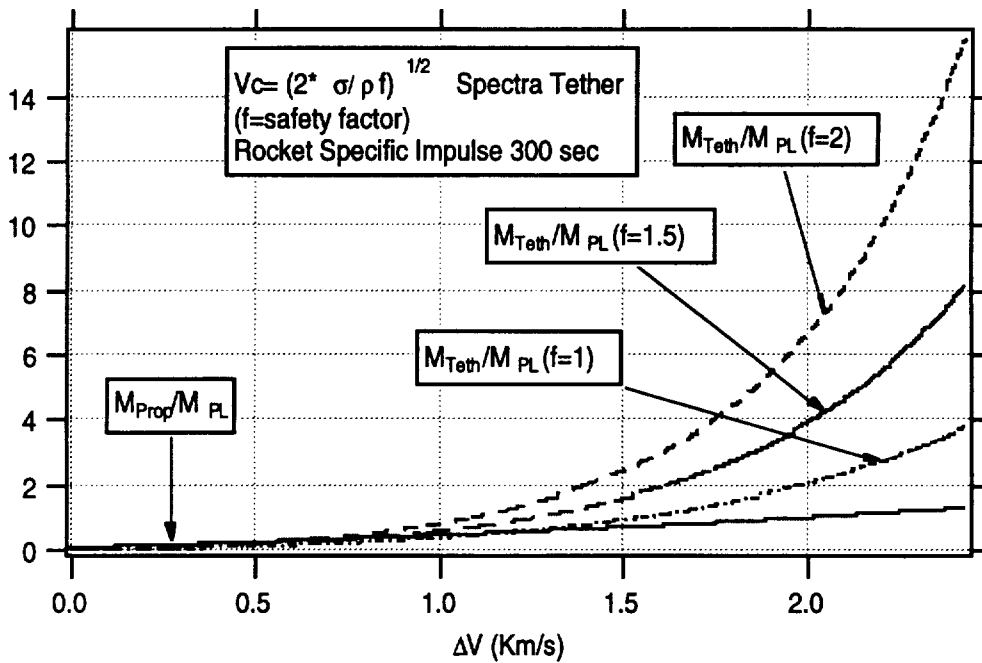
FIGURE 2-3. RATIOS OF TETHER AND PROPELLANT MASS TO PAYLOAD MASS VS.
IMPARTED ΔV.

Let us look now at the ΔV required for transferring a satellite from LEO to GEO. The required injection velocity to transfer a payload (with a Hohmann transfer) to a higher orbit is shown in Figure 2-5. The system must impart a ΔV of 2.4 km/s to inject a payload into GTO (apogee height = 35,786 Km) while an additional 1.4 km/s is needed to circularize the orbit. Consequently, if a single stage tether system (with present day technology) were to be used to transfer a payload from LEO to GTO, the mass of the tether would be about 9x the payload mass while from Figure 2-3 it can be concluded that the propellant (Hydrazine) mass would be less than 2x the payload mass. In other words, it would take about 5 launches for a single stage tether system to become competitive.

This is already an encouraging conclusion which however can be improved dramatically by looking into: (1) the trend in tether material improvement through the years in order to estimate possible values of the tether critical velocity 10-15 years from now; and (2) a two-stage system that by splitting the ΔV into two components utilizes the tethers at their best with present day technology. It will be shown later on in this report that a two stage tether system from LEO to GEO is more competitive, on a mass basis, than a present-day upper stage after only two launches.

The plot contains the following labels:

$V_c = (2^* \sigma/\rho f)^{1/2}$ Spectra Tether
(f=safety factor)
Rocket Specific Impulse 300 sec

$M_{Teth}/M_{PL}(f=2)$

$M_{Teth}/M_{PL}(f=1.5)$

$M_{Teth}/M_{PL}(f=1)$

M_{Prop}/M_{PL}
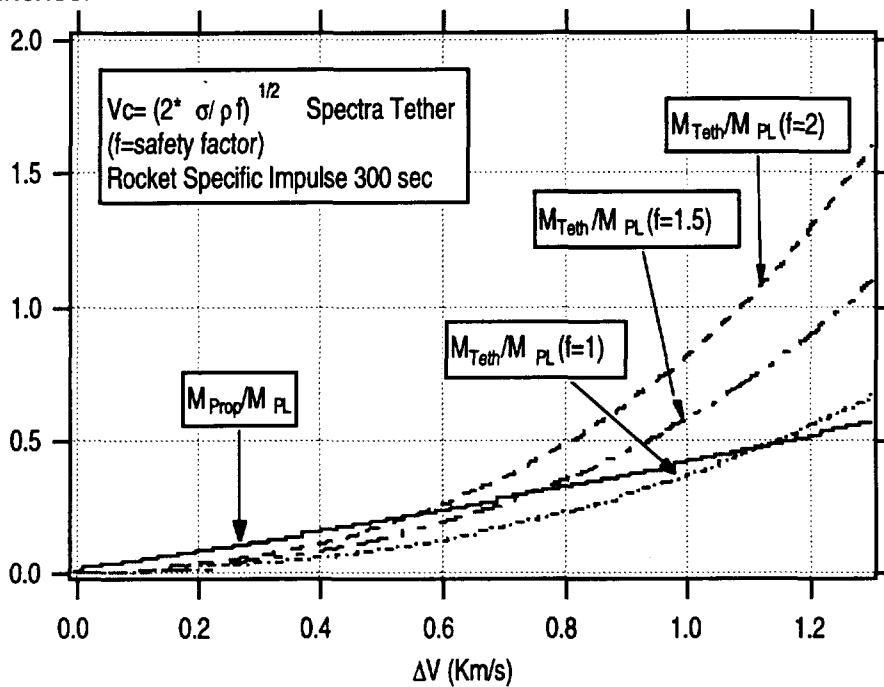
FIGURE 2-4. EXPANSION OF PREVIOUS FIGURE FOR ΔV < 1.25 KM/S.
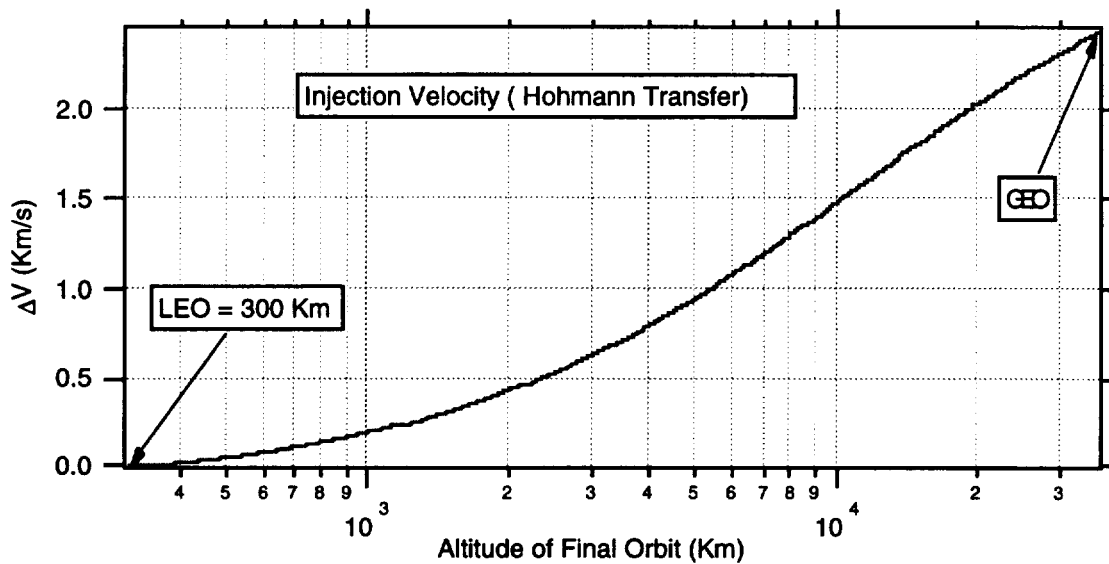
FIGURE 2-5. INJECTION VELOCITY REQUIRED TO TRANSFER A PAYLOAD FROM LEO TO A
GIVEN APOGEE.

2.2.3 Tether materials and future trends

The tether characteristic velocity depends on the material strength to density ratio. The change of this ratio through the years gives an indication of the future trend and the possible values of the tether characteristic velocity in the near future (see Figure 2-6).

Figure 2-6 shows that the strength to density ratio of tether materials had two distinct eras during this century: (a) the metal era before 1960 with a very slow increase of the strength to weight ratio, and (b) the carbon fiber era with a dramatic increase of the ratio after 1960. If we believe in the linear regression analysis shown in Figure 2-6, the strength to density ratio should be expected to increase by about 70% in the year 2010 with respect to the present value of Spectra 2000. Conversely, the tether critical velocity should increase by about 30% in the year 2010 with respect to the resent value of Spectra 2000. Consequently, the tether in the year 2010 could be a factor 3 lighter than at present for a single stage tether transportation system from LEO to GTO.

These improvements might seem dramatic but they would be completely eclipsed if experimental materials like Fullerenes come on line for the construction of long tethers. Fullerenes have demonstrated in the laboratory a strength to density ratio almost two orders of magnitude higher than Spectra 2000. At present, however, the samples being produced are only a few micron long [5] but several attempts are underway at making this new material suitable for forming tethers.
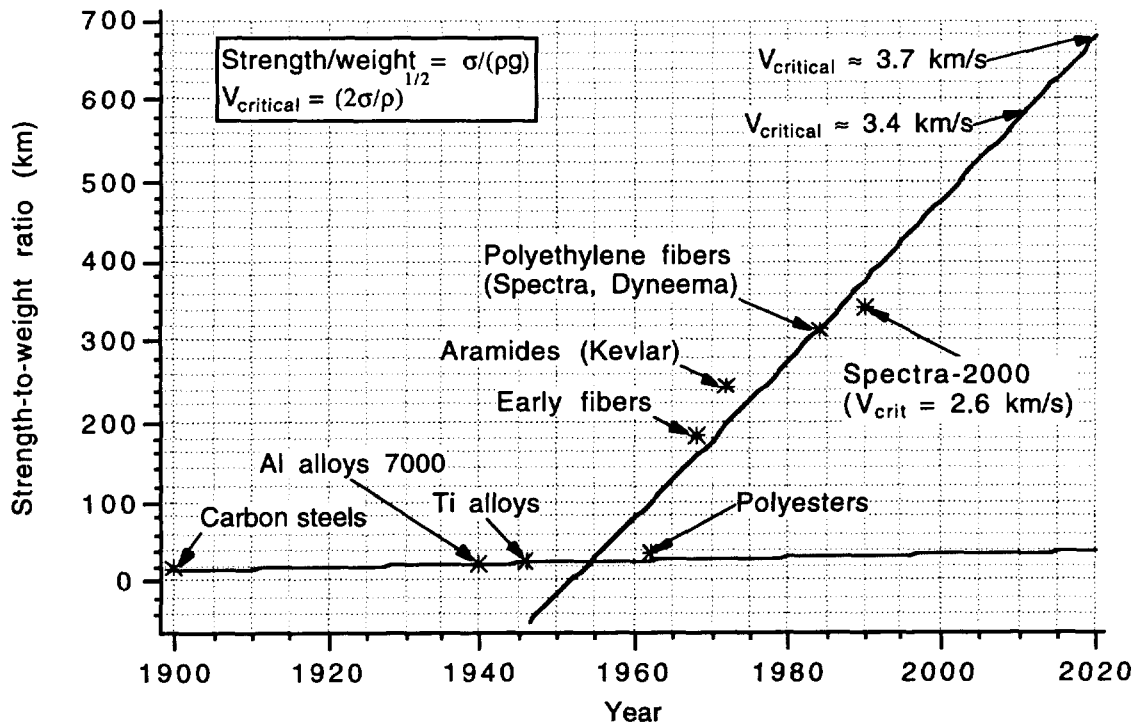
FIGURE 2-6 STRENGTH TO DENSITY RATIO OF TETHER MATERIALS THROUGH THIS
CENTURY AND BEYOND.

2.2.4 Mission Strategy

An alternative solution to reducing the mass of the tether system (with present day technology) is by designing a two stage system. The first stage spinning in LEO injects the payload into a higher orbit where it is captured by the second stage spinning in MEO. After the capture, the payload is released at a perigee passage into GTO. The 1st stage provides a velocity increase $\Delta V_1 = V_{TIP-1}$ where the latter is the tip velocity of the stage. The second stage captures the payload at the bottom of the spin, during its retrograde rotation, and releases it at the top of the spin, during its posigrade rotation. Consequently, it accelerates the payload (with respect to the speed of its CM) from $-V_{TIP-2}$ to $+V_{TIP-2}$ thereby providing a total velocity increase of $\Delta V_2 = 2V_{TIP-2}$. Since the masses of the first and second stages are determined by their tip velocities, we would expect that minimal tether mass configurations for a two stage system should be found for $\Delta V_2 > \Delta V_1$.

The optimal partition of ΔVs (or equivalently V_{TIP}) between the two stages has been computed and the results are shown in Figure 2-7. This figure shows the ratio between the total tether mass of the two stages and the payload mass vs. the ratio between the tip velocities.

The minimum is for a tip velocity ratio $V_{TIP-2}/V_{TIP-1} \approx 1.7$. The tether/payload mass ratio increases strongly for ratios $V_{TIP-2}/V_{TIP-1} < 0.8$, and it reaches a value of 9 (consistent with a single stage tether system) for $V_{TIP-2}/V_{TIP-1} = 0$. On the contrary, the tether/payload mass ratio changes only slightly for $V_{TIP-2}/V_{TIP-1} > 0.8$. Consequently, the partition of the ΔVs between the stages is rather free so long as $\Delta V_2 \geq 1.6\Delta V_1$ (remember that $\Delta V_2/\Delta V_1 = 2V_{TIP-2}/V_{TIP-1}$). It is worth noting that the optimum for a tether spinning system is for $\Delta V_2 > \Delta V_1$ unlike a conventional staging where the optimum is at $\Delta V_2 \approx \Delta V_1$.
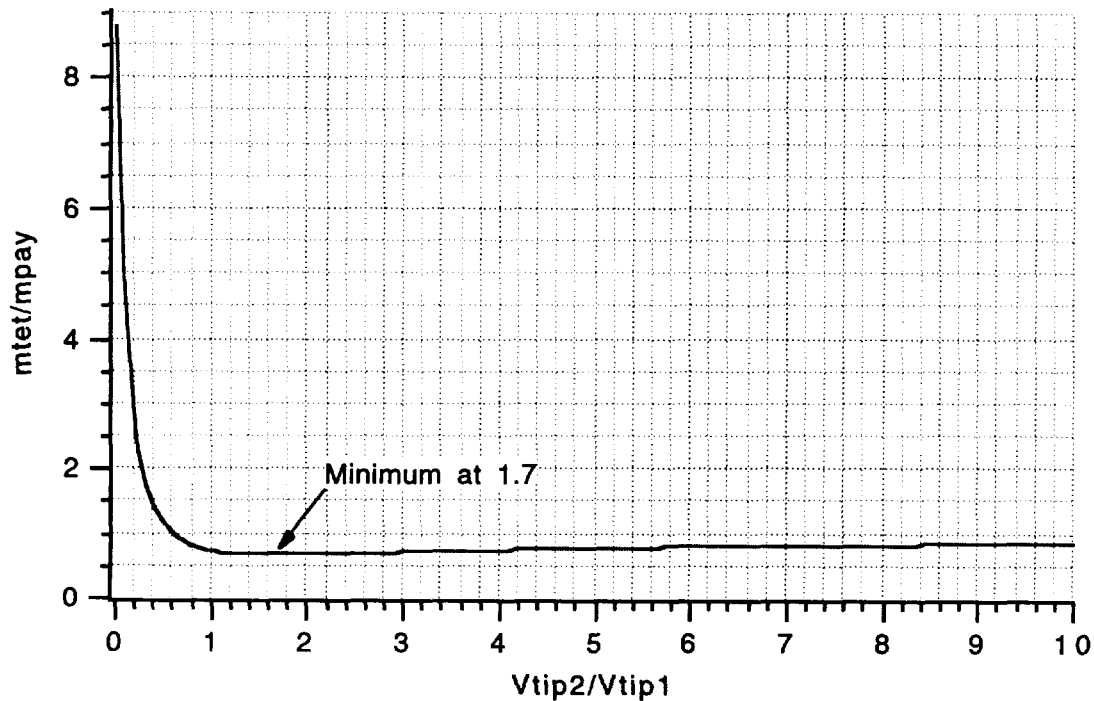
FIGURE 2-7 TOTAL TETHER MASS OVER PAYLOAD MASS FOR A TWO-STAGE TETHER SYSTEM VS. THE TETHER TIP VELOCITIES RATIO.

2.3 MISSION ANALYSIS

2.3.1 Orbital Mechanics of a Two-stage Tether System

In a two-stage tether system, the 1st stage tether rotates with angular rate ω_1 and, in general, orbits in a LEO orbit rp_1 x ra_1 defined by its perigee and apogee radii. The 2nd stage, which rotates with an angular rate ω_2, is at an intermediate orbit (MEO) between LEO and GEO. This orbit is also elliptical in order to provide a velocity match at perigee, at the capture of the satellite released from the first stage, between the tether tip velocity and the incoming satellite that follows the transfer orbit (TO). For best efficiency, ΔVs are imparted at perigee where the energy produced by a given ΔV is maximum because the orbital velocity is maximum (see Figure 2-8.)

An important consideration to keep in mind is the synchronicity [6] between the LEO orbit, the transfer orbit (TO) after release from the 1st stage and the MEO orbit of the 2nd stage. Synchronicity between the orbits (also called orbital resonance) of the first and the second stage provides frequent encounters between the two stages and, consequently, frequent launch opportunities. Synchronicity between the orbit of the second stage (MEO) and the transfer orbit of the payload (TO) provides multiple recapture opportunities if the first capture attempt is missed, i.e., there will be periodic encounters at the perigees of the two orbits after a miscapture.

The orbital periods of the TO orbit and of the MEO orbit can be expressed as follows:

$$P_{TO} = MP_1 \tag{5.1}$$

$$P_2 = N\,P_1 \tag{5.2}$$

where P stands for orbital period, the subscript 1 stands for 1st stage in LEO and 2 stands for 2nd stage in MEO. M and N do not have to be necessarily integer numbers for having periodic encounters but rather rational numbers. That is, M and N must satisfy the following equation in order to provide periodic encounters at perigee passages:

$$\frac{N}{M} = \frac{J}{K} \qquad \text{with J and K integer numbers} \tag{6}$$

The satellite is first released by the 1st stage at perigee, which must have the same orbital anomaly of the perigee of the 2nd stage. If the satellite is released when the tether crosses the local vertical (LV), the perigee of TO is also at the point of release. After a time Trev = NKP_1 (revisit time) the satellite passes through the perigee of TO when the 2nd stage passes through the perigee of MEO (i.e., multiple recapture opportunities). The relative position and velocity of the satellite with respect to the tether tip of the 2nd stage dictate that:

$$r_{pTO} = r_{tip2} \quad \rightarrow \quad r_{p1} + L_{12} = r_{p2} - L_2 \tag{7.1}$$

$$v_{tip1} = v_{tip2} \quad \rightarrow \quad v_{p1} + \omega_1 L_{12} = v_{p2} - \omega_2 L_2 \tag{7.2}$$

in which 1 stands for 1st stage and 2 for 2nd stage and $L_1 = L_{11} + L_{12}$, $L_2 = L_{21} + L_{22}$ are the overall lengths of the 1st and 2nd stage tethers, ω_1 and ω_2 are the rotational rates of the two tethers. After defining $\chi_1 = m_{sat}/m_{plat1}$ and $\chi_2 = m_{sat}/m_{plat2}$, we have:

$$L_{11} = \frac{\chi_1}{1 + \chi_1}\, L_1$$

$$L_{12} = \frac{1}{1 + \chi_1}\, L_1$$

$$L_{21} = \frac{\chi_2}{1 + \chi_2}\, L_2 \tag{8}$$

$$L_{22} = \frac{1}{1 + \chi_2}\, L_2$$
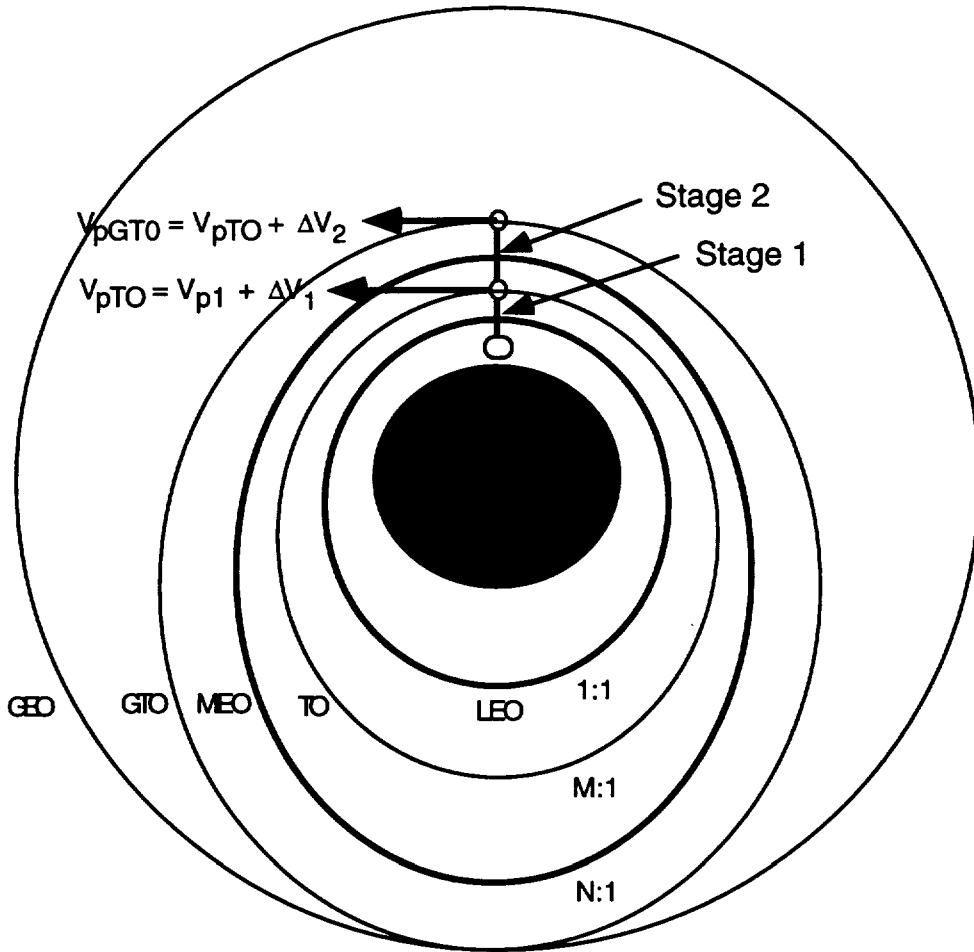
FIGURE 2-8. ORBITAL SKETCH OF TWO-STAGE TETHER SYSTEM FOR TRANSFERRING SATELLITES FROM LEO TO GEO. THE TWO STAGES ARE SHOWN AT THE RESPECTIVE PAYLOAD RELEASES WHICH, IN REALITY, ARE NOT SIMULTANEOUS.

In the following, we summarize the formulas for the computation of the orbital characteristics of satellite and platforms before release and after release for the general case of a first stage in an elliptical initial orbit. After defining μ the Earth's gravitational constant, the orbital velocity of the center of mass (CM) of the 1st stage at perigee is:

$$V_{p1} = \sqrt{\frac{\mu}{r_{p1}}}\sqrt{1 + e_1} \tag{9.1}$$

where r_{p1} is the perigee radius and e_1 is the orbital eccentricity. The velocities at perigee of the second stage before release and of the satellite on its transfer orbit TO are:

$$V_{p2} = \sqrt{\frac{\mu}{r_{p1}}}\sqrt{\frac{2}{(L_{12} + L_2)/r_{p1} + 1} - (1 - e_1)N^{(-2/3)}} \tag{9.2}$$

$$V_{pTO} = \sqrt{\frac{\mu}{r_{p1}}}\sqrt{\frac{2}{L_{12}/r_{p1} + 1} - (1 - e_1)M^{(-2/3)}} \tag{9.3}$$

2-10

Since $\omega_1 = \frac{1}{L_{12}}(V_{pTO} - V_{p1})$ and $\omega_2 = \frac{1}{L_2}(V_{p2} - V_{pTO})$, the rotational rates of the two stages are as follows:

$$\omega_1 = \frac{1}{L_{12}}\sqrt{\frac{\mu}{r_{p1}}}\left(\sqrt{\frac{2}{L_{12}/r_{p1} + 1} - (1 - e_1)M^{(-2/3)}} - 1\right) \tag{10.1}$$

$$\omega_2 = \frac{1}{L_2}\sqrt{\frac{\mu}{r_{p1}}} \cdot \tag{10.2}$$

$$\left(\sqrt{\frac{2}{(L_{12} + L_2)/r_{p1} + 1} - (1 - e_1)N^{(-2/3)}} - \sqrt{\frac{2}{L_{12}/r_{p1} + 1} - (1 - e_1)M^{(-2/3)}}\right)$$

The velocity increments ΔV_1 and ΔV_2 imparted by the first and second stage and the perigee velocity of TO are:

$$\Delta V_1 = \omega_1 L_{12} \tag{11.1}$$

$$\Delta V_2 = 2\omega_2 L_{22} \tag{11.2}$$

$$V_{pTO} = V_{p1} + \Delta V_1 \tag{11.3}$$

The second stage captures the incoming satellite at a velocity equal to $V_{CM-2} - \omega_2 L_{22}$ and accelerates it to a velocity $V_{CM-2} + \omega_2 L_{22}$, thereby producing a velocity increment $\Delta V_2 = 2\omega_2 L_{22}$. However, the tip velocities and not the ΔVs determine the structural strength of the stages. The first stage tether must be designed to withstand a tip velocity $V_{TIP-1} = \Delta V_1$ and the second stage a tip velocity $V_{TIP-2} = 1/2\Delta V_2$.

The perigee radius and velocity of the satellite in GTO after release (with the tether along LV) from the second stage are:

$$r_{pGTO} = r_{p1} + L_{12} + 2L_{22} \tag{12.1}$$

$$V_{pGTO} = V_{pTO} + \Delta V_2 \tag{12.2}$$

From conservation of energy and angular momentum we can readily obtain the apogee radius and velocity of the satellite after release as follows:

$$r_{aGTO} = \frac{r_{pGTO}}{\dfrac{2\mu}{r_{pGTO}V^2_{pGTO}} - 1} \tag{13.1}$$

$$V_{aGTO} = V_{pGTO}\frac{r_{pGTO}}{r_{aGTO}} \tag{13.2}$$

At the apogee of the GEO transfer orbit, the orbit must be circularized with an additional velocity increment ΔV_c as follows:

$$\Delta V_c = \sqrt{\frac{\mu}{r_{aGTO}}} - V_{aGTO} \tag{14}$$

This velocity increment can be supplied by conventional propulsion or (an option not included in this report) by an additional tether. The overall ΔV_{Tot} for the transfer from LEO to GEO is, therefore:

$$\Delta V_{Tot} = \Delta V_1 + \Delta V_2 + \Delta V_c \tag{15}$$

At this point it is necessary to establish a procedure for computing the orbital period ratios M and N (for different tether lengths and mass ratios) which satisfy eqn. (6) and produces the desired apogee altitude of the satellite after release from the second stage. This search could be conducted by trial and error but it would be very time consuming. A faster procedure is by utilizing eqn. (13.1). After substitution of the relevant expressions and assuming that L_1 and $L_2 \ll r_1$, eqn. (13.1) yields:

$$(1 + \chi_2)^2 \left(1 - \frac{1 - e_1}{2}N^{(-2/3)} + \frac{1 - e_1}{4}M^{(-2/3)} + \chi_2\left(1 - \frac{1 - e_1}{4}M^{(-2/3)}\right)\right)^{-2} - \frac{r_{p1}}{r_{aGTO}} - 1 \approx 0 \tag{16}$$

Equation (16) can be solved numerically to find N and M. Figure 2-9 shows solutions for three relevant pairs of orbital period ratios i.e., (a) M = 2, N = 4, (b) M = 1.5, N = 4.5, (c) M = 1.2, N = 3.6, and for two eccentricities of the LEO orbit. It is worth reminding that M is the ratio between the TO and LEO orbital periods while N is the ratio between the MEO and LEO orbital periods. From eqn (12) we can also see that the mass ratio χ_1 does not play any role in the orbit synchronicity while the ratio χ_2 plays an important role.
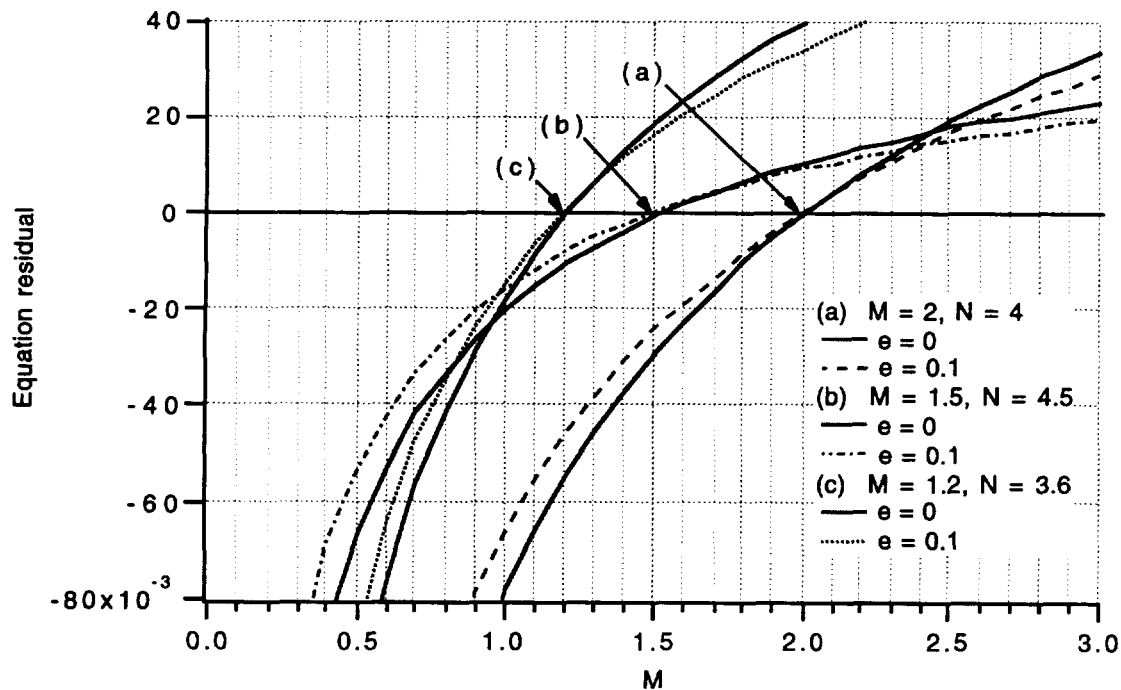
FIGURE 2-9. POSSIBLE ROOTS OF THE SYNCHRONICITY EQUATION.

Since $1/\chi_2$ is the platform_2/satellite mass ratio, the lower its value the lighter the platform of the second stage. The lightest platform of the second stage, among the cases of interest, is obtained for case (b) and its mass is about 1.3x the mass of the payload.

2.3.2 Platform Orbits after Release

Tethers (whether spinning or not) simply exchange angular momentum between the end bodies once they are cut. For this reason, if the satellite is propelled upward after release, the platform is propelled downward. The satellite altitude gain and the platform altitude loss depend upon the satellite over platform mass ratio. The orbital characteristics of the platform after release can be computed from conservation of energy and angular momentum.

The orbit of the platform of the 2nd stage after release is not critical because the MEO orbit is a high-energy orbit. Consequently, the mass of the 2nd stage platform is solely determined by the synchronicity equation as pointed out before. On the contrary, the mass of the 1st stage platform is determined by the characteristics of the LEO orbit and the velocity increment ΔV_1 imparted by the 1st stage. The first stage must be prevented from reentering the atmosphere after releasing the payload. From this point of view initial elliptical orbits are advantageous when compared to an equal-energy circular orbit because the ΔV (at perigee) causes a decrease of the apogee height after release in the former case and a (dangerous) decrease of the perigee height after release in the latter case.

The geocentric radius of the platform absidal point (that can either be a perigee or an apogee depending on the magnitude of the ΔV) opposite to the release point can be computed from conservation of energy and angular momentum, as follows:

$$r_{pl,s} = \frac{r_{pl,r}}{\dfrac{2\mu}{r_{pl,r}\, V_{pl,r}^2} - 1} \tag{17.1}$$

$$V_{pl,s} = V_{pl,r}\, r_{pl,r}/r_{pl,s} \tag{17.2}$$

and the platform velocity at release Vpl,r is given by

$$V_{pl,r} = V_{CM} + \Delta V_{pl} \tag{17.3}$$

$$\Delta V_{pl} = -\chi \Delta V \tag{17.4}$$

In eqns (17), the subscript pl stands for platform, r identifies the point at release and s the opposite absidal point, χ is the mass ratio and ΔV is the velocity increment of the payload. These equations can be applied either to the platform of the 1st or 2nd stage.

2.3.3 Tether masses

The tether mass for an optimally-tapered tether is proportional to the tip mass (satellite) according to the following formula:

$$m_{Tet} = m_{tip} \; \sqrt{\pi} \frac{V_{tip}}{V*} \exp\left(\frac{V_{tip}^2}{V*^2}\right) \text{erf}\left(\frac{V_{tip}}{V*}\right) \tag{18}$$

where m_{tip} is the tip mass and $V* = \sqrt{2\sigma/(\rho f)}$, σ is the ultimate stress, ρ the material density and f the safety factor. The tether material adopted for this study is Spectra-2000 with a density ρ = 970 kg/m3 and an ultimate strength σ = 3.25x109 N/m2. The tether safety factor is 1.75 as suggested for fail-safe tethers in Ref. 6.

The tether has its maximum cross section at the system CM and tapers toward the satellite and the platform. The cross section at the tether tip is given by (see Ref. 4)

$$A_{tip} = \frac{m_{tip} V_{tip}^2}{\sigma * L_d} \tag{19}$$

where $\sigma*$ = σ/f and L_d is distance from CM of the tip mass (either payload or platform).

The tether cross section at CM is readily obtained as follows:

$$A_{CM} = A_{tip} \exp\left(\frac{V_{tip}^2}{V*^2}\right) \tag{20}$$

where the ratio A_{CM}/A_{tip} is called the tapering ratio.

2.3.4 Accelerations

The maximum acceleration on the payload attached to a stage is simply:

$$a_{max} = V_{tip}^2/L_d \tag{21}$$

The relative acceleration (between the incoming payload and the rotating tip mass of the 2nd stage) can also be readily computed with respect to the LV-LH reference frame. From symmetry considerations, the LH component of the relative acceleration at capture is zero. In fact, the horizontal component of the orbital velocity is symmetric with respect to perigee and the horizontal component of the rotational velocity profile is also symmetric with respect to LV. The symmetry is preserved when we take the difference of the two velocities in order to compute the relative velocity. Consequently, the point of capture is a stationary point in the horizontal relative velocity profile which means that the horizontal acceleration at capture is zero.

On the contrary, the vertical orbital and rotational components are antisymmetric and, consequently, the vertical component of the relative acceleration is different from zero. Its numerical value can be simply computed by considering that the vertical component of the orbital acceleration at perigee is zero leaving only the non-zero vertical component of the rotational acceleration (at capture) at the crossing of LV. The vertical relative component of the acceleration at capture, therefore, is:

$$a_{LV}^{rel} = V_{tip}^2 / L_2 \qquad\qquad (22)$$

where L_2 is the tether length of the 2nd stage. The total tether length is used here because, if we assume for simplicity that the capture device has negligible mass with respect to the platform, the CM of the 2nd stage before capture coincides approximately with the platform.

From eqns. (21-22), longer tethers imply smaller accelerations when the satellite is attached to a stage and, more importantly, at capture. In the design of the system, we have limited the maximum tether lengths to ≤ 100 km which sets the lower limit of the accelerations as shown later on.

2.3.5 Numerical Cases

By using the equations derived above, several cases have been analyzed for different orbital eccentricities and synchronicity factors. The cases presented in this chapter were derived for the heaviest payloads predicted in the traffic model, that is, telecommunication satellites of the 9000-lb class (4082 kg) which are heavier than an Intelsat VII.

In order to perform a meaningful comparison, initial orbits with approximately the same energy were adopted. Equal energies of the initial orbits imply same semimajor axes and, for this reason, similar semimajor axis were adopted for the initial orbits. Also a minimum perigee altitude of 400 km (rp = 6778 km) was assumed for the orbits with the highest eccentricity.

The numbering of the cases (from 5a to 6d) presented in the Tables 2-1 to 2-5 may seem odd but it reflects the original numbering of the cases. We must preserve it in this report because the original numbering appears in several other related analyses.

2.3.6 System Mass

Tables 2-1 to 2-5 clearly show that, with present day technology, a single stage tether system from LEO to GEO would be about 4 times more massive than the best results obtained here with a two stage system (cases 6b, 6c and 6d).

The masses shown in the tables are end-of-life (EOL) masses. At the beginning-of-life (BOL) the system must include all the propellant needed for reboosting the stages after each transfer for the number of missions planned between propellant resupplies. The trade off among various thrust systems, carried out by D.J. Vonderwell at Boeing, Huntsville, AL [7], favors high specific impulse (Isp = 3000 s) ion thrusters. After assuming a 30-day reboost time, 2-year operations (time between propellant resupplies) and 12 missions per year, the propellant, power required and the BOL total masses of the systems for the various cases of interest have been computed as depicted in Table 2-7.

For the sake of clarity, the masses of the various components are expressed in term of multiplication factors of the maximum payload mass (4082 kg) in Table 2-6 for case 6d.

TABLE 2-1. KEY PARAMETERS OF A TWO-STAGE TETHER SYSTEM FOR TRANSFERRING A 4082-KG (9000 LB) SATELLITE FROM LEO TO GEO WITH ORBITAL RATIOS M = 2 AND N = 4 AND FOR A SINGLE STAGE TETHER SYSTEM. HERE THE INITIAL LEO ORBITS ARE CIRCULAR.

	Two stage	Single stage
Dimensions: All distances (km) All masses (kg)	$L_1 = L_2 = 20$ km $\chi_1 = 0.191; \chi_2 = 0.454$ $e_1 = 0$	$L_1 = 60$ km $\chi_1 = 0.107$ $e_1 = 0$
1st stage CM orbit (km) Altitudes (km) Semimajor axis (km)	7588 x 7588 1210 x 1210 7588	7588 x 7588 1210 x 1210 7588
2nd stage CM orbit	7624.8 x 30616	n/a
Satellite orbit after 1st stage release	7604.8 x 16486	7642.2 x 42165
Platform-1 orbit after 1st stage release Altitudes	6675.5 x 7584.8 298 x 1207	6681 x 7582.2 303 km
Satellite orbit after 2nd stage release	7632.3 x 42165	n/a
Platform-2 orbit after 2nd stage release	7612.3 x 20260	n/a
Rotational rate ω_1 (rad/s)	0.07277	0.04
Rotational rate ω_2 (rad/s)	0.03397	n/a
$\Delta V_1 = V_{tip\text{-}1}$ (km/s)	1.222	2.149
$\Delta V_2 = 2V_{tip\text{-}2}$ (km/s)	0.934	n/a
$\Delta V_{circularize}$ (km/s)	1.372	1.371
ΔV_{Tot} (km/s)	3.528	3.520
Platform-1 mass (kg)	21370	38150
Tether-1 mass (kg)	4720	23890
Platform-2 mass (kg)	8990	n/a
Tether-2 mass (kg)	700	n/a
1st stage mass (kg) 2nd stage mass (kg)	26090 9690	62040 n/a
EOL Mass Grand Total (kg)	35780	62040

TABLE 2-2. PARAMETERS OF TWO-STAGE TETHER SYSTEM FROM LEO TO GEO WITH ELLIPTICAL INITIAL ORBITS. FOR ALL CASES $L_1 = L_2 = 20$ KM, M = 2, N = 4.

	Case 5a	Case 5b	Case 5c	Case 5d
Dimensions All distances (km) All masses (kg)	$\chi_1 = 0.352$ $\chi_2 = 0.473$ $e_1 = 0.1$	$\chi_1 = 0.15$ $\chi_2 = 0.462$ $e_1 = 0.05$	$\chi_1 = 0.275$ $\chi_2 = 0.462$ $e_1 = 0.05$	$\chi_1 = 0.26$ $\chi_2 = 0.462$ $e_1 = 0.04$
1st stage CM orbit Altitudes Semimajor axis	6778 x 8397.2 400 x 2019 7588	7208 x 7966.7 830 x 1589 7588	7208 x 7966.7 830 x 1589 7588	7288 x 7895.3 910 x 1517 7588
2nd stage CM orbit	6812.8 x 31426	7245.4 x 30993	7243.7 x 30994	7323.9 x 30936
Satellite orbit after 1st stage release	6792.8 x 17296	7225.4 x 16863	7223.7 x 16865	7303.9 x 16798
Plat-1 orbit after 1st stage release Altitudes	6772.8 x 6788 395 x 410	7205.4 x 7232.6 827 x 855	6684.6 x 7203.7 307 x 826	6677.5 x 7284 300 x 906
Satellite orbit after 2nd stage release	6819.9 x 42165	7252.8 x 42165	7251 x 42165	7331.2 x 42165
Plat-2 orbit after 2nd stage release	6799.9 x 20878	7232.8 x 20556	7231 x 20558	7311.2 x 20492
Rot. rate ω_1 (rad/s)	0.07519	0.0672	0.0746	0.0743
Rot. rate ω_2 (rad/s)	0.03134	0.0327	0.0327	0.033
ΔV_1 (km/s)	1.112	1.17	1.17	1.18
ΔV_2 (km/s)	0.851	0.896	0.896	0.9
ΔV_{circ} (km/s)	1.452	1.41	1.41	1.4
ΔV_{Tot} (km/s)	3.415	3.476	3.476	3.48
Platform-1 mass	11600	27210	14850	15700
Tether-1 mass	4100	4100	4490	4530
Platform-2 mass	8630	8840	8840	8840
Tether-2 mass	600	650	650	650
1st stage mass 2nd stage mass	15700 9230	31310 9490	19340 9490	20230 9490
EOL Mass Grand Total	24930	40800	28830	29720

TABLE 2-3. PARAMETERS OF TWO-STAGE TETHER SYSTEM FROM LEO TO GEO FOR ORBITAL RATIOS M = 2 AND N = 4 AND DIFFERENT TETHER LENGTHS.

Dimensions Distances (km), Masses (kg)	Case 5d (repeated)	Case 5e	Case 5f
1st stage mass ratio 2nd stage mass ratio LEO eccentricity	$\chi_1 = 0.26$ $\chi_2 = 0.462$ $e_1 = 0.04$	$\chi_1 = 0.26$ $\chi_2 = 0.462$ $e_1 = 0.04$	$\chi_1 = 0.26$ $\chi_2 = 0.462$ $e_1 = 0.04$
Capture revisit time (hr:min)	7:18	7:18	7:18
LEO-GEO transfer time (hr:min)	16:23	16:23	16:23
1st stage tether length (km) 2nd stage tether length (km)	$L_1 = 20$ $L_2 = 20$	$L_1 = 60$ $L_2 = 20$	$L_1 = 100$ $L_2 = 30$
1st stage CM orbit Altitudes Semimajor axis	7288 x 7895.3 910 x 1517 7588	7298 x 7906.2 920 x 1528 7602	7308 x 7917 930 x 1539 7612
2nd stage CM orbit	7323.9 x 30936	7365.6 x 30946	7417.4 x 30947
Sat. orbit after 1st stage release	7303.9 x 16798	7345.6 x 16789	7387.4 x 16781
Plat-1 orbit after 1st stage release Altitudes	6677.5 x 7284 300 x 906	6689.5 x 7285.6 311 x 908	6701.3 x 7287.4 323 x 909
Sat. orbit after 2nd stage release	7331.2 x 42165	7373 x 42165	7428.4 x 42165
Plat-2 orbit after 2nd stage release	7311.2 x 20492	7353 x 20488	7398.4 x 20482
Rot. rate ω_1 (rad/s)	0.0743	0.0242	0.0142
Rot. rate ω_2 (rad/s)	0.0331	0.0331	0.0218
$\Delta V_1 = V_{tip1}$ (km/s)	1.18	1.15	1.12
$\Delta V_2 = 2V_{tip2}$ (km/s)	0.9	0.9	0.9
ΔV_{circ} (km/s)	1.4	1.4	1.39
ΔV_{Tot} (km/s)	3.48	3.45	3.41
Sat. acceleration on 1st stage	8.9	2.8	1.6
LV acceleration at capture (g)	2.2	2.2	1.4
LH acceleration at capture (g)	0	0	0
1st stage mass 2nd stage mass	20230 9490	20230 9490	20230 9490
EOL Mass Grand Total	29720	29720	29720

TABLE 2-4. PARAMETERS OF TWO-STAGE TETHER SYSTEM FROM LEO TO GEO. FOR ALL CASES $L_1 = L_2 = 20$ KM, M = 1.5, N = 4.5.

	Case 6a	Case 6b
Dimensions All distances (km) All masses (kg)	$\chi_1 = 0.4$ $\chi_2 = 0.75$ $e_1 = 0.04$	$\chi_1 = 0.54$ $\chi_2 = 0.753$ $e_1 = 0.1$
1st stage CM orbit Altitudes Semimajor axis	7268 x 7873.7 890 x 1496 7571	6778 x 8284.2 400 x 1906 7531
2nd stage CM orbit	7302.3 x 33969	6811 x 34244
Sat. orbit after release	7282.4 x 12559	6791 x 12946
Plat-1 orbit after release Altitudes	6677 x 7262 299 x 884	6683 x 6771 305 x 393
Sat. orbit after release	7305.2 x 42165	6813.8 x 42165
Plat-2 orbit after release	7285 x 14052	6793.8 x 14417
Rot. rate ω_1 (rad/s)	0.053641	0.0564
Rot. rate ω_2 (rad/s)	0.057751	0.0553
$\Delta V_1 = V_{tip1}$ (km/s)	0.77	0.73
$\Delta V_2 = 2V_{tip2}$ (km/s)	1.32	1.26
ΔV_{circ} (km/s)	1.40	1.45
ΔV_{Tot} (km/s)	3.49	3.44
Platform-1 mass	10470	7560
Tether-1 mass	1900	1900
Platform-2 mass	5440	5420
Tether-2 mass	1700	1550
1st stage mass 2nd stage mass	12370 7140	9460 6970
EOL Mass Grand Total	19510	16430

TABLE 2-5. PARAMETERS OF TWO-STAGE TETHER SYSTEM FROM LEO TO GEO FOR ORBITAL RATIOS M = 1.5 AND N = 4.5 AND DIFFERENT TETHER LENGTHS.

Dimensions Distances (km), Masses (kg)	Case 6b (repeated)	Case 6c	Case 6d
1st stage mass ratio 2nd stage mass ratio LEO eccentricity	$\chi_1 = 0.54$ $\chi_2 = 0.753$ $e_1 = 0.1$	$\chi_1 = 0.54$ $\chi_2 = 0.753$ $e_1 = 0.1$	$\chi_1 = 0.54$ $\chi_2 = 0.753$ $e_1 = 0.1$
Capture revisit time (hr:min)	8:10	8:10	8:10
LEO-GEO transfer time (hr:min)	16:50	16:50	16:50
1st stage tether length (km) 2nd stage tether length (km)	$L_1 = 20$ $L_2 = 20$	$L_1 = 40$ $L_2 = 40$	$L_1 = 60$ $L_2 = 80$
1st stage CM orbit Altitudes Semimajor axis	6778 x 8284.2 400 x 1906 7531	6778 x 8284.2 400 x 1906 7531	6798 x 8308.7 420 x 1931 7551
2nd stage CM orbit	6811 x 34244	6844 x 34211	6917 x 34259
Sat. orbit after 1st stage release	6791 x 12946	6804 x 12933	6837 x 12958
Plat-1 orbit after 1st stage release Altitudes	6683 x 6771 305 x 393	6687 x 6764 309 x 386	6709.7 x 6777 332 x 399
Sat. orbit after 2nd stage release	6813.8 x 42165	6849.6 x 42165	6928.2 x 42165
Plat-2 orbit after 2nd stage release	6793.8 x 14417	6809.6 x 14404	6848.2 x 14434
Rot. rate ω_1 (rad/s)	0.0564	0.0277	0.0181
Rot. rate ω_2 (rad/s)	0.0553	0.0272	0.0132
$\Delta V_1 = V_{tip1}$ (km/s)	0.73	0.72	0.71
$\Delta V_2 = 2V_{tip2}$ (km/s)	1.26	1.24	1.2
ΔV_{circ} (km/s)	1.45	1.45	1.44
ΔV_{Tot} (km/s)	3.44	3.41	3.35
Sat. acceleration on 1st stage	4.2	2	1.3
LV acceleration at capture (g)	6.2	3	1.4
LH acceleration at capture (g)	0	0	0
1st stage mass 2nd stage mass	9460 6970	9460 6970	9460 6970
EOL Mass Grand Total	16430	16430	16430

TABLE 2-6. MASSES OF COMPONENTS EXPRESSED AS MULTIPLICATION FACTORS OF THE MAXIMUM PAYLOAD MASS OF 4082 KG FOR CASE 6D. THE PROPELLANT MASSES ARE FOR 24 MISSIONS AT MAXIMUM PAYLOAD CAPACITY.

Component	Factor x satellite mass
1st stage platform	1.8x
1st stage tether	0.5x
2nd stage platform	1.3x
2nd stage tether	0.4x
1st stage propellant	0.7x
2nd stage propellant	1.2x
System (w/o payload)	5.9x

If we consider that the total mass of an IUS (Inertial Upper Stage) (which can transfer a 4-ton payload from LEO to GTO) is equal to 14800 kg [8], then it can be concluded that the tether system becomes competitive, from a system mass viewpoint, after only 2 missions, while it can accommodate 24 missions between propellant resupplies.

2.3.7 Tether sizes

Fail-safe tethers will likely be the preferable candidates for spinning tethers. If we assume, for the sake of picturing the size, that the tethers have solid cross section, the tether diameters for the best-case system under consideration (6d) average about 0.64 cm for the 1st stage tether and 0.48 cm for the 2nd stage. The ratio between the cross section at the tether tip and at the CM (i.e., the tapering ratio) is 1.1. Since the tapering ratio is close to unity, we could for simplicity of construction utilize non-tapered tethers of maximum cross sections at the expense of a small mass increase.

This last conclusion stems from the fact that in a two-stage tether system from LEO to GEO the ΔV provided by each stage is well below 1 km/s and, consequently, tapered tethers do not have a striking mass advantage over cylindrical tethers.

TABLE 2-7. POWER AND MASS REQUIREMENTS FOR THE LEO TO GEO TETHER SYSTEM [COURTESY OF BOEING, HUNTSVILLE, AL]

30 day reboost (12 missions/year)   Isp = 3000 s (ion engine)
tb/Period = 0.35   Efficiency = 0.75

Case	LEO Platform			MEO Platform			Total System* Mass (kg)
	Propellant Mass (kg)	Power Required (kW)	System* Mass (kg)	Propellant Mass (kg)	Power Required (kW)	System* Mass (kg)	
5a	4706	135.382	20603	2944	82.004	12301	32904
5b	4331	120.459	35827	3103	86.611	12727	48554
5c	4808	136.692	24351	3103	86.618	12727	37078
5d	4804	136.224	25237	3127	87.236	12751	37989
5e	4828	136.026	25262	3135	87.599	12760	38022
5f	4857	135.875	25293	3119	87.101	12743	38036
6a	2908	81.498	15403	5249	156.685	12605	28008
6b	2914	82.700	12498	4958	146.780	12134	24631
6c	2924	82.529	12508	4926	145.554	12100	24608
6d	2928	82.202	12512	4883	144.169	12055	24567

* - System mass does not include payload mass

2.3.8 Accelerations

The maximum acceleration at capture is 1.4 g (that is all in the vertical component because the horizontal component is zero) for the most interesting case 6d. The maximum accelerations on the satellite when attached to the 1st and 2nd stages are 1.3 g and 0.8 g, respectively for case 6d.

2.3.9 Mission Sequence

The three following slides [9] show the mission sequence and orbits for case 5f (the sequence for case 6d is qualitatively similar to this). The satellite is first released from the 1st stage at the appropriate phase angle (that depends upon the M/N ratio) with respect to the perigee. For case 5f the satellite is released from the 1st stage when the 2nd stage is at apogee (i.e., angle = 180 deg). After the satellite is captured by the second stage, the satellite is released one orbit later when the second stage passes again through perigee. The total transfer time from LEO to GEO in case the satellite is captured at the first attempt is 16:23 hr:min for case 5f (M = 2 and N = 4), and 16:50 hr:min for case 6d (M = 1.5 and N = 4.5).

2.3.10 Revisit and Transfer Times

The time Trev = NKP_1 is the periodic revisit time between the 2nd stage and the satellite released from the 1st stage in case of miscapture. Cases with M = 2, N = 4 have a slightly shorter revisit time than cases with M = 1.5, N = 4.5. In fact, in the former case N = 4 and K = 1 (see eqn. 6) while in the latter case N = 4.5 and K = 1. The revisit time is equal to 7:18 hr:min for cases with M = 2 and N = 4 and 8:10 hr:min for M = 1.5 and N = 4.5.

2.3.11 Payloads with different masses

The cases analyzed previously were all for the heaviest payloads of 4082 kg (9000 lb). The system however can handle any lighter payload with ease. Lighter payloads in fact only require adjustments of the rotational rates of the two stages. The adjustments of the orbits of the two stages are almost negligible. The orbit adjustments are only of a few kilometers in order to compensate for the fact that the CMs of the two stages have shifted somewhat because of the lighter payload. The orbital adjustment are therefore very minor and they can be simply incorporated into the reboost phases of the stages.

In the 9000-lb cases analyzed before, the rotational rates of the second stage at capture and at release of the payload were the same and equal to ω_2. This implies that the second stage does not need to be spun up or down after capture of a 9000-lb payload. For payloads lighter than 9000 lb, the rotational rate at release from the 2nd stage ω_{2b} is lower than at the rate at capture ω_{2a}. Consequently, the second stage must be spun down after capture. This can be accomplished by either lengthening the tether (i.e., because of the conservation of angular momentum, the tip speed changes inversely with the tether length) or by using electrical thrusters or a combination of the two techniques.

Table 2-8 shows the orbital characteristics and other relevant parameters of case 6d for payloads of 9000 lb (repeated), 5000 lb and 2000 lb. In the table, ω_1 is the rotational rate of the 1st stage and ω_{2a} and ω_{2b} are the rotational rates of the 2nd stage at capture and at release, respectively. It should be pointed out that the synchronicity of the orbits and the zero distance at capture is preserved for all payload masses thanks to the minor orbit adjustments indicated in the table.

Figure 2-10 shows the rotational rates ω_1, ω_{2a} and ω_{2b} vs. the payload mass for case 6d. After inspection of Table 2-8 and Figure 2-10, it appears that a possible design option is to choose an average payload mass as a nominal case (4243 lb is for example a factor 2.12 greater than 2000 lb and a factor 2.12 smaller than 9000 lb). By following this option, the rotational speed of the 2nd stage must be increased after capture for payloads > 4243 lb and decreased for payloads < 4243 lb. The advantage of this option is that the required rotational speed increases and decreases could be handled by a 2.12 increase or decrease of the 2nd stage tether length. Consequently, the tether length of the 2nd stage could be 17.8 km for 2000-lb payloads, 37.7 km for the design-point payloads of 4243 lb and 80 km for 9000-lb payloads.
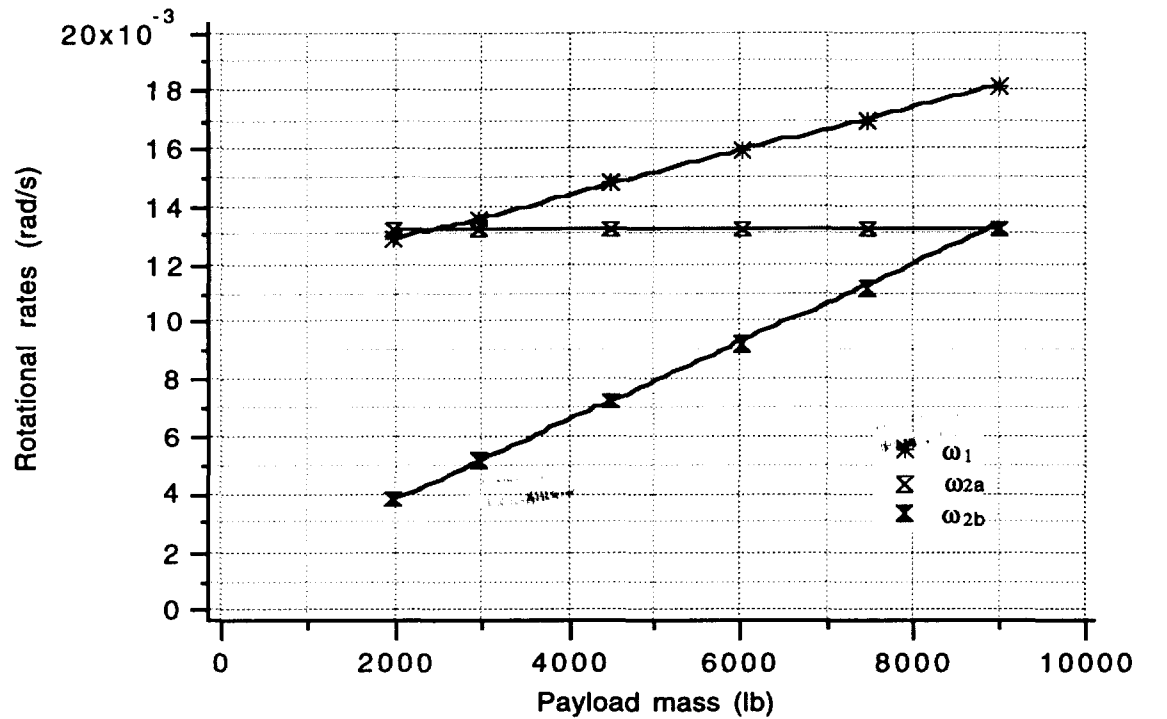
FIGURE 2-10. ROTATIONAL RATES OF THE 2 STAGES VS. P/L MASS. ω_1 = 1ST STAGE, ω_{2A} AND ω_{2B} = 2ND STAGE AT CAPTURE AND RELEASE

2.4 RENDEZVOUS AND CAPTURE

One of the important aspect of a two-stage tether system is the capture of the satellite by the second stage. A few important points must be stressed regarding this particular rendezvous and capture as follows: (a) the relative velocity at capture is zero; (b) the horizontal component of the relative acceleration is zero; (c) the vertical component of the relative acceleration is about 1.4 g; and (d) the timing of the rendezvous maneuver is faster than a conventional rendezvous.

Considering that the vertical acceleration is the only non-zero component at capture, the capture maneuver is fairly similar to capturing an object, thrown in the air from the ground, at the top of its parabolic trajectory with the hand moving at the same horizontal velocity of the object. The only non-zero component at capture is, in both cases, the vertical acceleration that is equal 1 g on the ground and 1.4 (cases 6d and 5f) for the tether system in space.

While the above simple example can help understanding the rendezvous and capture dynamics, accurate simulations of this phase have been made by H. Dionne at Boeing, Huntsville, AL [10].

The relative distance, velocity and acceleration profiles are shown in Figures 2-11 to 2-18 for the cases of greatest interest. In the figures, the x-axis is along LV and the y-axis is along LH. The figures show clearly the important points about this rendezvous and capture that were previously highlighted.

TABLE 2-8. KEY PARAMETERS OF LEO TO GEO SYSTEM FOR CASE 6D FOR DIFFERENT PAYLOAD MASSES. FOR ALL CASES M = 1.5, N = 4.5, e_1 = 0.1.

Dimensions Distances (km), Masses (kg)	Case 6d_1 9000-lb payload	Case 6d_2 4500-lb payload	Case 6d_3 2000-lb payload
Capture revisit time (hr:min)	8:10	8:10	8:10
Transfer time to GEO (hr:min)	16:50	16:50	16:50
1st stage tether length (km) 2nd stage tether length (km)	L_1 = 60 L_2 = 80	L_1 = 60 L_2 = 80	L_1 = 60 L_2 = 80
1st stage CM orbit Altitudes Semimajor axis	6798 x 8308.7 420 x 1931 7551	6798 x 8308.7 420 x 1931 7551	6798 x 8308.7 420 x 1931 7551
2nd stage CM orbit	6917 x 34259	6925.2 x 34251	6931.6 x 34244
Sat. orbit after 1st stage release	6837 x 12958	6845.2 x 12950	6851.6 x 12944
Plat-1 orbit after 1st stage release Altitudes	6709.7 x 6777 332 x 399	6785.2 x 7455.2 407 x 1077	6791.6 x 7914.7 414 x 1537
Sat. orbit after 2nd stage release	6928.2 x 42165	6961.4 x 42165	6988.7 x 42165
Plat-2 orbit after 2nd stage release	6848.2 x 14434	6881.4 x 20953	6908.7 x 26980
Rot. rate ω_1 (rad/s)	0.0181	0.0148	0.0129
Rot. rate ω_{2a} (rad/s)	0.0132	0.0132	0.0132
Rot. rate ω_{2b} (rad/s)	0.0132	0.0072	0.00384
Sat. acceleration on 1st stage	1.3	1.1	0.9
LV acceleration at capture (g)	1.4	1.4	1.4
LH acceleration at capture (g)	0	0	0
1st stage mass 2nd stage mass	9460 6970	9460 6970	9460 6970
EOL Mass Grand Total	16430	16430	16430

FIGURE 2-11. LV DIFFERENTIAL ACCELERATION AT RENDEZVOUS AND CAPTURE OF
SATELLITE BY 2ND STAGE.
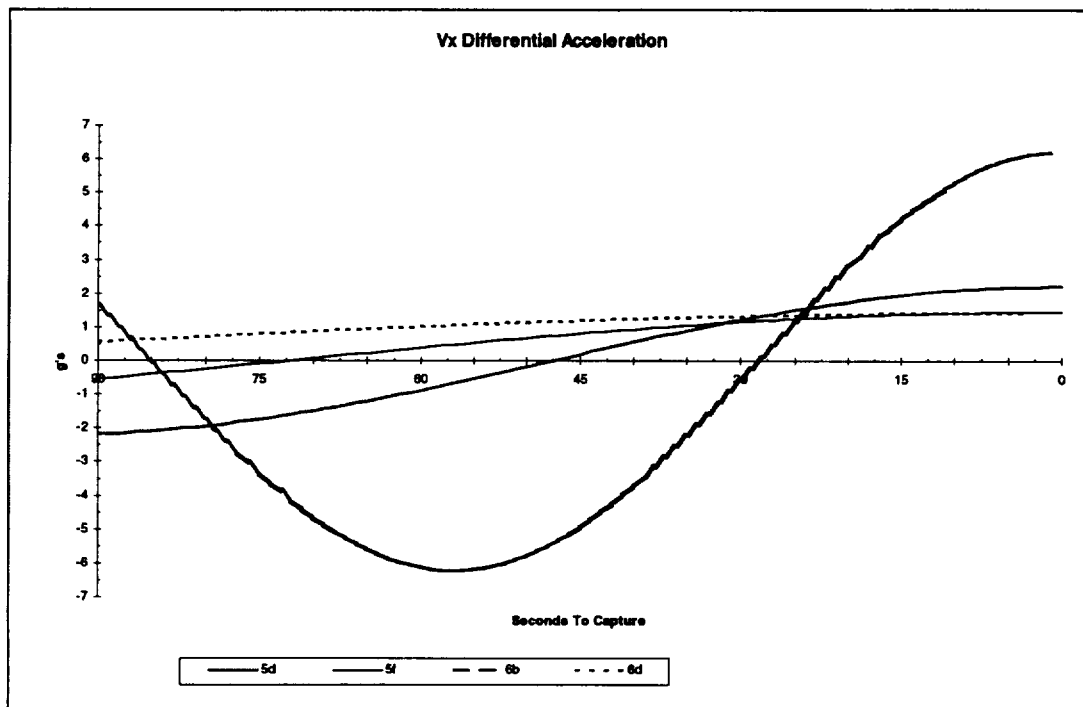
FIGURE 2-12. DETAIL OF LV DIFFERENTIAL ACCELERATION AT SATELLITE
RENDEZVOUS & CAPTURE BY 2ND STAGE.
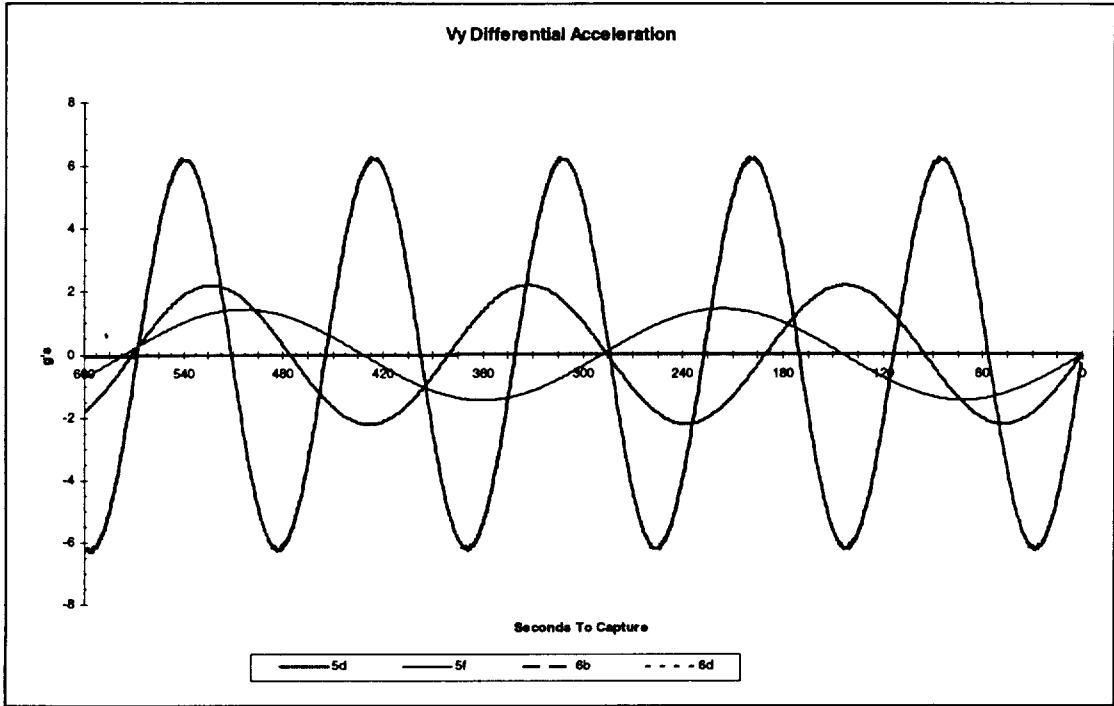
FIGURE 2-13. LH DIFFERENTIAL ACCELERATION AT RENDEZVOUS AND CAPTURE
OF SATELLITE BY 2ND STAGE.
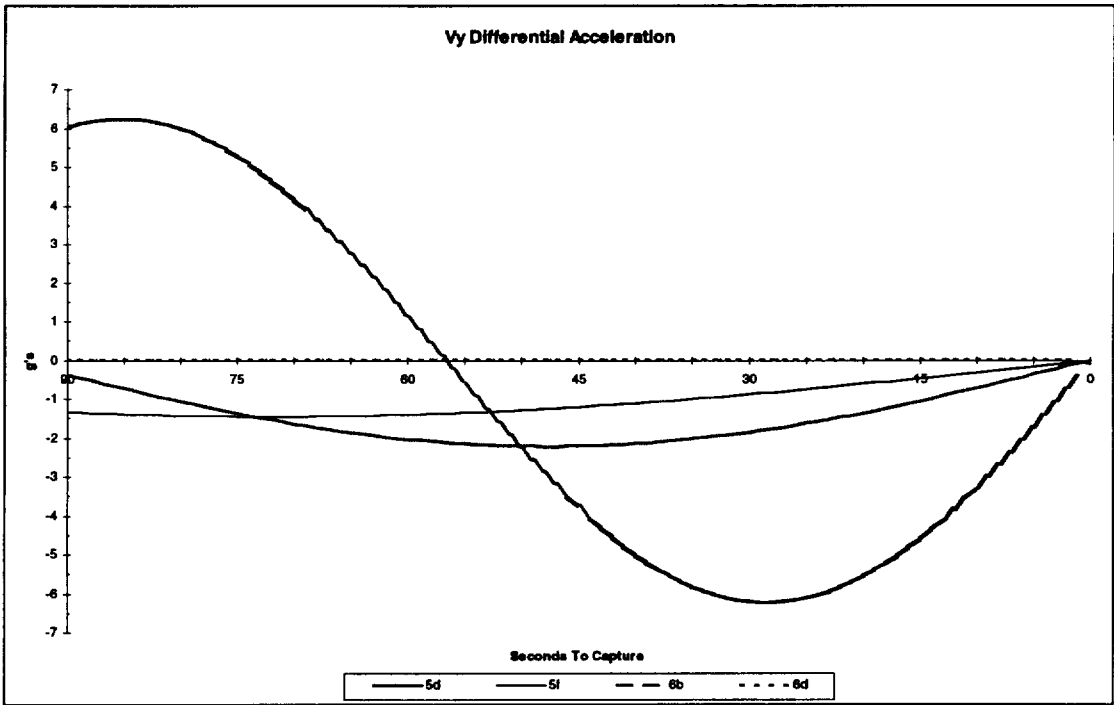
FIGURE 2-14 DETAIL OF LH DIFFERENTIAL ACCELERATION, SATELLITE
RENDEZVOUS & CAPTURE BY 2ND STAGE.
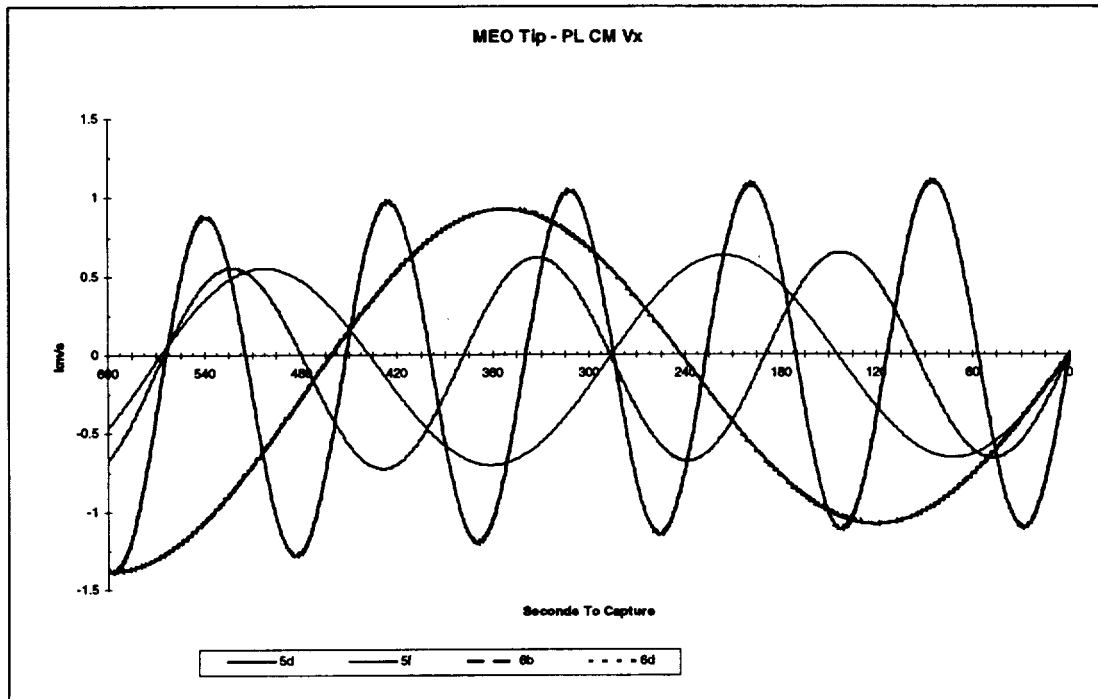
FIGURE 2-15 LV DIFFERENTIAL VELOCITY AT RENDEZVOUS AND CAPTURE OF
SATELLITE BY 2ND STAGE.
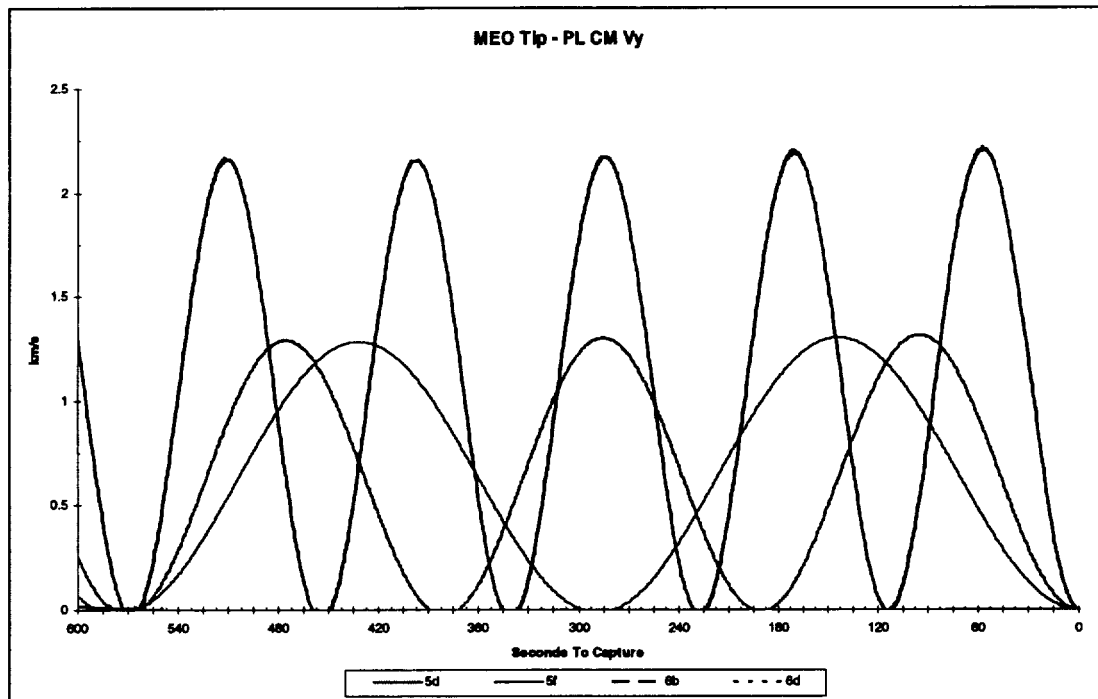
FIGURE 2-16 LH DIFFERENTIAL VELOCITY AT RENDEZVOUS AND CAPTURE OF
SATELLITE BY 2ND STAGE.
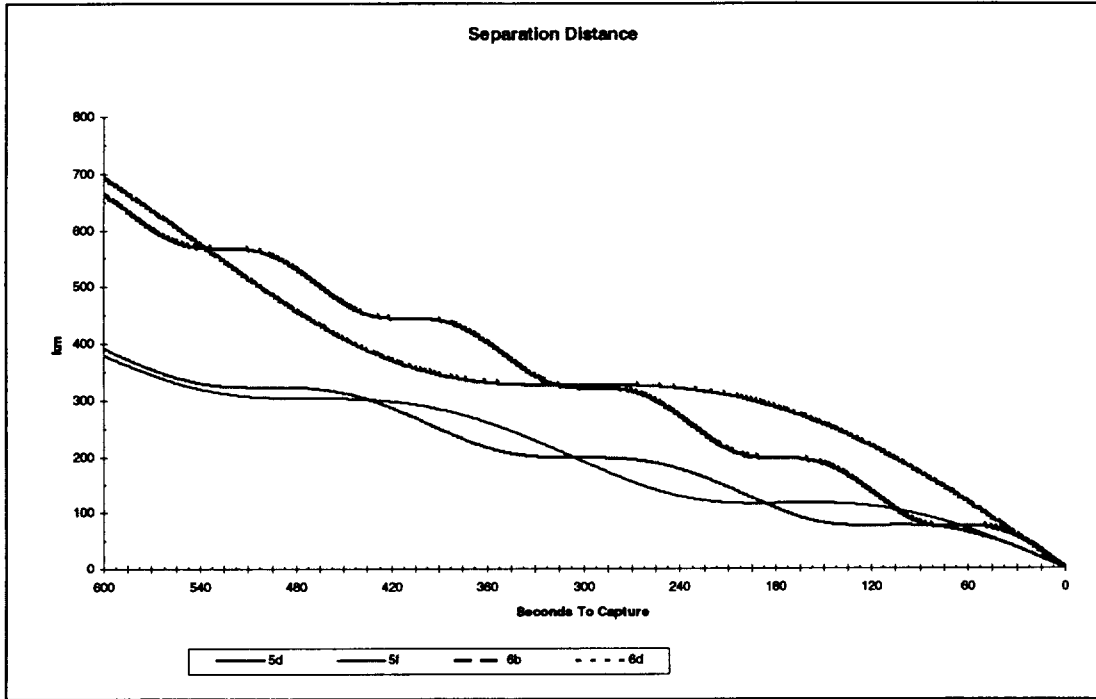
FIGURE 2-17 SEPARATION DISTANCE AT RENDEZVOUS AND CAPTURE OF
SATELLITE BY 2ND STAGE.
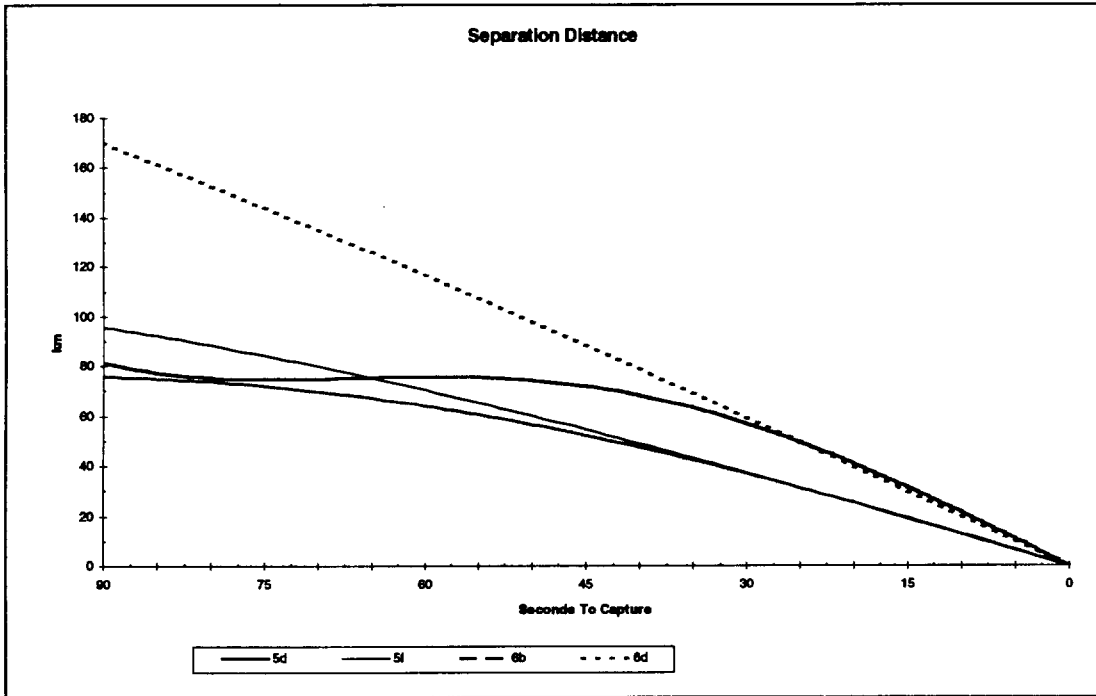
FIGURE 2-18 DETAIL OF SEPARATION DISTANCE AT RENDEZVOUS AND CAPTURE
OF SATELLITE BY 2ND STAGE

2.5 ADDITIONAL CONSIDERATIONS

The tether system discussed here is reversible: it can be used to transport spent satellites from GEO to LEO. In this case the 2nd stage would capture the satellite at the top of its spin and release at the bottom of its spin to rendezvous with the 1st stage. Another interesting feature is that because of conservation of angular momentum, if a satellite is transferred to GEO and an equal-mass satellite is retrieved from GEO at the next available opportunity, then no propellant is required for reboosting the stages. Clearly, in a realistic situation the return traffic will be different from the outgoing traffic and some propellant will be necessary for making up the deficit of angular momentum. The return traffic, however, besides being important in itself can also provide sizable savings to the propellant budget of the system.

2.6 SUMMARY

A two-stage tethered system of reasonable size and relatively small mass can be designed for transferring satellites with a mass up to 9000 lb from LEO to GEO (with the circularization ΔV provided by the kick motor of the satellite). The transfer times from LEO to GEO for the two-stage systems examined here are between 16:23 hr:min and 16:50 hr:min which is competitive with the 5:30 hr:min from LEO to GEO of a conventional upper stage.

The best estimate of the end-of-life system mass is about 16500 kg for the two stages without propellant. If we then consider that the system will be reused 24 times over 2 years and that it will conservatively always launch 9000-lb satellites, about 8000 kg propellant for the ion engines must be added to the end-of-life system mass. The total mass estimated for 24 missions at maximum payload capacity is, therefore, 24500 kg. The tether system, therefore would become competitive with respect to a present upper stage (e.g., IUS) on a mass basis after only two launches.

The orbital mechanics of the system is designed with resonant orbits so that there are frequent conjunctions (or visits) between the 1st and 2nd stage and there multiple opportunities for capture of the satellite in case of miscapture by the 2nd stage (the revisit time ranges between 7:18 hr:min and 8:10 hr:min for the cases analyzed).

In summary, the tether system combines the efficiency of electrical propulsion (high specific impulse) and the delivery speed to GEO of a chemical system.

A single stage tether system from LEO to GEO would be >3 times more massive than a two stage system with present day tether technology. However, an increase of the strength-to-weight ratio of 70% (which is conceivable over the next 15 from the current trend) would reduce the tether mass by a factor three and consequently make the single stage tether system much more attractive than at present.

As a final comment, the tether system can not only be used to deliver payloads to GEO but also to return satellites from GEO to LEO. In a future scenario, not analyzed in this report, the return traffic could be used to offset a large portion of the propellant used for reboosting the stages.

Section 3

SYSTEM DEFINITION AND REQUIREMENTS

3.1 MISSION

The mission of the in-space tether transportation system is to capture payloads, up to a mass of 9000 lb each, in LEO and to deploy them to GEO. The payloads are delivered to LEO by a launch vehicle. The system shall be capable of deploying payloads at a maximum rate of one per month. The payload maximum mass and rate of deployment were derived from the Commercial Spacecraft Mission Model Update, dated 25 July 1996 [2]. The system shall be available to accomplish its mission in 2010 and shall have a 10-year life.

3.2 SYSTEM ARCHITECTURE AND REQUIREMENTS

Figure 3-1 is a top-level system architecture block diagram of the tether transportation system. As explained in the previous section, the system consists of two tether facilities, one in LEO, the second in MEO. The facilities are in a common orbital plane. The LEO facility captures and deploys the payload toward MEO for rendezvous with and capture by the MEO facility. The MEO facility subsequently deploys the payload into a geosynchronous transfer orbit (GTO). Each facility consists of a base facility from which the tether is deployed and spinning and a Payload Capture and Release Assembly (PLCRA) at the deployed end of the tether.
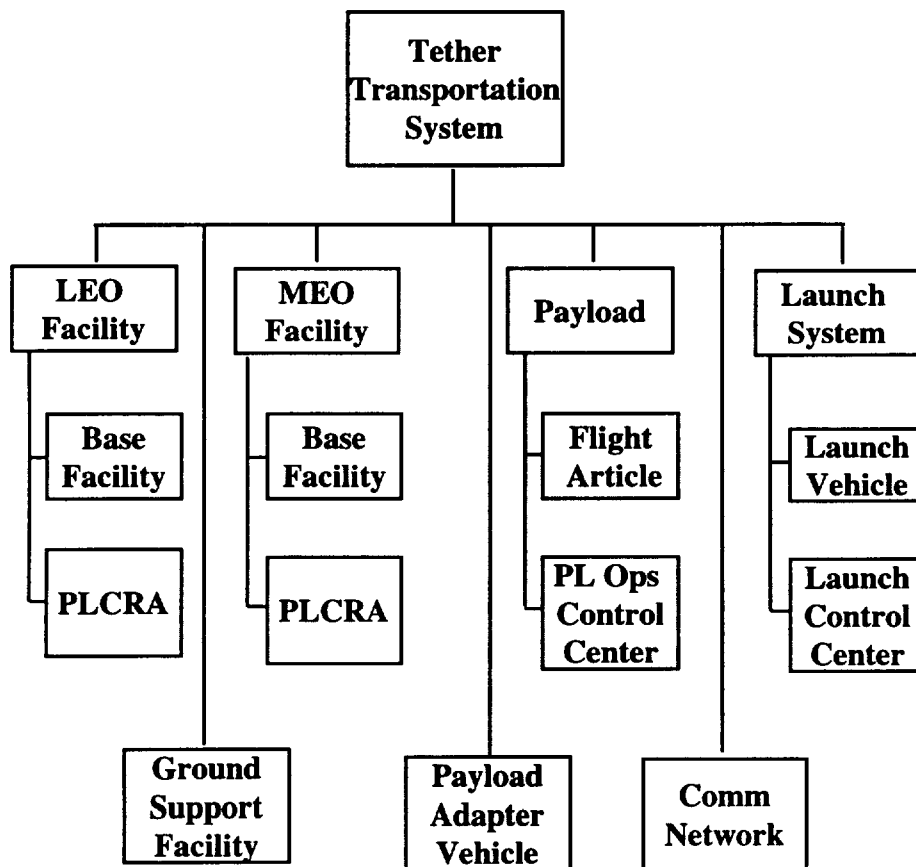
FIGURE 3-1. ARCHITECTURE OF THE LEO AND MEO TETHER FACILITIES

In order to provide an interface of the payload to the PLCRA and to circularize the payload in GEO, the system also includes a Payload Adapter Vehicle (PAV) to which the payload is mated prior to launch. Other elements of the tether transportation system include the payload flight article and operations control center, the launch system consisting of vehicle and control center, and the communications network for monitoring and controlling flight elements.

3.3 OPERATIONS CONCEPT AND FUNCTIONAL REQUIREMENTS

3.3.1 Overview and Approach

For engineering analysis of the tether transportation system, the operations concept was divided into three phases:
A. initial launch and deployment of the LEO and MEO facilities
B. recurring mission operations - i.e. recurring deployment of payloads from LEO to GEO
C. end-of life disposal of facilities

Engineering analysis initially focused on the second phase, recurring mission operations. Only when engineering definition and analysis of the system provided confidence of system feasibility did the study address the other phases. Study results relative to the first phase, initial deployment of the LEO/MEO facilities, are presented in Section 6.

3.3.2 Recurring Mission Operations

The operations concept for recurring mission operations was developed using functional analysis. That is, a top-level flow diagram was generated, shown in Figure 3-2.
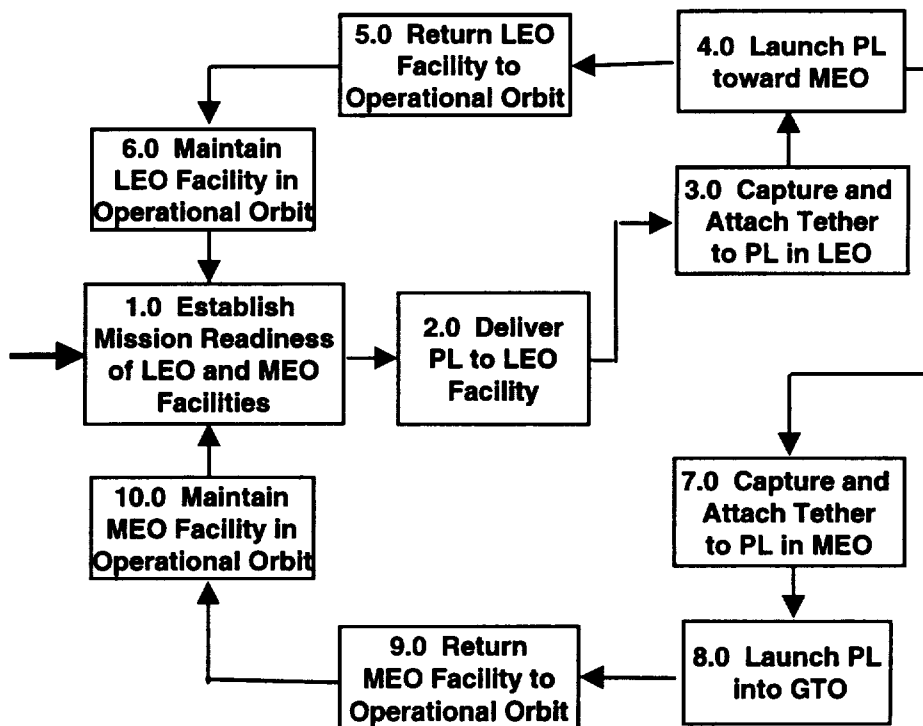
FIGURE 3-2. RECURRING MISSION OPERATIONS

Each functional block was then decomposed into more detailed functional activities, as shown in Table 3-1. These detailed functional activities were used to identify functional requirements to be implemented by the major system elements. In turn, this allowed definition of the subsystems comprising major system elements, in particular the LEO and MEO tether facilities.

Initial conditions for the top-level concept of recurring mission operations are that the LEO and MEO facilities are in "survival mode" in their respective operational orbits. The initial step to executing a mission operation (i.e., a payload delivery to GEO) is to establish the readiness of the LEO and MEO facilities. This readiness is a major consideration constituting the criteria to commit to launch of the payload.

3.3.3 RLV Launch Capabilities

The launch vehicle chosen as the design focus for this study is the VentureStar Reusable Launch Vehicle (RLV) [11]. The RLV should significantly reduce the cost to LEO; its development schedule (figure 3-3) indicates operational status by the year 2005. This fulfills the system requirement set forth in Section 3.1 of accomplishing a mission in 2010. The RLV's launch capabilities, which were used to evaluate the initial deployment of the LEO/MEO facilities, are summarized in Table 3-1

TABLE 3-1. RLV LAUNCH CAPABILITES SUMMARY

Gross Lift Off Weight (GLOW):	2,186,000 lb_m
Propellant Weight:	1,929,000 lb_m
Empty Weight	197,000 lb_m
Payload to 100 Nmi/28.5° orbit	59,000 lb_m
Payload Bay Size	15 x 45 ft
Isp (sea level)	347 s
Isp (vacuum)	455 s
Isp (average)	438 s
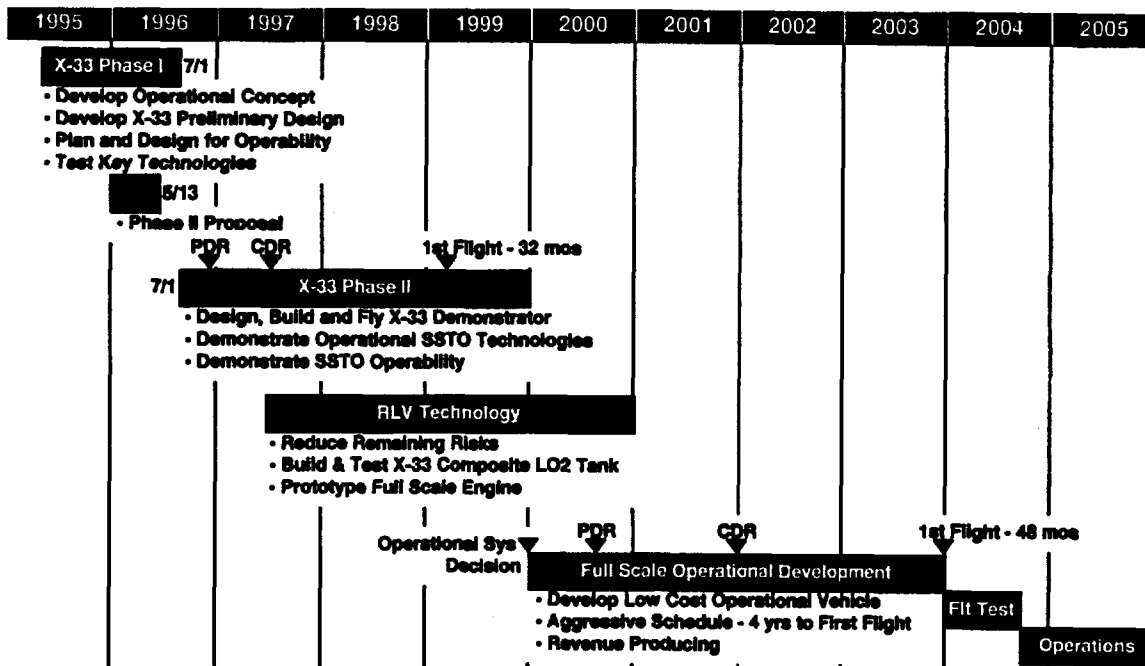
FIGURE 3-3. X-33/RLV PROGRAM SCHEDULE

Section 4

SUBSYSTEMS CONCEPTS AND TRADES

4.1 OVERVIEW

As explained in Section 3, the functional analysis of recurring mission operations was used to identify the functional requirements to be satisfied by major system elements. Also, the functional requirements were used to define the major subsystems and assemblies comprising the LEO and MEO facilities.

As stated above, figure 3-1 is a block diagram of the architecture of the LEO and MEO tether facilities, illustrating the major subsystems and assemblies. The facilities consist of the standard subsystems of orbiting spacecraft; however, the tether retrieval, deployment and spin control subsystem and the PLCRA are unique to the mission of these orbiting facilities.

4.2 ATTITUDE DETERMINATION AND CONTROL

4.2.1 Normal Operations

The LEO and MEO facilities are essentially spin-stabilized systems. This simplifies things somewhat since spin-stabilized systems are simple and are effective in any orientation. Many proven technologies currently exist that can be implemented on the LEO and MEO facilities. Attitude control will be accomplished by using thrusters (gas and/or electric), momentum wheels (in one axis only to control the twisting about the tether axis), and/or magnetic torquers. However, the high g levels on the facilities caused by the rotation may rule out the use of momentum wheels.

Three possible attitude determination methods that can be applied to the LEO and MEO facilities. They are:
- Interferometric methods – use multiple antennae and carrier phase measurements.
- Velocity vector matching – Use one antenna during the facility orbital maneuvers (e.g. reboost)
- Attitude vector matching techniques – Use two GPS antennae during spacecraft rotation.

The main method of GPS-based attitude determination is the interferometric method, which requires more than two antennae and at least 4 visible GPS satellites at each antenna. The interferometric mode provides attitude information to an accuracy of less than a tenth of a degree. Attitude determination requires the estimation of the carrier phase ambiguity, which is the number of carrier cycles between the master antenna and the satellite. Resolution of this ambiguity is facilitated by a rate of change in the line of sight vector from the satellite to the antenna baseline. If the satellite alone provides this rate of change, (i.e. the antenna system is stationary in the local level coordinate system), then the time to resolve the ambiguity can be of the order of a few minutes. A larger baseline provides greater attitude accuracy, however, a baseline as small as 1 meter can provide an accuracy of 0.1 degrees, and not suffer from flexure in the antenna baseline structure. [12]

4.2.2 Rendezvous/Capture and Release Operations

This area is currently undergoing further investigation. Due to the low thrust rate of the LEO and MEO facilities, the attitude (and location) of each facility must be precisely controlled. This will require a high degree of precision from the attitude control sensors selected for use

on the facilities. Simulations are currently underway to determine the rendezvous and approach velocities of the RLV to the LEO facility as well as the payload to LEO and MEO facilities. These results will lead to a sample rate analysis or trade study to be performed as the facility designs mature. The resulting required sample rate might be the design driver for the attitude control system. Considering the large mass and the low thrust rates of the LEO and MEO facilities, the Payload Adapter Vehicle (PAV) will assume the responsibility for all final attitude corrections prior to capture.

For rendezvous and capture of the payload by each facility, it is necessary to use relative GPS navigation. The relative mode of operation of the navigation system is enabled when the target vehicle data (LEO or MEO facility) is available to the PAV via a communications data link. The simplest form of relative navigation processing synchronizes the navigation output from two receivers and computes the line of sight position and velocity vectors. This mode requires that the GPS receivers in the target and payload are tracking identical satellites and use similar processing methods to obtain the highest possible accuracy. It is therefore important that the Leo and MEO facilities have the capability of transmitting satellite selection information along with position, velocity, and time information. Relative navigation is enabled when the payload vehicle is between 200 km and 10 km of the target (this depends on the characteristics of the data link and accuracy of the docking sensor for close proximity operation). During close proximity operation, the system will hand navigation and control functions from the GPS based system to the docking sensor. More study of close proximity operations is necessary in order to define the capture envelope for the mission.

4.2.3 Mission Profile

To achieve Payload to LEO or MEO facility automated rendezvous, it is important to standardize the mission profile to the extent possible thereby simplifying the on-board targeting methodology. The mission profile must have phase (central angle between the payload facility and the tether facility) adjustment capability to compensate for launch time variation across the launch window, orbit transfer errors, navigation errors, orbit propagation errors, and target ephemeris errors. There are a number of mission profiles and phasing strategies that can be automated in order to achieve the desired rendezvous mission. A baseline mission profile from Payload launch through delivery of the payload to its final orbit is required. Further investigation in this area is needed

4.3 ELECTRICAL POWER

4.3.1 Introduction

In order to obtain high performance, minimize propellant consumption and ensure long operational life, electric propulsion options are required. This, of course, drives the system design to higher power requirements (on the order of 100's of kilowatts.) The propulsion system duty cycle for re-boosting is characterized primarily by short tangential burns at the perigee and apogee of the orbit. The remainder of the time the propulsion system is used periodically to perform attitude control. The exact duration of the burns has not been determined but is assumed to be approximately 35% of the orbit period for the preliminary design analysis. Longer or continuous burn times will decrease the power required by the propulsion system (by permitting the use of smaller electric thrusters) but, at the same time, tend to circularize the orbit (if no active thrust vector control is implemented.) Additional trade studies should be conducted to determine the optimum burn duration in order to

minimize the current draw on the battery system. The rest of the tether platform power requirements are relatively stable over the course of the orbit.

In an effort to ensure practicality, an attempt was made to develop a system based on current technology. Unfortunately, most storage systems flown to date proved unsuitable for this application. The high current demands on the battery system (due to the high current pulses required by the propulsion system) are well outside current qualification limits. Extrapolations to future systems now under development, or that are just now being deployed, are therefore considered.

4.3.2 Requirements

The Tether Transfer system consists of the LEO and MEO facilities (tethers, winches, thrusters, etc.) which are the reusable elements of the system, and the Payload Adapter Vehicle (PAV), which is the expendable element. Their functions and their expected lifetimes drive the power requirements for the different elements. The PAV power system requirements resemble those of an upper stage, such as:
- Limited lifetime (days if not hours)
- Power storage only
- Moderate power requirements (not quantified in this study)

Both the LEO and MEO tether facilities have requirements more similar to the space station, namely:
- 10+ year lifetime
- High power requirements (90 - 150 kW)
- Serviceability
- Power generation and storage

Power requirements by major subsystem areas and by element are shown in table 4-1. The subsystem power requirements, excluding the propulsion elements, are similar to typical on-orbit platforms. For the LEO and MEO tether facilities, the power requirement for the propulsion subsystem is several orders of magnitude greater than all the other subsystems combined. The Payload Capture and Release Assembly (PLCRA) and the PAV do not use large electrical propulsion elements and therefore have considerably lower power requirements.

4.3.3 Power Generation

Primary batteries will likely be used to supply electrical power for the PAV. Communication, tracking, and maneuvering during rendezvous dominate power requirements for the PAV. The interface between the PAV and the LEO and MEO tether facilities is the PLCRA, which includes the communication and tracking systems and the active capture mechanism. The sole interface between the PLCRA and the tether platform (for both the LEO and MEO facilities) is the tether itself, therefore power generation and storage capabilities are included aboard each PLCRA. The estimated power required for the PLCRA is 1380 W, however, further design effort on the details of the capture system may revise this figure. A barrel-style array with an area of 15.61 m^2 would provide sufficient power for battery charging to account for eclipse times. This also includes an allowance to compensate for the losses associated with the constantly changing sun angle due to rotation of the tether facility.

TABLE 4-1. TETHER FACILITY SYSTEM POWER ESTIMATES

Element	Subsystem	Power (Watts)
Platform	C&DH	150
	ALDCS	5
	Secondary Prop.-Attitude	155
	Main Prop. (LEO / MEO)	82000 / 140000
	Thermal control	200
	Power management system	705
	Retrieval, deployment	10000
	Communications	50
	Total Power (LEO/MEO)	**93265 / 151265**
Payload Capture and Release Assembly	C&DH	150
	ALDCS	5
	Propulsion	872
	Thermal control	100
	Power management system	75
	Docking sensors, actuators	28
	Communications	50
	Final lock-on, capture system	100
	Total Power	**1380**
Payload Adapter Vehicle	C&DH	110
	ALDCS	5
	Propulsion	872
	Thermal control	200
	Power management system	100
	Beacon system	20
	Communications	35
	Total Power	**1342**

A major component of the total power required for the LEO and MEO platforms is the power required by the ion thrusters during reboost following deployment of the payload. For this study, the following assumption was made with regards to power usage: the platforms do not combine any tether reeling with a reboost operation. This is thought to be valid based on the scenario that reeling operations are primarily associated with payload capture and release, whereas reboost takes place over 30 days with no payload. A more in-depth study of platform operations is required to confirm this assumption.

The sum of reboost and subsystem power requirements is estimated to be 93 kW for the LEO platform and 151 kW for the MEO platform. Both power levels support a robust reeling rate for payload capture and release operations. To provide the required power for the LEO platform, with sufficient margin for battery recharge, a total array area of 1093 m2 is needed. This can be provided by four wing pairs, each slightly larger than those planned for International Space Station. For the current design, the MEO platform drops further after payload deployment (due to it supplying a larger portion of the required DV to the payload) and requires six wing pairs for a total area of 1495 m2. These estimates are based on multi-junction photovoltaic cells of 24% efficiency, an annual degradation of 2.75%, and a worst case seasonal sun angle of 24 degrees off normal (equatorial orbit). The eclipse times for the LEO and MEO platforms are 0.6 hr and 1.48 hr, respectively. These values are taken from the Satellite Took Kit (STK) software and represent worst-case eclipse times for a "typical" mission scenario.

Table 4-2 presents some of the power generation systems considered for this study. A brief description of some of the systems is presented below.

TABLE 4-2. POWER GENERATION OPTIONS

TECHNOLOGY PARAMETER	SD (STIR.)	SD (BRAY.)	PV (SI)	PV (GAs)	MULTI JUNCTION	CPV	TPV
MATURITY (YEAR)	1999	1998	1960	1980	1998	1998	2000
FLIGHT HISTORY	NONE	NONE	LOTS	SOME	NONE	NONE	NONE
MASS (Kg/KW)	46	46	10-20	8-16	6-12	32	54
ENERGY STORAGE	YES	YES	NO	NO	NO	NO	YES
EFFICIENCY	25%	25%	12%	17%	23%	25%	25%
DISTURBANCE POTENTIAL	SOME	SOME	NONE	NONE	NONE	NONE	NONE
COST (00 $'s/KW)	$52,000	$60,000	$240,000	$280,000	$320,000	$40000	$44,000
FRONTAL AREA (M ²/KW)	3.6 M²	3.6 M²	12-24 M²	8-16 M²	6-12 M²	3.6M²	3.6 M²
ROBUSTNESS	> 10 Years	> 10 Years	> 10 Years	> 10 Years	> 10 Years	> 10 Years	> 10 Years
SCALE ECONOMIES	MED.	MED.	HIGH	HIGH	MED.	MED.	MED.

Silicon solar arrays are the cheapest available at present, but silicon also has the highest degradation percentage (about 3.75% per year) of all available materials. Silicon solar array efficiency has held constant at about 14% since the early 1980's, but new high-efficiency silicon materials are being tested. Scientists anticipate an increase in efficiency to about 18% by the next decade through use of these new materials.

Gallium-arsenide arrays are more expensive than silicon, but have a lower degradation percentage (about 2.75% per year). GaAs arrays were invented in the early 1980's with an efficiency of about 16%. This efficiency has steadily increased since then. Scientists believe there is a high potential for GaAs arrays within the next decade.

Multi-junction arrays have a higher efficiency than GaAs arrays, offering 21-22% efficiency at present. The degradation percentage is 2.75%, since they are made of the same material as GaAs arrays.

Indium phosphide arrays offer about 19% efficiency at present, but have a high cost, which outweighs the increased efficiency. Indium phosphide is the most expensive material available. Scientists have experimented with less expensive strains of indium phosphide, but in the process of lowering the cost, the efficiency has dropped back to 12-13%.

AMTEC, or Alkali Metal Thermal to Electric Converter, is a new material being tested for use in solar arrays. The alkali metal used in the process is sodium. High temperatures (1100 K) are used to vaporize the sodium, then high pressure pushes the sodium vapor through the BASE (beta-alumina-sodium-electrolyte), leaving the electrons behind. This leaves the electrons on one side and the protons on the other side, creating a battery. AMTEC has reached about 19% efficiency in the labs and is predicted to reach at least 30% (possibly 35%) within the next decade. Because of a degradation percentage very near 0%, AMTEC has a very promising future on Earth and in space. This due is mainly to the system being composed primarily of steel and sodium. Its cost is comparable to that of gallium arsenide and multi-junction arrays.

Terrestrial solar cells were investigated for this study but were rejected due to the anticipated price decrease for space-qualified solar cells in the near future. Prices are expected to decrease considerably due to the large increase in solar cell production needed to meet commercial demands.

Figure 4-1 presents an historic perspective of the solar-based power generation systems. As can be concluded from the curves, there has been considerable increase in the performance of the various elements over that last 20 years. Projections to 2005/10 are based on vendors' input and represent conservative estimates. In some cases, the higher efficiencies are currently being demonstrated in laboratory tests and can be reasonably expected to mature into space-qualified systems.
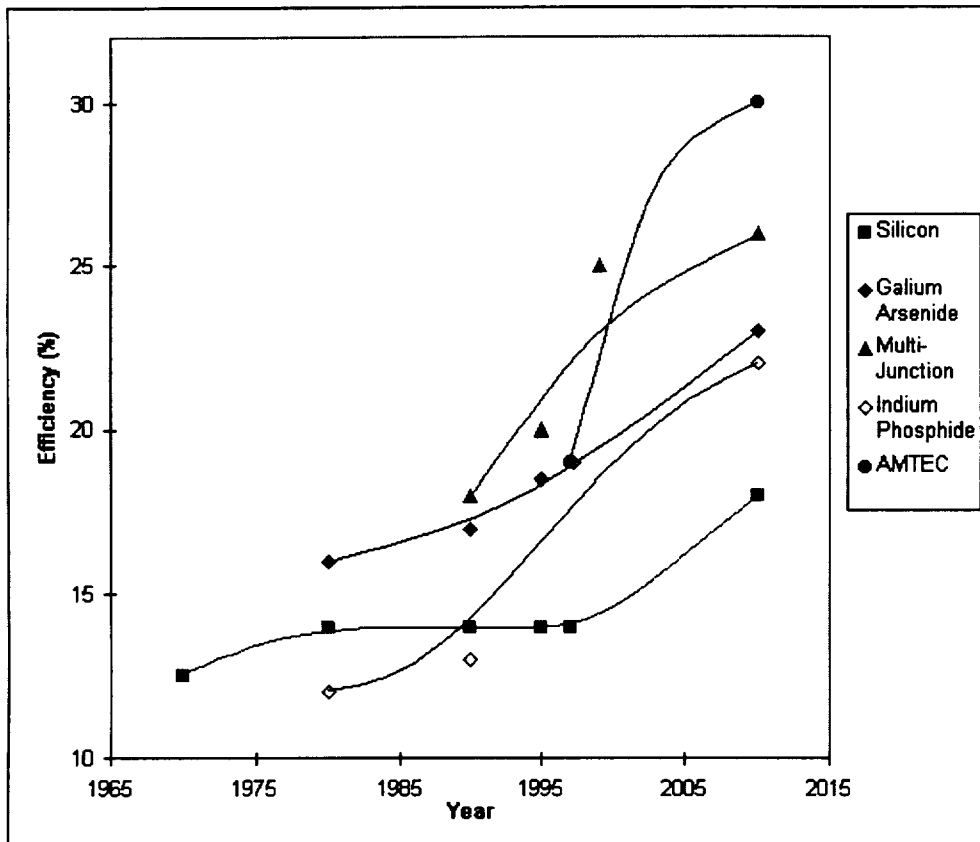
FIGURE 4-1. TRENDS IN POWER GENERATION EFFICIENCIES

4.3.4 Power Storage

A number of cycle life tests are currently being performed on Ni-H$_2$ batteries. Cycle life tests on the order of 50,000 cycles at 60% depth of discharge (DOD) have been performed for simulated LEO conditions. Based on this information, a DOD of 70% is assumed available by 2010 and is used for the battery sizing calculations reported below. A specific energy of 60 Whr/kg was assumed for all calculations. One 50 Ahr Ni-H2 battery, weighing approximately 25 kg, can satisfy power storage requirements for the PLCRA. It is important to note that the PLCRA storage requirements were calculated based on the orbit parameters for the LEO platform. This represents worst-case values for required cycle life, orbit period, and eclipse duration.

The LEO and MEO platforms require considerably larger power storage. A total of 1476 kg of batteries (equivalent to approximately 64 batteries similar to the one used for the PLCRA) is required for the LEO platform. Due to the higher power requirements of the MEO platform, approximately 5912 kg of batteries is required. This is equivalent to 253 of the PLCRA batteries. Significant weight savings could be seen if a storage system with a higher specific energy is used. Another possible option for energy storage is to use flywheels, which are currently being planned for first use in space around 2002. Based on ground test data, a mass density of 9.6 kg/kW for flywheels (vs. 53 kg/kW for Ni-H$_2$ batteries) is anticipated with a depth of discharge of approximately 60% by 2000. Super capacitors being developed by Auburn University were also examined as another possible storage system.

Another option for power storage is to utilize the kinetic energy in the rotation of the tether facilities, which is on the order of megawatts. Power would be put into the system by reeling in the tether. This increases the rotation rate, and therefore the kinetic energy of the system. The power would then be extracted by allowing the tether to reel out, with the reel motor acting as a generator. Practical limitations to this technique would include limits on the rotation rate to avoid over-stressing the structure and/or tether, as well as the overall dynamics of the tether system. Table 4-3 presents a comparison of the power storage systems that were considered in this study.

TABLE 4-3. ENERGY STORAGE OPTIONS

PARAMETER \ TECHNOLOGY	FLYWHEEL	NIH$_2$	NICd	NIMH	LI ION	Reel Generator
MATURITY (YEAR)	2000	1980	1970	TBD	TBD	TBD
FLIGHT HISTORY	NONE	LOTS	LOTS	NONE	NONE	NONE
MASS (Kg/KW)	9.6	53.2	374	53.2	37.6	TBD
VOLUME (M³/KW)	0.028	0.08	0.14	0.04	0.04	TBD
DEPTH OF DISCHARGE	60%	50%	8%	20%	50%	TBD
COST (00 $'s) / 40 AH	$300,000	$300,000	$300,000	N/A	N/A	TBD
SYSTEM ENG. DENSITY	72+ WH/Kg	60 WH/Kg	30 WH/Kg	14 WH/Kg	80-120 WH/Kg	TBD
ROBUSTNESS	>10 YEARS	>10 YEARS	10 YEARS ?	TBD	TBD	TBD
SCALE ECONOMIES	HIGH	MED.	MED.	HIGH	HIGH	TBD

4.4 COMMUNICATIONS

4.4.1 Communication Key Design Requirements and Drivers

The major driver for the communications system is the overall system performance. This requires that accurate position information be exchanged over the entire orbit. The communication system will also most likely function as the beacon to allow the use of

differential GPS. Besides the need to exchange position and attitude information there is the standard requirements to provide periodic health and status information. While no specific requirements were identified, it is expected that some part of an auxiliary payload onboard will require use of the communication bandwidth. This will occur on a "as available" basis and will not be a design driver. Communication between the PAV, the PLCRA, and the tether platform will exist for both stages. Besides inter-element communication, each element must communicate with the ground. To obtain communication over the entire orbit will require the use of a Telemetry Data Relay Satellite System (TDRSS) like system. For periods of direct Field of View (FOV) the communication will be direct between the elements.

The PAV will emit a continuous RF beacon that can be used in conjunction with the 2010 version of the GPS constellation to produce a differential GPS. This type of differential GPS is being developed for Automated Rendezvous and Capture.

The maximum data exchange will be during capture and release events where direct FOV exists, ensuring relatively high link margins. Non-operational phases will require much lower data rates to exchange housekeeping, diagnostics, and maintenance data. Inter-element traffic rates are estimated to be no greater than 10 mbps peak, which is well within current technology.

Although the spectrum has not yet been established, optical links could be used since the majority of the high data rate phases are performed while in direct line-of-sight, but RF links will be adequate. Current developments in space-based optical links are progressing rapidly with near term commercial applications being planned for some commercial programs.

4.4.2 Communication - Reference Design Major Features

Figure 4-2 presents a schematic of the system showing the various links required. The links will form a network that allows multiple paths to be used to ensure data transfer. These links can also be used to support position and attitude determination.

The ground links will operate at near real time but will not require ground intervention to complete a capture or release event. The function of the ground station will be to monitor the LEO and MEO tether systems, make go/no-go determination prior to a payload release, and support contingency activities if required. The actual capture and release activities progress too fast for ground functions to support the events real-time.

Multiple antennae on each element will be installed to provide the required reliability as well as ensure that communications can occur at any phase of the orbit. For this report, current-technology RF hardware has been selected for sizing activities. Due to the large amount of ongoing commercial investment, there is now considerable expansion in the arena of RF antennae and this issue should be revisited for future studies.

4.4.3 Summary

Clearly, a communication system is required to meet the mission objectives. The communications systems will provide for the exchange of position and attitude information. In addition, it well function as a beacon for use as a part of a differential GPS. No major technology design drivers in the communications area were identified. All of the communications requirements can be meet with current hardware and software.
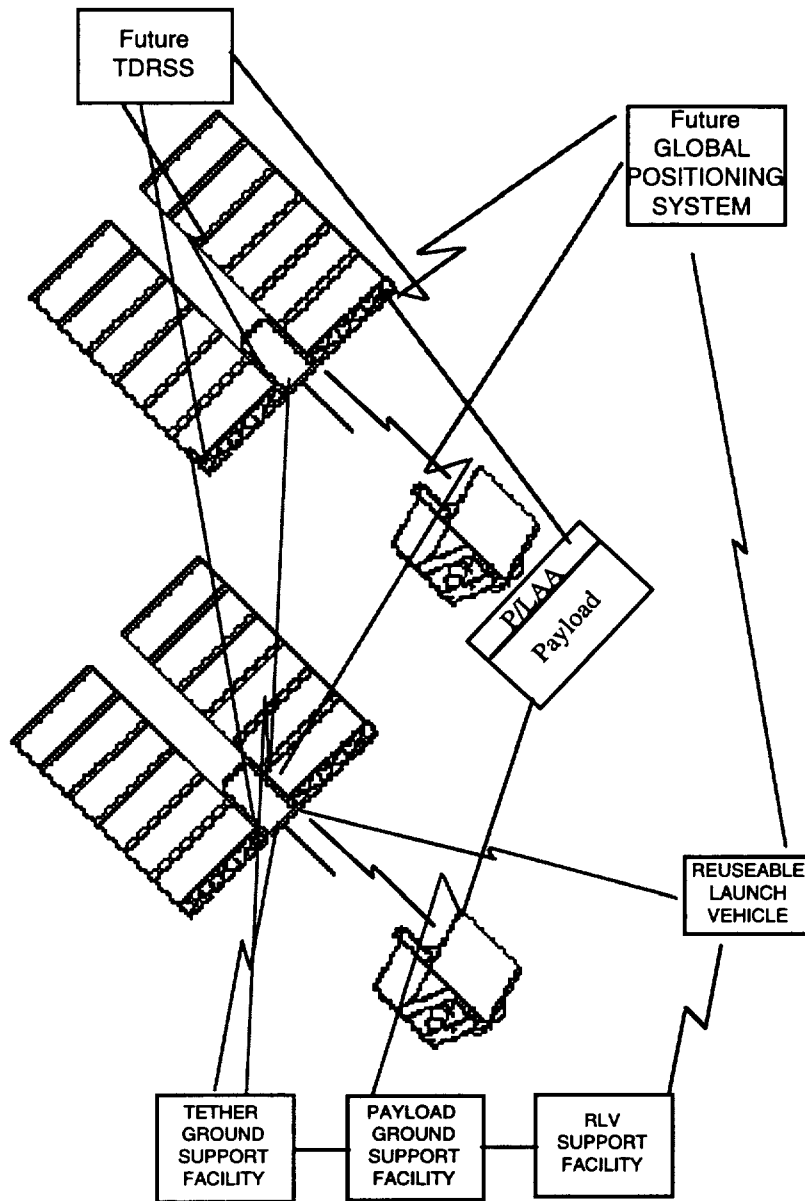
FIGURE 4-2. SYSTEM SCHEMATIC SHOWING VARIOUS REQUIRED LINKS

4.5 COMMAND AND DATA HANDLING

4.5.1 Introduction

The Command and Data Handling (C&DH) subsystem will perform three main functions: computing, data storage, and data routing. As Figure 4-3 demonstrates, the C&DH subsystem will interface with each of the other subsystems. As each subsystem gathers information, data is sent to the C&DH subsystem. C&DH then processes the data, determines which subsystems are affected by the data, and sends commands to those subsystems as necessary.
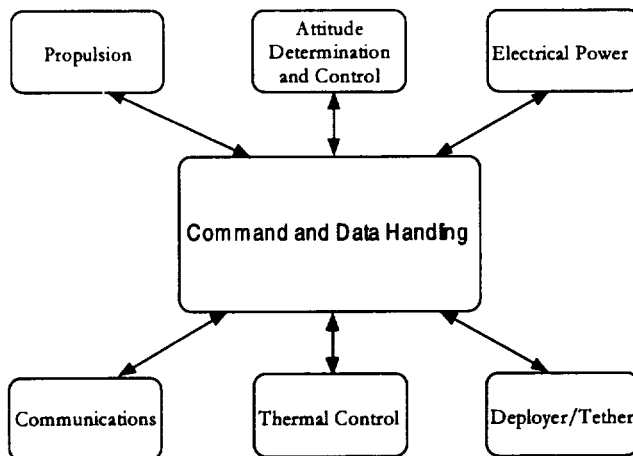
FIGURE 4-3. C&DH SUBSYSTEM INTERACTION

4.5.2 Computing

As Figure 4-4 suggests, the C&DH subsystem will be made up of a number of CPU's. The MEO and LEO platform computers will control command and telemetry processing, attitude sensor processing, location determination, complex autonomy, fault detection, power management, thermal control, and deployer/reel control. The PLCRA computers will control the same functions as the platform computers along with payload-rendezvous data processing and beacon data processing. The PAV computer will control the same functions as the platform computers except for the deployer/reel control. However, for the PAV, less processing complexity is necessary. The PLCRA and PAV computers will be local to the PLCRA and PAV, respectively.
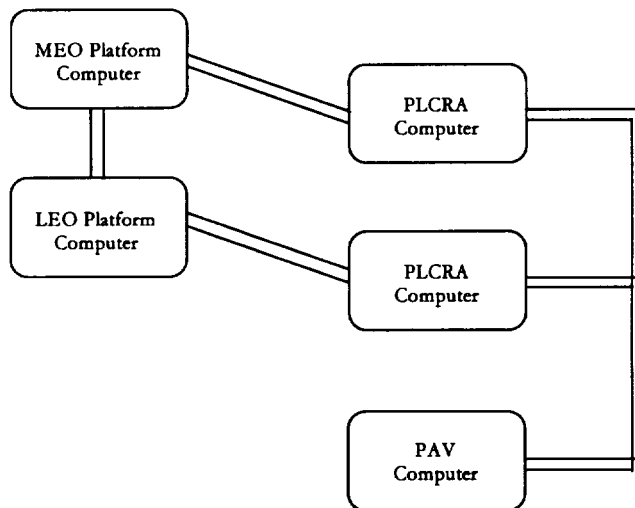
FIGURE 4-4. C&DH COMPUTER SYSTEM

Table 4-4 lists typical throughput values for on-board applications of a bus computer. These typical values, taken from Space Mission Analysis and Design [13], are based on a 1750A architecture and 16-bit words. The table further lists an engineering estimate of the expected throughput values for the tether platform and PLCRA computers based on the typical throughput values.

TABLE 4-4. TYPICAL THROUGHPUT VALUES

	Typical Throughput (KIPS)	Expected Tether Throughput (KIPS)
Communications		
Command Processing	7.0	28.0
Telemetry Processing	3.0	12.0
Attitude Sensor Processing		
Rate Gyro	9.0	18.0
Sun Sensor	1.0	2.0
Earth Sensor	12.0	24.0
Magnetometer	1.0	2.0
Star Tracker	2.0	4.0
Attitude Determination & Control		
Kinematic Integration	15.0	15.0
Error Determination	12.0	36.0
Precession Control	30.0	60.0
Magnetic Control	1.0	1.0
Thruster Control	1.2	2.4
Reaction Wheel Control	5.0	5.0
Ephemeris Propagation	2.0	8.0
Complex Ephemeris	4.0	8.0
Orbit Propagation	20.0	80.0
Autonomy		
Complex Autonomy	20.0	40.0
Fault Detection		
Monitors	15.0	15.0
Fault Correction	5.0	10.0
Other Functions		
Power Management	5.0	5.0
Thermal Control	3.0	3.0
Kalman Filter	80.0	160.0

Because the platform computers perform the most complex data manipulation, the most powerful processor is needed here; however, the necessary complexity does not exceed the standard processor capabilities expected within the next few years. Furthermore, it would be financially wise to use the same processors for both the platform and PLCRA computers as the difference in complexity between the two is small (the PAV computer requires a less powerful processor.) With the high rate of increase in processor capability, it is expected that standard off-the-shelf processors of the future will meet the needs of the platform, PLCRA, and PAV computers.

4.5.3 Data Storage

In the past, magnetic tapes have been used for data storage in satellite systems. Currently, solid state storage is the most common. The amount of RAM and ROM necessary is mostly driven by the needs of the Attitude Determination & Control System (ADCS). The satellite

will be able to store and retrieve data real-time. The size and specs of the storage will be based on the requirements of the ADCS. Currently, solid-state storage devices are often used and usually meet the demands of the ADCS and perform in real-time. Current standard off-the-shelf solid-state data storage devices will meet the requirements of the platform, PLCRA, and PAV computers.

4.5.4 Data Routing

Current protocols widely used for data routing include MIL STD 1553, MIL STD 1773, & VME. The MIL STD 1553 and MIL STD 1773 are both serial data buses. Serial data buses have been found more efficient and more flexible than parallel data buses for long distances. It is expected that the next generation of data buses will be wireless. The amount and type of data buses necessary are dependent upon the requirements of the system. For the platform computer, the highest amount of data traffic will occur as the attitude control sensors relay their data to the processor. The most traffic for the PLCRA and PAV occurs as the sensor measurements and controls are transmitted. MIL STD 1553 is currently the best data bus for platform-to-subsystem communication because of the possible distance over which each must communicate information. Within the PLCRA and PAV, a VME bus is the best choice. MIL STD 1553 and VME buses are currently available. Wireless data buses may be standard in the future and will be acceptable substitutions.

4.6 PROPULSION

4.6.1 Introduction

The ΔV required for both LEO and MEO platform reboost after payload deployment, as well as the desired multi-year mission lifetime, drive the propulsion system requirements to high specific impulse (Isp) systems (i.e. electric thrusters) to minimize the total required propellant. Typical chemical (monopropellant or bipropellant) systems offer Isp values from 150 to 450 seconds. For the proposed 30 day reboost, two-year refuel case, a system with an Isp of 450 seconds would require a total ideal propellant mass of 19,416 kg for reboost of the LEO platform and 31,957 kg for the MEO platform (based on case 6d_1.) For the LEO platform, this is more than twice the minimum platform dry mass needed to avoid reentry of the platform at the end of a two-year mission. Electric propulsion offers Isp values from 500 to 5,000 seconds, providing the opportunity for significant propellant mass savings. For a system with an Isp of 5,000 seconds only 1,845 kg of propellant are required for reboost of the LEO platform. This increase in Isp does come at a cost. Current ion thrusters have efficiencies around 70-75% (with 90% being quoted by some sources.) Assuming an Isp of 5,000 seconds and a power conversion efficiency of 90%, the power required to generate the needed thrust levels is on the order of 130 - 240 kW for the LEO and MEO platforms.

For the purpose of this study, a system with an Isp of 3,000 seconds and power conversion efficiency of 75% is assumed. These values are consistent with the performance of currently available xenon ion thrusters. Table 4-5 shows the required propellant masses, power, and total system masses for cases 5a-f, 6a-d(1-3). Cases 5a-f and 6a-d_1 are for 9,000 lb. payload, case 6d_2 for a 4,500 lb. payload, and case 6d_3 is for a 2,000 lb. payload.

As shown in Table 4-5, case 6d_1 offers the lowest propellant mass, power requirement, and total system mass for the 9000 lb. payload. The power requirements for LEO and MEO may seem excessive, but it is important to note that these values are based on today's technology. If an ion thruster with the same specific impulse of 3,000 seconds, but a higher

efficiency of 90% is used the total power required drops to 69 kW for LEO platform reboost and 120 kW for the MEO platform.

TABLE 4-5. CASE SUMMARY (CURRENT TECHNOLOGY)

Case	LEO Platform			MEO Platform			Total System* Mass (kg)
	Propellant Mass (kg)	Power Required (kW)	System* Mass (kg)	Propellant Mass (kg)	Power Required (kW)	System* Mass (kg)	
5a	4706	135.382	20603	2944	82.004	12301	32904
5b	4331	120.459	35827	3103	86.611	12727	48554
5c	4808	136.692	24351	3103	86.618	12727	37078
5d	4804	136.224	25237	3127	87.236	12751	37989
5e	4828	136.026	25262	3135	87.599	12760	38022
5f	4857	135.875	25293	3119	87.101	12743	38036
6a	2908	81.498	15403	5249	156.685	12605	28008
6b	2914	82.700	12498	4958	146.780	12134	24631
6c	2924	82.529	12508	4926	145.554	12100	24608
6d_1	2928	82.202	12512	4883	144.169	12055	24567
6d_2	1483	41.017	11007	1790	50.919	8836	19842
6d_3	663	18.147	10151	535	14.785	7528	17679

* System mass does not include payload mass

It is also of interest to note that if the same tether platforms are used to transfer smaller payloads the propellant and power requirements drop almost proportionally for the LEO platform, as shown by case 6d_2 (4500 lb. payload) and case 6d_3 (2000 lb. payload). Due to the already low propellant to platform ratio (LEO) of case 6d_1, the total mass reduction for the LEO platform is not significant. The large decrease in MEO propellant mass (and therefore system mass) is due to the significant reduction in the ΔV imparted to the payload by the MEO platform for the reduced payload masses.

4.6.2 Background

In order to more accurately predict the total propellant required for a two-year mission (24 reboost operations of the LEO and MEO facilities) an Excel spreadsheet model was built. The reboost missions were modeled by starting with the final payload transfer and working backwards in time to the first mission. The propellant required for reboost of the platform for each payload transfer was calculated using the ideal rocket equation:

$$m_p = m_f \left[\exp\left(\Delta V / g_c I_{sp} \right) - 1 \right] \tag{23}$$

Where:

m_f = final (inert) mass of the system after release of the payload (kg)

ΔV = velocity increment from orbital analysis (m/s)

g_c = gravitational constant (9.80665 m/s^2)

I_{sp} = specific impulse (s)

After calculating the required propellant for the final reboost, the sum of this propellant mass and the inert mass becomes the new inert mass for the next iteration (previous reboost

mission). This updated platform mass (dry platform mass + propellant mass) is used to calculate the new mass fraction (χ) of the system (payload mass/platform mass). The platform orbit after payload release is recalculated (this is for the previous payload transfer) using the new value for χ and the equations derived by E. Lorenzini. From this, the new reboost ΔV and the required propellant mass are determined. This process is then repeated until the desired number of reboost operations have been completed (i.e. for a two year mission, assuming a 30 day reboost, a total of 24 reboost operations are required.) The propellant for each reboost is summed to give the total mass of propellant for the two-year mission.

It is important to note that this is not the most accurate means for calculating the total propellant needed. Each payload release is a unique event due to the difference in platform mass (propellant is consumed for each reboost), requiring its own analysis to determine the correct tether length and/or spin rate of the system for proper orbit transfer of the payload. It would be more accurate to perform a detailed analysis of the entire two-year mission, taking into account these changes for each reboost calculation. It should be stated, however, that the current method of analysis is conservative. The current method of calculation uses the numbers (tether length, spin rate, etc.) calculated by E. Lorenzini for the end of life mass (minimum platform mass) required to avoid reentry of the platform after payload release. This minimum platform mass corresponds to the largest reboost ΔV, and hence the largest propellant mass. As the platform mass is increased (i.e. decreased mass ratio), in order to maintain the same ΔV imparted to the payload by the facility the spin rate and/or tether length have to decrease. This results in a decrease in the drop of the platform after payload release, which in turn corresponds to a lower reboost ΔV and lower propellant mass. Therefore, using the end of life spin rate and tether length for each reboost calculation over-predicts the total propellant mass required for the two-year mission.

No budget for orbital maintenance is included in the two-year propellant mass. The amount of propellant required for orbit maintenance, assuming worst-case scenario, is less than 10% of the total two-year propellant budget. Using numbers from STK (provided by H. Dionne), it was determined that the LEO platform spent 14% of its orbit between 400 km and 500 km altitude, 16% from 500 km to 700 km, and 10% from 700 km to 1,000 km altitude (the remaining 60% is above 1000 km.) Using worst-case values from an Earth Satellite Parameters table [13] for ΔV to maintain orbit altitude, the total propellant mass required for orbital maintenance was calculated to be less than 150 kg for a two year mission (assuming a system with an Isp of 3,000 seconds.)

Once the propellant mass is known the required thrust and power can be determined based on the orbital period, number of days for reboost, and percent of the orbit over which thrust is applied.

$$F = \dot{m}\, I_{sp}\, g_c = \left(\frac{m_{P_{tot}}}{t_{b_{tot}}} \right) I_{sp}\, g_c = \left(\frac{m_{P_{tot}}}{t_b n} \right) I_{sp}\, g_c \qquad (24)$$

Where:

$$t_{b_{tot}} = t_b * n = \text{total burn time}$$

$$t_b = (\text{percent of orbit period})\, p_{ave}$$

$$n = \text{total number of burns} = INT\left(\frac{\text{days for reboost}}{p_{ave}} \right)$$

The average orbital period (pave) is simply the average between the initial orbit of the tether facility (at time of payload release) and the final orbit of the platform after payload release. This is assumed accurate enough for this level of investigation.

Knowing the average thrust required for a given orbit, the power can be calculated from:

$$P = \frac{F\,I_{sp}\,g_c}{2\eta}$$

(25)

Where: η = conversion efficiency

Knowledge of the average thrust per reboost also permits determination of the number of a given type of electric thruster required to supply this thrust level. As with any analysis, there are a certain number of assumptions built into the calculations. Here are some of the more important ones for this study:

- thrust acts through the center of mass of the system for reboost (i.e. no torque is induced on the system)

- each period of thrust (35% of p_{ave}) is applied symmetrically about the perigee and each burn can be modeled as "impulsive".

- ΔV for orbital maintenance is negligible (as stated above.) If some estimate of orbit maintenance and ADCS propellant budget is desired, 10-15% can be added to the total propellant mass for the two year mission.

4.6.3 Parametric Analysis and Discussion

As stated above, the power required for reboost is directly proportional to the Isp of the propulsion system (linear relationship as seen in figure 4-5). Also presented here are the plots of required thrust and propellant mass versus Isp (figures 4-6 and 4-7, respectively.)
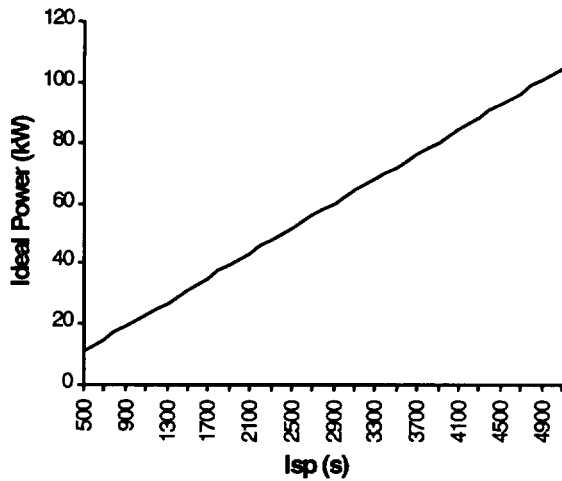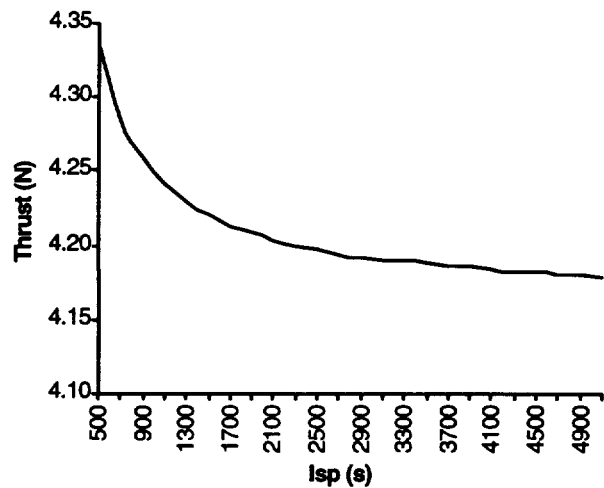
FIGURE 4-5. IDEAL POWER VS. ISP   FIGURE 4-6. MINIMUM THRUST VS. ISP
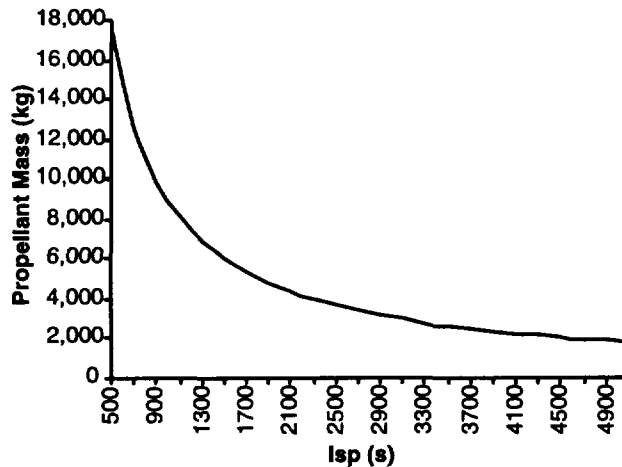
4-15

FIGURE 4-7. PROPELLANT MASS VS. ISP

As seen in figures 4-6 and 4-7, increasing the Isp has only a small effect on decreasing the required thrust, but significantly reduces the propellant required. Increasing the system Isp by an order of magnitude decreases the required propellant by an order of magnitude (but at the expense of a large increase to the power required.) This trend is not seen for the required thrust. The order of magnitude change in Isp only decreases the required thrust by less than 5%.

Some other trends that are obvious upon close examination of the equations presented above are that thrust (and therefore power) required for reboost is inversely proportional to the number of days for reboost. Doubling reboost time reduces the required thrust level by half. The same relationship is true of the percentage of the orbit over which thrust is applied.

4.6.4 Future Work

The system presented above requires thrust levels on the order of 4 - 8 N. Currently, most high Isp electric thrusters provide thrust in the mN range, however some electric thrusters are available producing 1-2 N of thrust. Additional research needs to be done on the effects of scale up on electric thrusters, namely on how this affects efficiency (specific power consumption) and specific impulse.

Materials degradation on-orbit is another area of concern. Maximum power consumption (i.e. maximum required thrust) is at the end of a two year mission when the facility is lightest. Because of this, cathode erosion (in today's ion thrusters) and degradation of photovoltaics (or whatever power system is selected) over a two year mission are issues which need to be addressed. Thruster life can be a limiting factor as well. For a typical two-year mission the thrusters will be cycled over 10,000 times.

As noted above in Section 4.6.2, a more detailed analysis combining the orbital analysis and propulsion work should be performed. This will allow a more accurate prediction of the total system mass and pave the way for optimization of the overall LEO to GEO system. Part of this effort should be concentrated on performing a detailed trade between the end-mounted versus center-mounted platform concepts. It would also permit analysis of the trade-off between the cost of a higher initial platform mass and the total propellant required over an extended period (10+ years) of time.

Advances in on-orbit power generation are needed. Due to the large power requirements during reboost of the tether facilities (~120 kW), any increase in the efficiency of solar to electric conversion (photovoltaics, solar dynamic, etc.) will result in a significant weight savings for both tether facilities.

Electrodynamic tethers have the potential to provide reboost capability for both LEO and MEO platforms, with little to no propellant consumption. Preliminary calculations indicate that reboost of the LEO platform with an electrodynamic tether can be achieved for roughly the same available power required for reboost using ion thrusters.

4.6.5 Summary

From a propulsion standpoint, orbit transfer of a 9,000 lb. payload from LEO to GEO using a two-stage tether platform system is feasible assuming a two year refuel. The total propellant mass for a two-year mission can be significantly reduced by going to higher Isp thrusters, if the power requirements can be met. Further investigation into the orbit mechanics of the two-stage system could yield a solution where the LEO and MEO platforms are nearly identical.

4.7 THERMAL CONTROL

4.7.1 Thermal Control–Key Design Requirements and Drivers

The Tether Platform, the PAV, and the PLCRA are the main elements requiring thermal control. Each element's thermal control will maintain its subsystem and tether hardware within their temperature limits and protect the hardware from extremes of the thermal cycles induced by alternating sun and deep space exposure. The thermal control will also reject waste heat from active components.

The goal is to maintain the temperature of sensitive equipment within allowable limits. In general, the electronics base temperatures are limited to typical temperature limits (range of 32°F to 140°F). A major requirement is to control structural thermal gradients for the 10 or more year lifetime. Excessive thermal gradients over a long period can cause materials to fail. Therefore, this must be considered due to the addition of the on-orbit structural loads introduced during the payload capture and release events, as well as the presence of significant centrifugal loading during the entire mission life.

4.7.2 Thermal Control - Reference Design Major Features

A passive thermal control system was selected for the baseline design. This represented the minimum power demand, very low development risk, the lowest cost and the most flexibility. The primary heat rejection path, via radiation, is from the side panels to space. The effective surface area for heat rejection for each element is listed below in Table 4-6. Surface temperatures can be controlled using surface optical properties without the use of louvers or variable emissive surface treatments. A mix of white paint (a/e =0.25 / 0.9) and Second Surface Mirror (SSM) (a/e =0.1 / 0.8) surface treatments can be used to maintain the expected temperature range requirements.

The electronics are "heat sinked" to surface panels or to structural components that have good thermal contact to the surface panels. This allows designers to custom-design to the heat rejection requirements of each of the major subsystems. Sufficient heat rejection

margin exists to "cold bias" the system allowing the fine-tuning of individual Line Replaceable Units (LRU) using heater strips.

TABLE 4-6. EFFECTIVE HEAT REJECTION SURFACE AREA

Element	Surface Area (m²)
Tether Platform	105.6
PLCRA	9.5
PAV	5.7

The use of active thermal control was considered. No specific need for heat pipes as a means of thermal control was identified in this preliminary study. Active thermal control using fluids such as ammonia or water represents additional complexity over traditional approaches due to the artificial gravity. Obviously, a pure passive system is highly desirable; therefore, a preliminary analysis of a passive thermal control system was conducted.

4.7.3 Thermal Control - Preliminary Analysis

A preliminary, conservative analysis shows adequate margin for the subsystems to use pure passive thermal control methods for all elements but the PVA. This assumes that adequate conduction paths can be developed for all of the subsystems' hardware and that no time phasing of heat loads occurs. The later assumption is very conservative since in most cases the battery system or power distribution system is not sized to allow simultaneous use of all hardware. The tether reel assembly thermal design may require limiting the cycle times and/or rate of motion in order to ensure passive limits can be maintained. Additional studies will be required to validate this once the design matures.

A conservative assumption of required rejected heat equaling the required power was made for the preliminary thermal analysis of each element. Most of the Tether Platform's subsystem hardware is mounted within the truss structures that should provide a sufficient heat rejection path to space. The thrusters mounted on the ends of the Platform were assumed to be the major heat contributors. The thrusters have an efficiency of 75%; the remaining 25% of the required power was assumed to be the Tether Platform's required heat rejection. Table 4-7 provides a summary of the required heat dissipation for each element.

TABLE 4-7. ELEMENT HEAT DISSIPATION SUMMARY

Element	Heat Dissipation (Watts)
Tether Platform (re-boost/ peak)	13700 / 27400
Payload Capture and Release	1380
Payload Adapter Vehicle	1342

The design cases assumed a tether system in either the re-boost or the peak states. Figures 4-8 through 4-10 present the pure passive cooling assessments for all three elements. External surface temperatures will be less for the rotating state of both platforms and the PLCRA. The effective radiative sink temperatures presented below are for a surface directly exposed to the sun at steady state. The actual radiative surface temperature will be less than 0°F for the rotating cases. The MEO platforms will be colder due to the higher altitude with less earth albedo and a greater view of deep space.
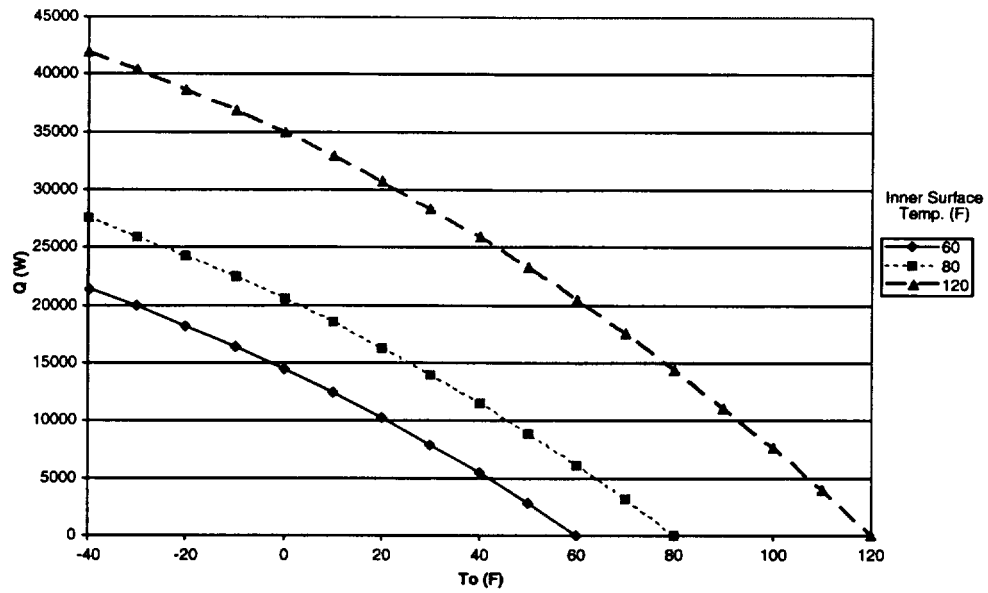
4-18

FIGURE 4-8. PLATFORM HEAT REJECTION VS. FULL SUN RADIATIVE HEAT SINK

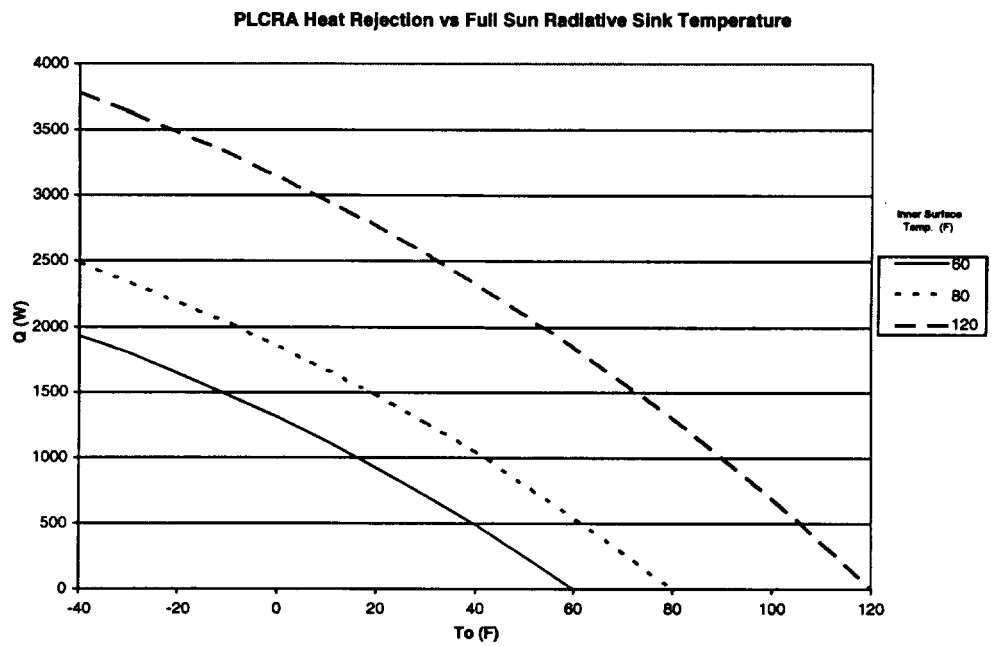PLCRA Heat Rejection vs Full Sun Radiative Sink Temperature

FIGURE 4-9. PLCRA HEAT REJECTION VS. FULL SUN RADIATIVE SINK
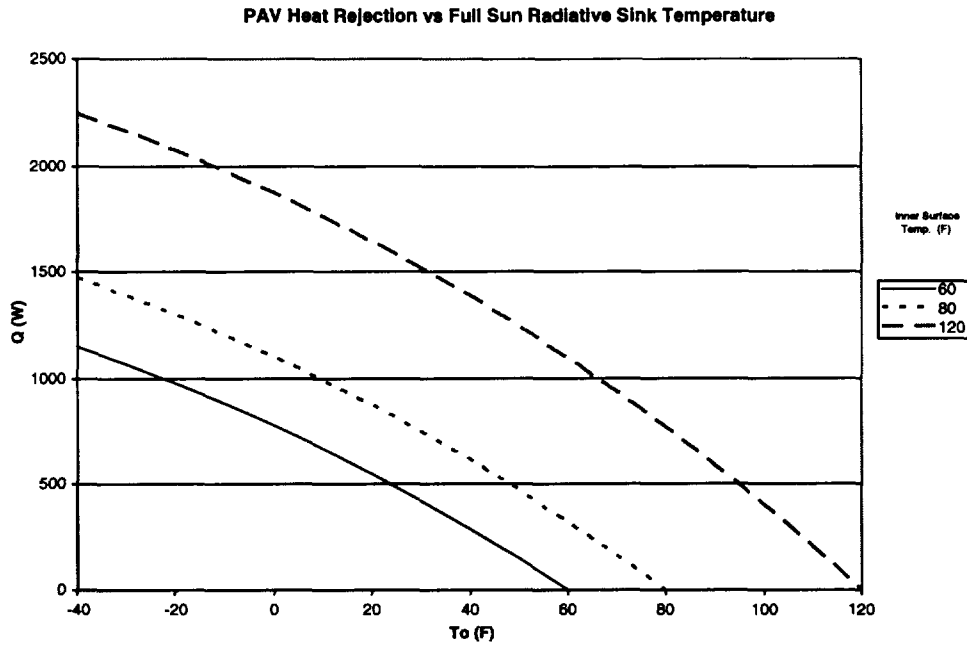TEMPERATURE

FIGURE 4-10. PAV HEAT REJECTION VS. FULL SUN RADIATIVE SINK TEMPERATURE

This simple analysis used the effective radiative sink temperature to bracket the worst-case heat rejection capabilities. Three average surface temperature curves were computed for 60, 80 and 120 °F, consistent with a maximum LRU baseplate of 140 °F. This assumes that the design will provide for sufficient conduction to the surface to reject the required heat. Experience indicates that if we maintain the surface temperatures less than 120 °F it is possible to design a structure that will conduct the heat to the surface and maintain the required junction temperature limits. Obviously, if the baseplate temperatures are more restrictive, colder surface temperatures will be required. Local hot spots were not considered for this phase of the design.

The surface optical properties must be controlled to provide the required heat rejection and minimize the solar absorption. The curves provide a reference point for two typical spacecraft optical properties using Second Surface Mirrors (SSM) and white paint such as Chemglaze. If the worst case optical properties for white paint (10 years of degradation) are considered, the radiative temperature will increase to 102 °F for these steady state cases. Therefore, the radiative surfaces will need to be maintained somewhere between the new white paint surfaces and the SSM.

A reasonable heat rejection of 27,400 watts can be achieved for the primary platform depending on optical property mix. The PLCRA can also be maintained passively. The PAV represents more of a challenge, but simple time phasing of the loads will reduce the effective heat load to a range that can be maintained passively.

The thermal control physical provisions for all three elements are limited to surface treatments and heater strips, where required. Selective application of surface treatments will be made to achieve the desired thermal result. The design will consider the 10 year (or more) lifetime to ensure that optical property degradation will not adversely impact the performance of the system. There are several mechanisms to obtain the required surface properties over the lifetime of the system including robust surface treatments, louvers to vary

exposed surface areas, or surfaces with variable emissivity that can be controlled electronically. Surface optical property selection and the flight elements' surface treatment distributions will be based on location of the heat sources and the requirements of the surfaces. These include surface materials selection (life), compatibility with UV exposure and tolerance, and Atomic Oxygen exposure and tolerance. Proper thermal balancing can minimize the application of heater strips, which would be provided more for contingency usage than for standard operations.

The electronics layout will be managed to ensure optimal placement of hardware to distribute heat loads between the external panels. This will be easier for the platforms than for the other elements because of their large surface area available within the truss structures. Optimum electronics placement for the PRCRA and PVA will require more effort but are well within the current experience base.

The typical thermal control system design relies heavily on analysis using proven tools and techniques. This allows the developer to limit the amount of thermal vacuum testing required. For example, thermal vacuum testing on the initially developed payload adapter vehicle (PAV) will be expected but will not be repeated after the design and the processes are validated. Integrated thermal models will assess the system response to the full range of heat loads and to orbital environmental extremes including:
- Full sun conditions
- Transient cold conditions in earth shadow
- Tolerance to contingency conditions will be assessed in accordance with FMEA process
- Heater power loss
- Heater failure
- "Unusual" attitudes

4.7.4 Summary

The selected reference thermal design represents a low cost technical solution based on proven spacecraft design approaches. There is some risk inherent in relying on passive mechanisms, but our preliminary analyses indicate that sufficient surface areas exist for all elements but the PAV for the worst case internal heat loads. The PAV can be accommodated by time phasing the heat loads and could actually use the payload (which is inactive during these phases of the mission) as a heat sink. No new technology requirements were identified.

Section 5

CONFIGURATIONS

5.1 SYSTEM CONFIGURATION OVERVIEW

The flight segment of the Tether Transfer System (case 6d) consists of the LEO facility with 60 km tether, the MEO facility with 80 km tether, and the Payload Adapter Vehicle (PAV). Two general LEO/MEO facility configurations are shown in Figure 5-1. Both the LEO and MEO facilities consist of one or more tethers, a Payload Capture and Release System, and a platform with power generation and storage, tether control subsystems, and reboost propulsion. The platform can be mounted on the end or at the center of mass (CM) of the facility. The PAV provides an interface between payloads and the Payload Capture and Release System and provides final circularization ΔV to the payload. Each facility captures the payload, releases it at the appropriate point, and then reboosts itself to its nominal operational orbit for the next mission. Due to its unique functions, the PAV stays with each payload; therefore, a new PAV is required for each mission.
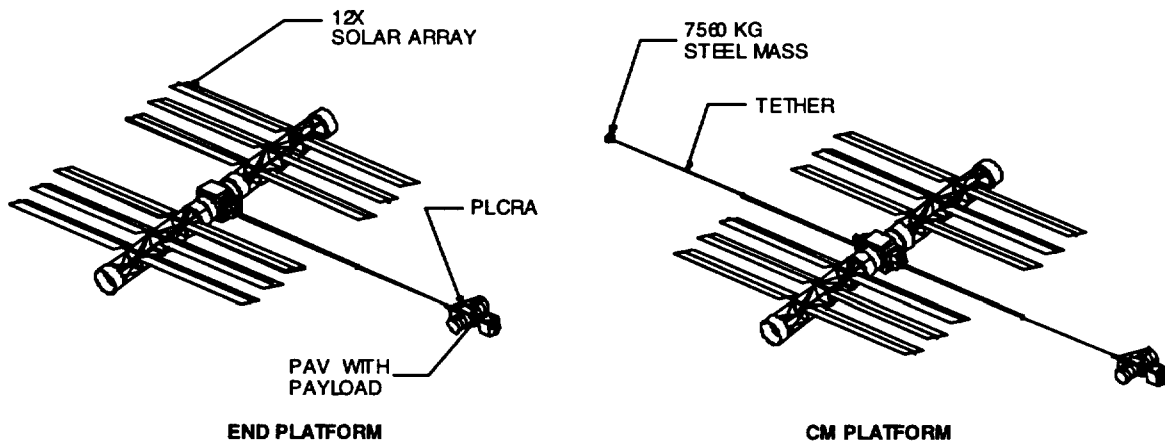
FIGURE 5-1. TETHER TRANSPORT SYSTEM CONFIGURATIONS

5.2 PAYLOAD ADAPTER VEHICLE

5.2.1 Design Drivers

The requirements that drove the design of the Payload Adapter Vehicle (PAV) included the following:
- Launch vehicle/payload interface
- Payload/facility interface
- Payload maneuverability
- Final circularization ΔV

The payload needs to interface with the launch vehicle and the LEO/MEO facilities' Payload Capture and Release Systems. The payload should have its own subsystems to maneuver itself and aid payload capture. The payload also requires propulsion, guidance/ navigation, power storage, and communication subsystems to be propelled from GTO to GEO after being hurled from the MEO facility (final circularization ΔV needed).

5-1

5.2.2 Subsystems and Parameters

The PAV, shown in Figure 5-2, provides the interfaces between both the launch vehicle and the tether facilities. The PAV will mimic the interfaces of current upper stages to both the payload and the launch vehicles in order to be transparent to the users of the system. The PAV will also provide the final circularization ΔV for the payload and therefore will have the fuel load, thrusters, guidance and control, and other subsystems of an autonomous spacecraft. This will enable the PAV to perform much of the terminal maneuvering leading up to capture.

The PAV is envisioned to consist of a structural ring connecting the launch vehicle to the payload. This structural ring will contain deployable grapple systems for capture by the tether facilities, fuel tank and propulsion components, reaction wheels, primary batteries, and the computer and communication system. Rendezvous beacons and antennae would be mounted to the outside of the cylinder and attitude control thrusters would penetrate the cylinder. Additional aft-facing thrusters would be provided for the circularization burn.

SCALE: 1/60
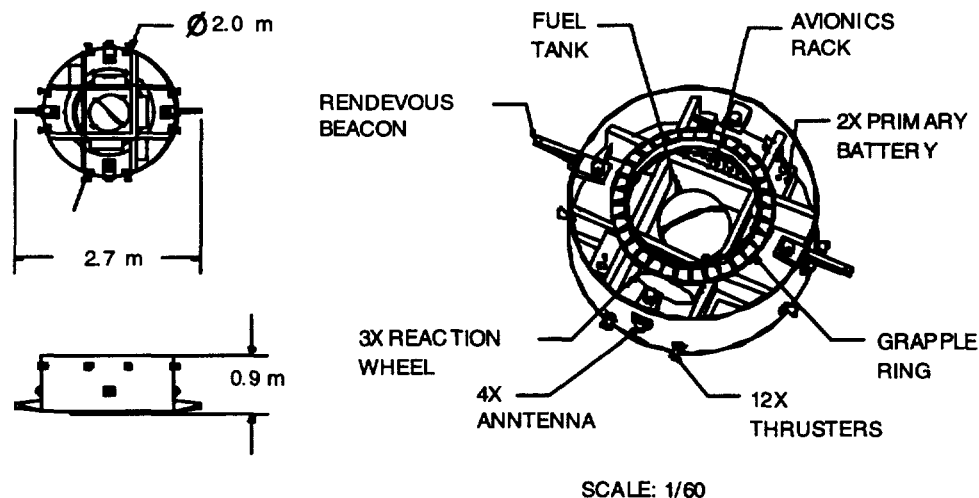
FIGURE 5-2. PAYLOAD ADAPTER VEHICLE

5.3 PAYLOAD CAPTURE/RELEASE ASSEMBLY

5.3.1 Design Drivers

The requirements that drove the design of the Payload Capture/Release Assembly (PLCRA) included:
- Facility rotation
- Payload capture transient loads
- PAV capture scenarios
- Payload mass

The constant rotation of the facility drives the design due to the constant load and the continuously changing sun angle on the solar arrays. Transient loads at capture and release and during acceleration of the payload to the facility spin rate are also significant design conditions.

PAYLOAD CAPTURE/
RELEASE ASSEMBLY
(PLCRA)

TRAPEZE

PAYLOAD
ADAPTER
VEHICLE (PAV)

INTELSAT-7
CLASS PAYLOAD
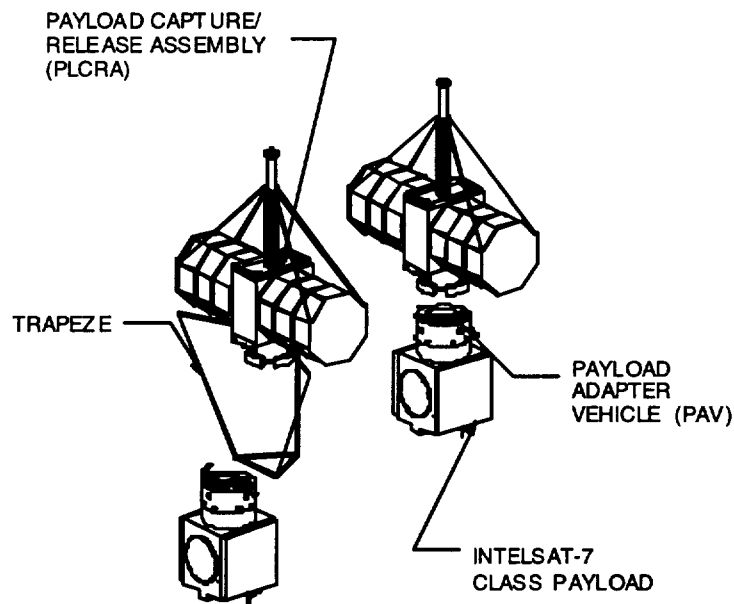
TRAPEZE CAPTURE   DIRECT RENDEVOUS

FIGURE 5-3. CAPTURE METHODS

Capture and release methods for the PAV are another major design driver. Two extreme scenarios are shown in Figure 5-3. The one scenario of flying the payload directly to a hard dock is mechanically simpler but levies very tight requirements on rate and attitude control, as well as position and velocity control (measured in centimeters). The other scenario would deploy a trapeze (larger than the PAV's uncertainty box) and guides. The trapeze and the PAV work together to accomplish a soft dock followed by reeling in the trapeze to a hard grapple. The final design approach selected will likely be between these extremes.

5.3.2 Subsystems and Parameters

A PLCRA will be located at one end of each tether facility. It will consist of
- a capture and grapple mechanism
- a structural tether interface
- a communication and tracking subsystem (for PAV rendezvous and capture)
- attitude control sufficient to maintain alignment for capture
- power generation and storage to accomplish these functions

The PLCRA communication and tracking subsystem will work with the incoming PAV during rendezvous and capture. It will contain attitude control sufficient to maintain alignment for capture and power generation and storage to accomplish these functions. Interfaces to the platform would be limited to communications and the tether itself.

The PLCRA configuration, shown in Figure 5-4, consists of a conical structure which flares from the tether attachment to the Marmann-clamp style grapple ring. Shelves surrounding the central cone provide mounting for subsystem equipment and the barrel-style solar arrays. A deployable boom extends from the top of the cone to inhibit wrapping of the tether around the PLCRA. The boom also serves as a kingpost to brace the solar arrays against the transient loads resulting from payload capture. The functional and load requirements on

5-3

the PLCRA identified thus far for the LEO and MEO facilities are similar enough that the same design would suffice for both..
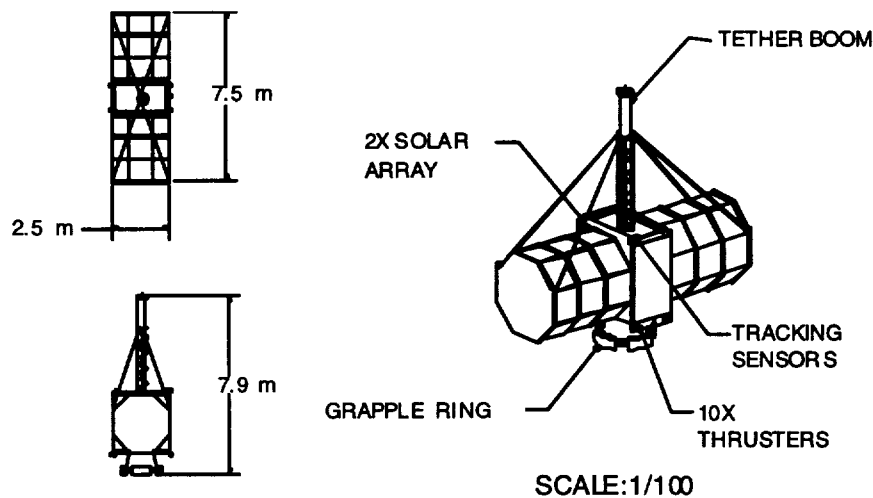

FIGURE 5-4. PAYLOAD CAPTURE/RELEASE SYSTEM

The barrel configuration for the PLCRA solar arrays was selected for simplicity and rigidity. The arrays are small enough that the added area would not be prohibitively heavy or expensive. This is particularly true when compared to the cost of constantly rotating planar arrays robust enough to withstand capture and release transient loads. The steady state load due to rotation is a function of desired ΔV and tether length. Early in the study, a 20 km tether was assumed, which resulted in steady state loads of the order of 9 G. The current configuration, however, provides a more benign 1.26 G for LEO and 0.8 G for MEO. Further studies should address overall natural frequency requirements to ensure that the PLCRA does not interact with any tether modes

5.4 PLATFORM

5.4.1 Design Drivers

The platform design drivers included
- Reboost requirements
- Facility rotation
- Tether dynamics
- Refueling and servicing
- Assembly

Reboost requirements and operations will drive the design. After each payload deployment, the facility's orbit will drop, and will have to be propulsively raised to the required deployment orbit. Electric propulsion will be used, since pure chemical systems become too massive, so the power requirements are driven by reboost as well. The constant rotation of the facility results in continuously changing sun angles, which impact power generation, and constant load on the platform and its appendages. The platform must be designed to ensure that its natural frequencies and modes do not interact with the tether, and must be arranged to prevent fouling the tether both during normal operation and in case of a tether break. Design of the facilities must consider servicing, given the ten-year life and the replacement cost. Furthermore, the fuel required for reboost during the facilities' lifetime may outweigh

the platforms and make periodic refueling a requirement. The mass and dimensions of the LEO and MEO platforms will require multiple launches and on-orbit assembly. This in turn requires breaking the platforms up into launch packages, and ensuring that appropriate subsystems are distributed among the launch packages so that the partially assembled platforms can maintain their orbits and control their attitudes during the assembly process.

5.4.2 Subsystems and Parameters

The Platform segment of each facility will provide tether control, facility rotation control, and facility reboost after each payload deployment cycle. Additionally the platforms will be capable of recovery to a safe or operational mode in case of a tether break. The platforms will provide servicing and refueling interfaces, but will only interface to the payloads via the tether and PLCRA.

A fuel load of 2928 kg will provide 2 years of reboost propellant for the LEO facility, while 4883 kg will suffice for the MEO facility. The LEO facility will require average orbital power of 82.2 kW, while the MEO facility will require 144.1 kW. The required average orbital power drove the platform solar array configuration to planar arrays, as the barrel arrays become prohibitively heavy and expensive.

To maintain optimum solar array alignment, simplify reboost operations, and mitigate docking complexity, a two-part platform design is recommended. The platform consists of a despun axle supporting the solar arrays and containing the propulsion tankage and thrusters with a rotating bearing structure surrounding the axle, to which the tether reels are mounted. Power to the reels is transferred via slip ring, and spin motors maintain a positive rate to control orientation of the platform axle. The facility extends symmetrically to either side of the tether plane to stay clear of the tether. Spare tether reels are provided for recovery in the case of a tether failure. A spare PLRCA would be pre integrated for immediate deployment as soon as a failure is detected.

The platform may be located at the end of the tether (Figure 5-5) or at the CM of the system (Figure 5-6). Table 5-1 summarizes some pros and cons of mounting the platform at the end and the CM of the facility.
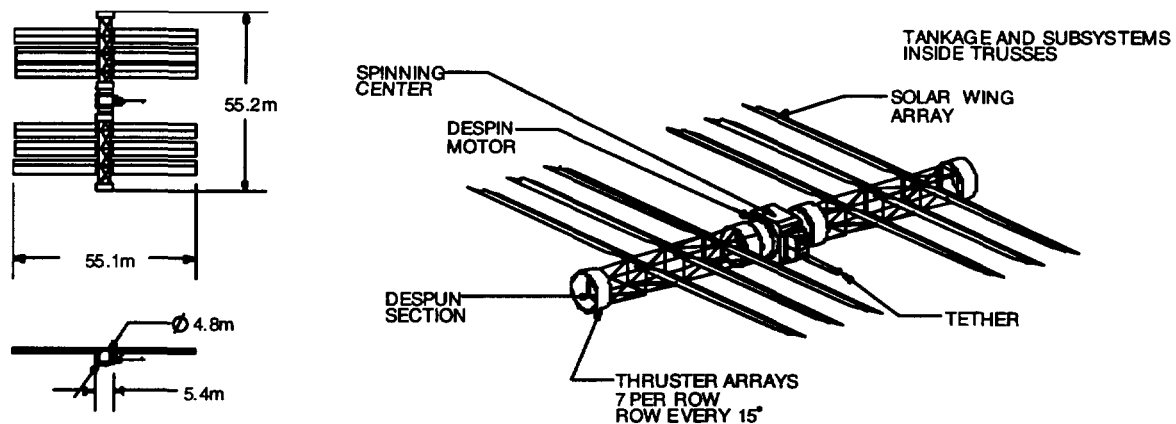

FIGURE 5-5. END PLATFORM
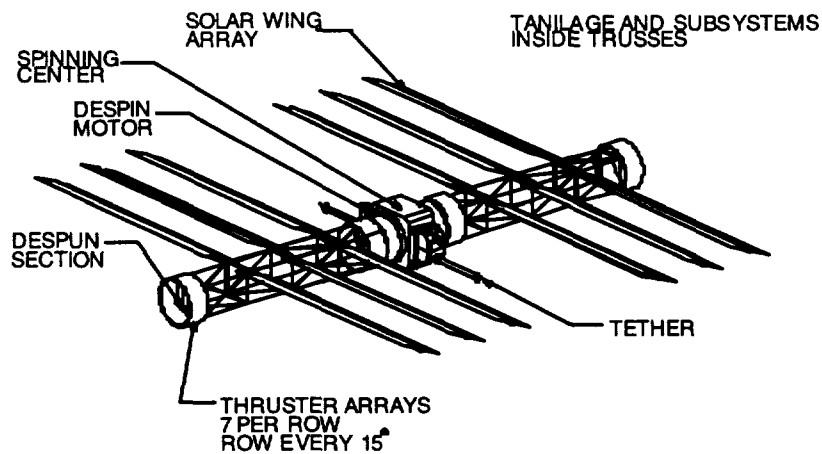
FIGURE 5-6. CM PLATFORM

TABLE 5-1 END PLATFORM VS. CM PLATFORM

	End Platform	CM Platform
Weight	Heavier structure due to rotation loads No extra endweight required	Lighter structure Endweight required
Structures	high platform loads drive heavier possibly more expensive structure	lower platform loads, but structure must be sized for tether-break conditions which would create similar loads to end platform
Reboost	Complex due to moving thrust line	Thrust line stationary relative to CG
Propulsion	higher propellant management system requirements	lower propellant management system requirements
Tether control	Simpler, only one tether to contend with, but more CM shift after payload release	Two tethers to operate but less CM shift after payload release
Docking / servicing	Complex docking – Orbital mechanics plus a rotating target Service operations complicated by constant load	Simpler docking – orbital mechanics only Service operations similar to other space servicing
Cost	Only one set of reels and one PLCRA required (and spares) Possibly more expensive structure Reboost more complex, more demands on software More expensive servicing operations due to load conditions	Two sets of reels, one PLCRA, and one endweight (and spares) Less expensive servicing Less demanding reboost operations, fewer demands on software

If the platform is at the tether end, its mass will serve as the counterweight to the system; if the platform is located at the system CM, a separate counterweight will be required, adding to the total system mass. Docking of servicing vehicles will also be complicated for the end

5-6

platform and might require that the system be despun, at a great cost in energy. If the platform is located at the system CM the platform will have to constantly adjust the tether to remain at the CM during payload capture and release. Docking and thrusting will be much simpler with the platform located at the CM and the loads due to rotation significantly less. For the platform located at the CM, the tether is split between a long segment going out to the PLRCA and a short segment going to the counterweight. Spare tethers are provided for both segments, and a spare PLRCA and counterweight would be stowed as well.

5.5 WEIGHT SUMMARY

TABLE 5-2. MAJOR ELEMENTS WEIGHT SUMMARY

Payload Adapter, wet	541 kg
Fuel Load	54 kg
Payload Adapter, dry	**487 kg**
Structure	242 kg
Tankage/propulsion Sys	29 kg
Electrical Power	121 kg
Command, Comm & tracking	30 kg
ADCS	39 kg
Thermal Control	5 kg
Grapple mechanism	20 kg

Payload Capture and Release Assembly (PLRCA)	631 kg
Payload Capture & release mechanism	200 kg
Structure	156 kg
Electrical Power	230 kg
Command, Comm & tracking	30 kg
ADCS	8 kg
Thermal Control	7 kg

Base (Stage 1) Platform, Wet	21632 kg
Fuel Load	2928 kg
Base (Stage 1) Platform, Dry	**18704 kg**
Tether	**1900 kg**
Reel assembly	**1000 kg**
Ballast	0 kg
Spare PLRCA	631 kg
Spare Tethers	2900 kg
Power Generation	3146 kg
Power Storage	1245 kg
Structure	4668 kg
Tankage/propulsion	506 kg
Electrical power control & distribution	2455 kg
Command, Comm & tracking	222 kg
ADCS	5 kg
Thermal Control	26 kg

Base (Stage 2) Platform, Wet	31314 kg
Fuel Load	4883 kg
Base (Stage 2) Platform, Dry	**26431 kg**
Tether	**1550 kg**
Reel assembly	**816 kg**
Ballast	0 kg
Spare End Masses	631 kg
Spare Tethers	2366 kg
Power Generation	4648 kg
Power Storage	5388 kg
Structure	5808 kg
Tankage/propulsion	799 kg
Electrical Power control & distribution	4104 kg
Command, Comm & tracking	272 kg
ADCS	5 kg
Thermal Control	44 kg

Section 6

INITIAL DEPLOYMENT OF FACILITIES

6.1 GROUND RULES, ASSUMPTIONS, AND DESIGN DRIVERS

In order to minimize deployment cost, the total number of launches required per platform is minimized. Assume the RLV is used to place the tether platform system components into a LEO parking orbit for assembly. Due to the components' packaging bulk and the RLV payload bay size constraints, three launches per platform (consisting of the facility hub and two photovoltaic (PV) array assemblies) are required. Currently, case 6d offers the lowest total system mass (LEO and MEO platforms) but with the MEO platform performing a larger part of the payload boost (ΔV increment). Due to this, the MEO platform is considerably more massive than the LEO facility. With further iteration of the ΔV division between the two platforms (limited by the requirement for synchronous orbits), an optimal design using identical LEO and MEO platform facilities can be determined in the future.
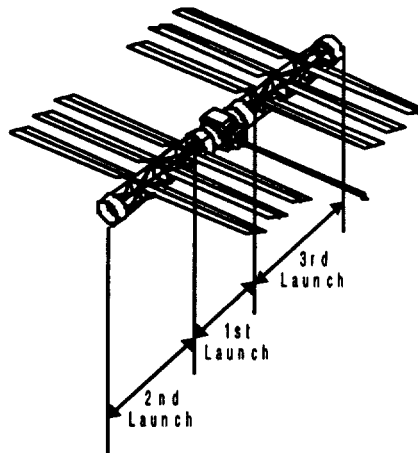

FIGURE 6-1. PAYLOAD COMPONENTS FOR THREE LAUNCHES

The facility hub is launched first, followed by the two PV assemblies. The weight of each payload is less than half the design payload capability of the RLV to a 100 Nmi orbit. Preliminary calculations indicate the RLV can place the reduced-mass payloads into the LEO facility operational orbit for case 6d. Anticipated turn around on the RLV is one week, therefore the first payload in orbit (facility hub) will need to maintain a stable orbit, accessible by the RLV, for more than two weeks (coarse pointing requirements). A body-mounted PV array on one side of the facility hub could provide up to 900 W of power to the ADCS and GNC systems. This takes the time lag associated with payload delivery for on-orbit facility assembly into account. Because the second and third payloads (PV's) will link with the facility hub, they do not require any ADCS or GNC. Once the facility is fully integrated, full-up power and systems check out will be performed, including tether deployment. If any problems arise during on-orbit assembly and check-out, using the RLV provides the opportunity to repair or retrieve the tether platform.

MEO checkout in LEO will be restricted to assembly, power-up, and systems check. Tether deployment will be performed after MEO platform is boosted to its operational orbit. Three main options are available for MEO platform boost and are discussed below.
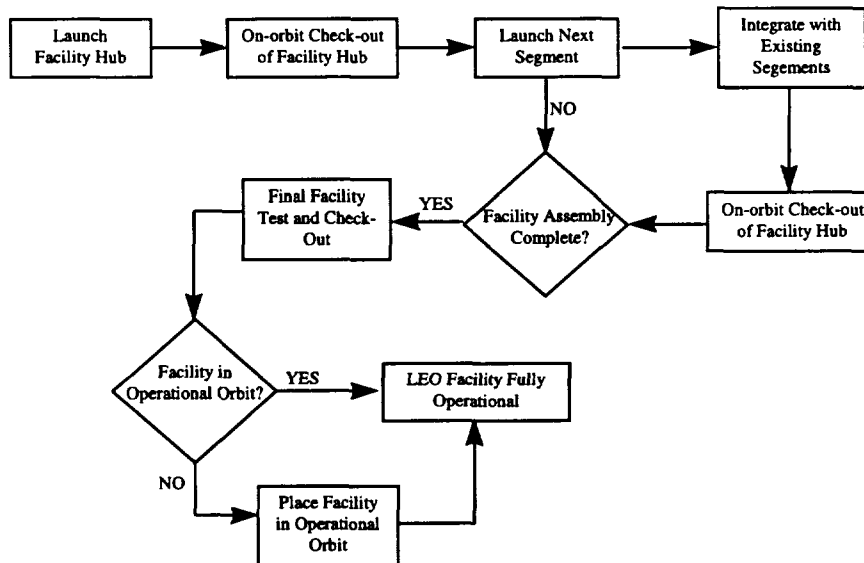
FIGURE 6-2. LEO FACILITY INITIAL DEPLOYMENT

6.2 MEO FACILITY DEPLOYMENT TRADES

- Systems check in LEO, self-boost to MEO, full propellant load
- Systems check in LEO, self-boost to MEO, minimal propellant load
- Systems check in MEO, LEO facility swings second facility to MEO transfer orbit

After assembly and checkout in LEO, the MEO platform with a full propellant load can boost itself to its operational elliptical orbit. Assuming the MEO platform starts in the LEO platform's operational orbit, the required propellant is on the order of 1,940 kg. This represents almost 40% of the total propellant capacity of the platform and would require refueling the MEO platform within one year of establishing on-orbit operations. Though refueling would be necessary within one year, this option is the most conservative of the three and will more than likely insure a fully functional MEO facility in the desired operational orbit.

The second option still involves the MEO platform boosting itself to an operational orbit, but with a reduced propellant load. Instead of boosting the MEO platform with a full propellant load, the minimum propellant required to attain its operational orbit could be used. This option still requires a significant amount of propellant, about 1,740 kg. The 200 kg of propellant "saved" equates to one reboost of the MEO platform (not a significant savings). Add to this the fact that the MEO platform immediately needs refueling after arriving in its operational orbit and this option becomes less attractive.

The third option involves using the LEO facility to impart some ΔV to the MEO platform. The amount of boost the LEO can perform is limited by the mass ratio of the two systems and the requirement to avoid reentry of the LEO platform, but could significantly decrease the propellant required to boost the MEO platform. There are some issues associated with this option. If full-up assembly and checkout of the MEO platform in LEO is still desired, the issue of g-loads on the PV arrays comes into play. This issue depends on how much ΔV can be imparted to the MEO platform without de-orbiting the LEO platform, the spin rate of the hooked facilities, and the tether length. If g-loads are an issue, then another case of keeping the PV arrays undeployed until after entering a MEO transfer orbit could be analyzed. The

6-2

MEO facility's recapture accessibility to the RLV and the LEO facility should be considered in case of a system's check failure. In addition, some sort of payload adapter assembly (PLAA) would be required to allow the MEO facility to be captured and released by the LEO facility. It is unlikely this PLAA would ever be used again; it would become extra weight or orbital debris.
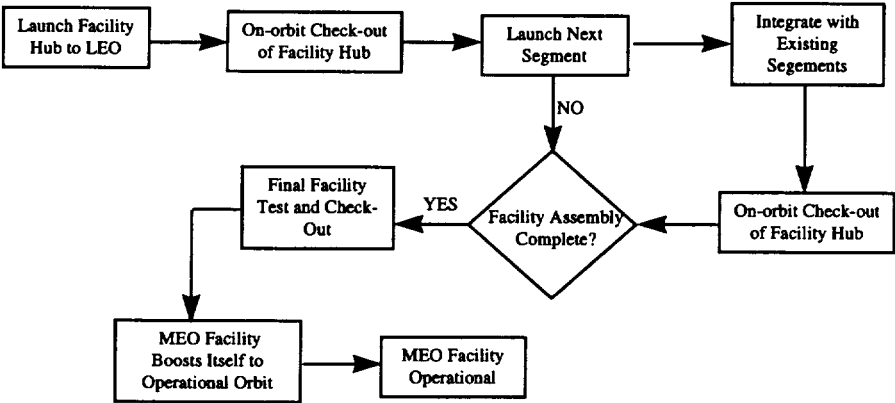

FIGURE 6-3. MEO FACILITY INITIAL DEPLOYMENT

The RLV summary information assumed for this analysis was presented above in section 3.3.3 (see Table 3-1).

Section 7

SYSTEM PERFORMANCE

7.1 INTRODUCTION

This section describes the major design issues and the performance of the system to deliver a payload to the correct orbit. Obviously, the major design issues section is focused on the problems that have not been solved at this time. None of the major design issues appear to be insurmountable and as would be the case for any study similar to this there are obvious problems that need to be solved. We do not offer the final answer here but do offer suggestions on potential mechanisms that these could be solved. Finally, the system performance is compared to other transportation systems. This system offers transfer times comparable to those provided by chemical upper stages with performance comparable to the electrical propulsion systems.

7.2 MAJOR DESIGN ISSUES

As a part of this study a determination was made as to defining the major design drivers and issues for this system to:
- Determine the overall feasibility
- Identify areas where future investment is required to develop enabling or enhancing technologies.

The most significant issue identified for the two-stage system is the Rendezvous and Capture (R&C) activities. The most sensitive phase is between release from the first stage and transition and capture by the second stage. This capture is not perform in the fashion that R&C activities have been performed at present with manned spacecraft such as the Shuttle or the Russian Mir re-supply missions. The tether system R&C has high approach velocities and very short capture periods. The previous sections describe the R&C approach which is very rapid when compared to the automated R&C now being explored by NASA or is being used by the Russians. In those activities the vehicles fly in formation for a long period of time and close the gap in a slow system approach that may take several hours to complete that last 10 meters for the Shuttle activities. The recent Mir accident clearly demonstrated the risk of an accident during even these slower docking activities.

The analysis discussed earlier does demonstrate that zero differential velocities and accelerations are possible with properly designed orbits. Essential aspects for this system to be successful require high precession of the knowledge and control of the payload and the rotating tether system. Position / state data accuracy not verified but expected to be on the order of tenths of meters. In order to enable this approach, knowledge of the orbital positions and orientation will be required for the entire orbit. At present, the only mechanism to obtain this position accuracy and orientation information is from optical sensors located on the ground. With the advent of a space based differential GPS or space and ground automated optical system this accuracy could be obtained. Future GPS constellations are being considered with modifications to improve space based navigation and attitude control. This combined with positioning beacons on the PAV and the PLCRA would provide sufficient information to determine and control the positions to within 10's of cm or better.

A detailed sensitivity analysis is required to determine the precision and accuracy required but has not been performed to date. Future studies should address this to ensure that the capture and release process is practical.

Another issue is the post capture dynamics, loads and tether management. The tether system will experience significant loading following the capture event. The tether was designed to account for the shock loads but these will be mitigated by managing the tether length just after capture very similar to what occurs after capturing a fish with rod and reel. This reeling out and then back in operation is described very well in the report produced by Joseph A. Carroll [14].

These dynamics where not simulated in this study but are acknowledged to be an issue that needs to be addressed in subsequent studies. The motion of the payload and the tether system will damp out rapidly after capture. The combination of reeling in and out can be used to ensure that the damping occurs in a reasonable period. A single orbit is planned prior to the second release event but additional orbits can be used. The single orbit was chosen to minimize the total transfer time. The use of additional orbits to damp the perturbations introduced is not expected but only penalizes the total transfer time.

The study used ideal solutions to the orbital dynamics and ignored the real world perturbations introduced by lunar and non-spherical earth. Drag make-up and solar pressure off-setting was included in the energy calculations. The introduction of these perturbations will drive the propulsion systems and power system requirements up. To account for these a 20% penalty was included in the overall calculation to size the propulsion and power systems. The rotation of the tether system will minimize these impacts but they will accumulate with time. Additional studies will be required to validate the control and resource requirements and should be included in the sensitivity analysis of capture events.

The power system for reboost and tether management is large when compared to the current generation of spacecraft but it is comparable to the ISS power system. The total power requirements are 93 to 151 kW for this study. There are indications that this could be reduced by as much as 50% with new technologies.

The issue of collision avoidance is brought up consistently but has a very low probability of occurrence even with the entire tether fully extended. The cross sectional area exposed to collision varies with rotation about the center of mass and the actual orbit is an orbit that is not being used by most satellites of commercial or national interest. The zero degree inclination is not a prime orbit for communication satellites and the limited ground area coverage limits earth resource missions. The probability of collision has not been determined since the satellites in the tether facilities operational orbits, as well as those with orbits that cross these orbits, are not known at this time. Because of the low thrust levels and the rigidity of the rotating masses, it is not practical to provide for sudden orbit changes (to accommodate collision avoidance maneuvers) by propulsive means. Orbit tracking of other material in the appropriate orbits will be performed to ensure that sufficient time exists to maneuver and avoid potential collisions.

7.3 SYSTEM PERFORMANCE

A two-stage tethered system of reasonable size and relatively small mass can be designed for transferring satellites with a mass up to 9,000 lb from LEO to GEO (with the circularization ΔV provided by the kick motor of the satellite). The transfer times from LEO to GEO for the two-stage systems examined here are between 16:23 hr:min and 16:50 hr:min which is competitive with the 5:30 hr:min from LEO to GEO of a conventional upper stage.

The best estimate of the end-of-life system mass is about 16,500 kg for the two stages without propellant. If we then consider that the system will be reused 24 times over 2 years

and that it will conservatively always launch 9,000 lb satellites, about 8,000 kg of propellant must be added to the end-of-life system mass. Therefore, the total mass for 24 missions at maximum payload capacity is estimated to be 24,500 kg. The tether system therefore would become competitive with respect to a present upper stage (e.g., IUS) on a mass basis after only two launches.

The orbital mechanics of the system is designed with resonant orbits so that there are frequent conjunctions (or visits) between the 1st and 2nd stage and there multiple opportunities for capture of the satellite in case of mis-capture by the 2nd stage (the revisit time ranges between 7:18 hr:min and 8:10 hr:min for the cases analyzed).

The two-stage system is flexible as demonstrated by the ability to boost payloads of varying masses. Payloads as small as 2,000 lb resulted in only minor adjustments in the system that could be easily accommodated for by the baseline system. Adjustments in tether length and/or rotation rates can be made to accommodate a wide range of payload masses. The total propellant required for platform reboost is directly related to the payload mass. Lighter payloads result in less momentum exchanged and therefore less propellant and power required for each. Further, the tether length can be used to adjust the accelerations on the payload to maintain loads within design limits.

7.4 SUMMARY

In summary, the tether system combines the efficiency of electrical propulsion (high specific impulse) and the delivery speed to GEO of a chemical system. The system is flexible and can be adjusted to limit payload accelerations and can adjust for a range of payload masses. The total power/energy requirements are manageable and are comparable to ISS levels. The power and propulsion system is one of the pacing technology areas for this tether system to be successful. The study here addressed using existing technologies, but with advancements now being developed in both the power and electrical propulsion arenas the solutions will be less demanding then assumed here. A single stage tether system from LEO to GEO would be >3 times more massive than a two stage system with present day tether technology. However, an increase of the strength-to-weight ratio of 70% (which is conceivable over the next 15 years from the current trend) would reduce the tether mass by a factor of three and consequently make the single stage tether system much more attractive than at present. As a final comment, the tethered system can not only be used to deliver payloads to GEO but also to return satellites from GEO to LEO. In a future scenario, not analyzed in this report, the return traffic could be used to offset a large portion of the propellant used for reboosting the stages.

7.5 RECOMMENDATIONS

From the results obtained in this study, the tether system from LEO to GEO appears to be highly competitive from a mass standpoint vs. the present chemical upper stages. This tether system is well worth of further detail analyses of its key aspects as follows:

1)   The influence of environmental perturbations over time and the necessary adjustments to the orbital design.

2)   The guidance and control during rendezvous and docking.

3)   The capturing of payloads launched incoming from the Earth's surface by the 1st stage, with consequent propellant savings of the launcher.

4)   The flow of angular momentum and the use of return traffic to restore the momentum.

5)   The use of the spinning tethers for storing electrical energy and reduce the requirement on batteries.

6)   The investigation of alternative orbital scenarios which enable the 2nd stage to provide also the circularization ΔV at apogee.

7)   The detail analysis of the system architecture and the identification of the most favorable configuration.

Section 8

SYSTEM COST

8.1 COST TRADE STUDY OBJECTIVES, REQUIREMENTS, AND ASSUMPTIONS

The purpose of the cost development was to provide a reasonable assessment of the cost of developing this tether system. A top level cost model was developed to assess the system costs, perform trade studies and to provide a mechanism to compare major subsystem costs. As is the case for any cost estimating exercise, a set of ground rules and assumptions was developed. The major assumptions are as follows:

- The government will develop any of the required technologies prior to initiating full scale development of the tether platforms and then actual full scale development will be a commercial effort
- Commercial financing will be used
- An internal rate of return of 25% is required
- To minimize interest expense, the development period is 3 years
- The lifetime for the initial configuration is 10 years but the system will be designed to allow periodic upgrades. No credit was given for subsequent investments and extension beyond a 10-year life.
- The nominal mission rate is 12 flights per year, once per month. Smaller payloads can be accommodated more often but the one/month is the minimal requirement.
- A 30% market share will be targeted by this system.
- Cost of Money (COM) is included in model
- The cost for the IUS and the Centaur were used for comparison, the costs for these programs are based on full and continuous production of these upper stages. This assumes that the production lines are fully active and providing upper stages at the optimal production rate.
- The Reusable Launch Vehicle (RLV) will be used to launch payloads and perform initial assembly operations.
- Costs are addressed for the upper stage activities only. The payload launch to low earth orbit will be the same for both missions. This does not give credit for the upper stage mass that must be launched with each payload. The PAV will be launched with each payload but is considerably smaller and less expensive than the IUS or Centaur.
- Redundant Payload Capture and Release Assemblies (PLCRA) were not included due to the fact that the reliability analysis performed indicated a very high mission success for the exposed tether at the altitudes of interest.

The assumptions and ground rules above were based on experience from involvement with commercial communication satellite constellation development activities. The internal rate of return is somewhat lower than what is used in many commercial efforts but is a realistic rate of return to be considered for a major system integration contract.

8.2 APPROACH TO COST ESTIMATES

The cost model used is the NASA COst Model (NASCOM). Versions of this model have been distributed to industry for use on a variety of programs including manned and unmanned space efforts. NASCOM uses historical costs to develop cost estimating relationships for each of the subsystems and each phase of the program development. The subsystem costs are based on averages from of the unmanned spacecraft database.

All cost estimates were expressed in current year dollars (FY 97). A discount was used for the system integration based on modern commercial development practices. The tether material costs are based on the recent tether missions. The software development costs were based on similarities to other programs with an inflation factor to provide some degree of conservatism.

The operations cost was assumed to be 3% of the development costs based on historical data for unmanned systems. This estimate is still fairly conservative since the ground systems would not be fully staffed except during the actual capture and release events. The yearly cost estimates for this program are comparable to estimates being used for the operations of the major commercial communications constellations that are now being developed.

8.3 RESULTS

The results indicate that the per launch costs compare very favorably with chemical upper stages for the class of payloads that were examined (9000 lbm). Financial payback occurred very quickly. Comparisons for the cost of nuclear and solar upper stages were desired but there was no recent cost data available.

The costs were integrated for the development and amortized across the ten-year life for a total of 120 missions. System development costs are presented in the table below and result in a total system cost of $456 Million.

TABLE 8-1. TOTAL SYSTEM DEVELOPMENT COSTS BASED ON EXISTING TECHNOLOGY

	DDT&E	Flight Unit	Total
Payload Adapter Vehicle	45	21	66
Payload Capture and Release Assembly	57	29	86
Base (Stage 1) Platform	118	98	216
Base (Stage 2) Platform	27	61	88
Initial Launch Cost		150	150
Total	247	359	606

The first column addresses design, development, test and evaluation (DDT&E) for each element. The flight unit costs are those required to produce the actual flight hardware. Although the MEO facility is expected to be very similar to the LEO facility, the MEO facility has a larger power system. In addition, the MEO facility must boost itself to its operational orbit. The use of unique development cost for the MEO facility provides a more conservative cost estimate. The use of a unique development cost for the second stage provides a more conservative cost estimate.

Figure 8-1 presents the time phased cost model for this system and indicates that the yearly operational costs will be approximately $14 million / year. The total cost phased over the ten-year period is compared to the revenue required to obtain the required internal rate of return on the program of 25%. The required revenue is $181M/year. The initial unit cost of the PAV reflects the cost developing the processes and procedures and does include a

learning curve effect for subsequent launches. Efficiencies and long term production can be expected to drive these costs down considerably. Targeted costs of less than $5 million per PAV appear to be obtainable. This would result in a total cost of $20 million per launch, which is less than 50% of the cost of comparable chemical upper stages.

One aspect of cost projections is the sensitivity to the major ground rules and assumptions. Figures 8-2 through 8-5 present the sensitivity of the costs elements to the major assumptions. Figure 8-2 presents the cost per mission versus the total development costs. The horizontal line indicates the cost of a representative chemical upper stage. Figure 8-3 presents the rate of return as compared to the cost of individual flights and indicates that there is room for increasing the rate of return or profit levels. The operations costs are not major success drivers since they occur during the periods that the system is receiving revenues. The final figure presents the impact of increasing or decreasing the number of flights per year. In this case, a minimum of five flights per year is required for the system to be viable. Obviously as the number of flights increase there are more flights to spread the development costs across, allowing increased profit margins or decreasing customer costs.
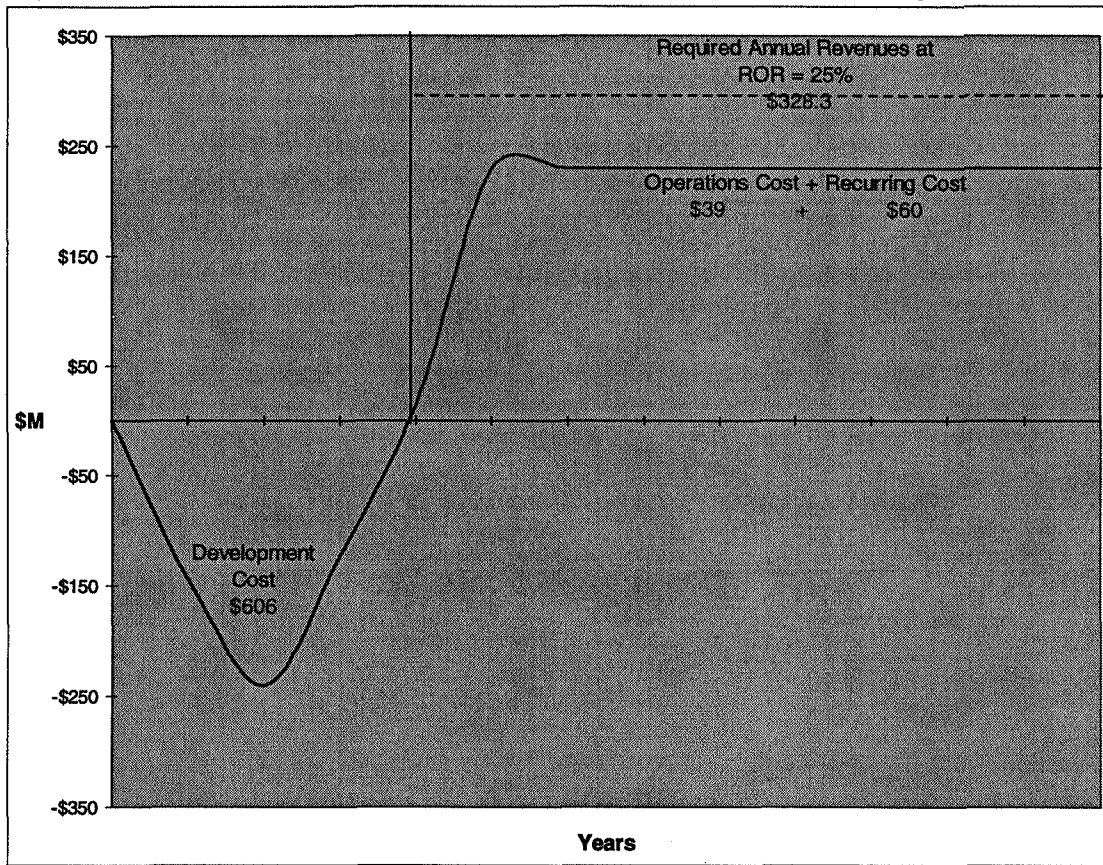

FIGURE 8-1. CASH FLOW MODEL

Total Price/Flight vs DDT&E
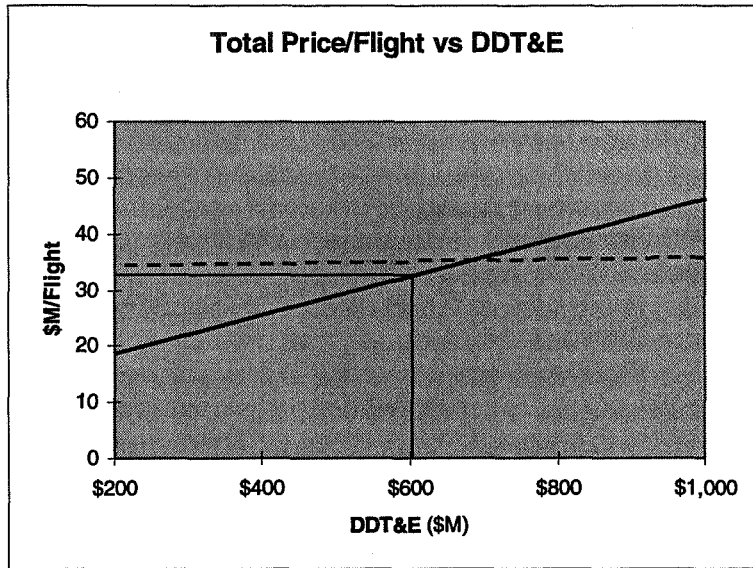
FIGURE 8-2. FLIGHT COST VS. DDT&E
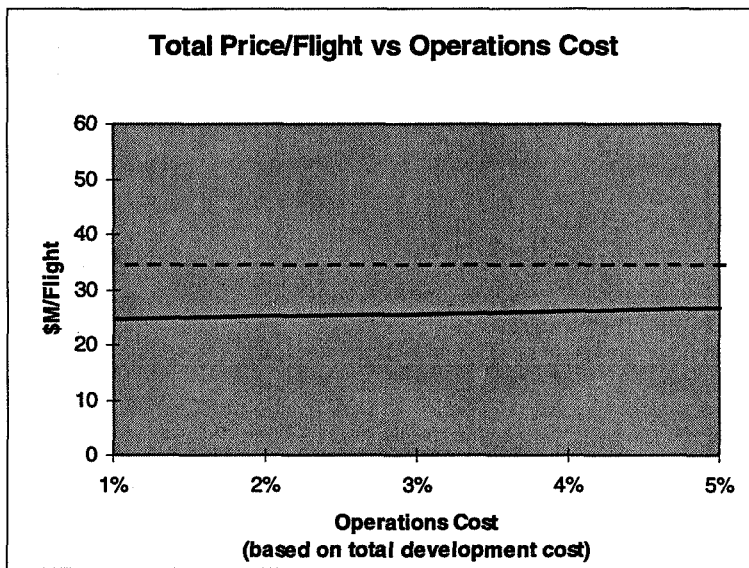

Total Price/Flight vs Operations Cost

FIGURE 8-3. FLIGHT COST SENSITIVITIES VS. OPERATIONS COST

NOTE: Dashed line represents assumed $5M for RLV upper stage unit cost + $30M RLV launch cost of upper stage

Total Price/Flight vs Rate of Return

FIGURE 8-4. FLIGHT COST SENSITIVITIES VS. RATE OF RETURN

Total Price/Flight vs Market Rate

FIGURE 8-5. FLIGHT COST SENSITIVITY VS. NUMBER OF FLIGHTS PER YEAR

NOTE: Dashed line represents assumed $5M for RLV upper stage unit cost + $30M RLV launch cost of upper stage

Section 9

SUMMARY

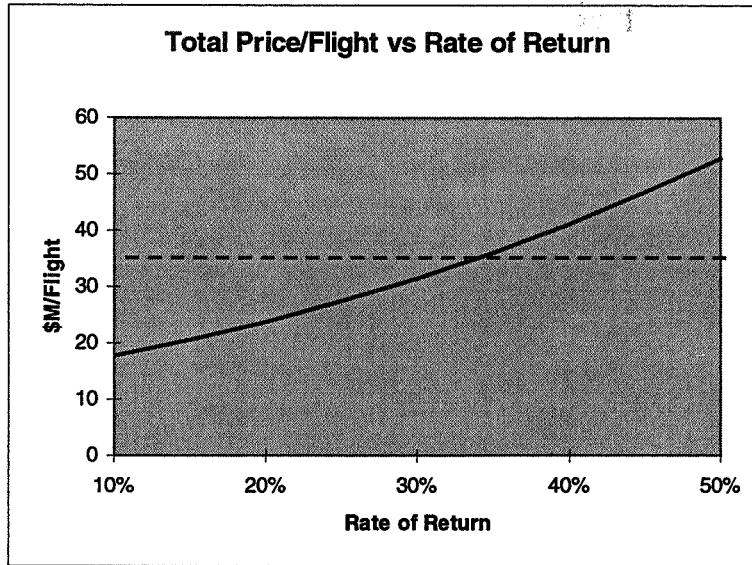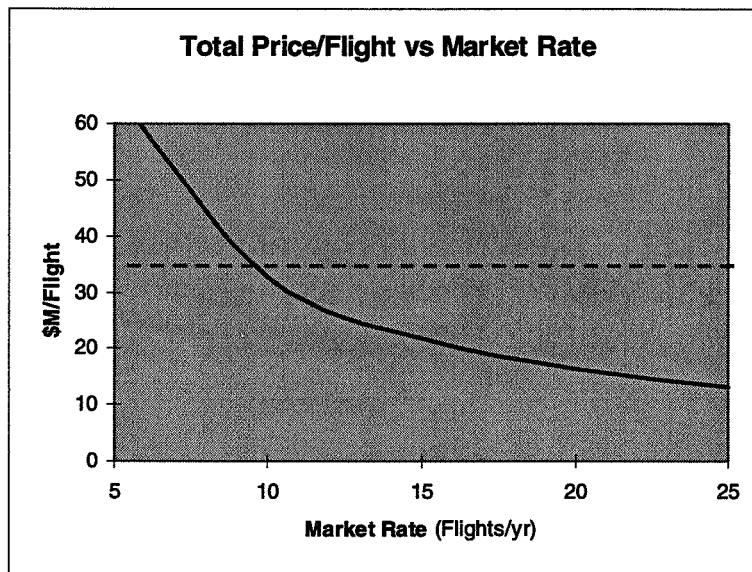### 9.1 CONCLUSIONS

The results of this study indicate that it is feasible and cost effective to obtain the transfer times of chemical upper stages with the efficiencies of electrical propulsion systems by using the momentum transfer between either a single or two stage tether transfer system. A single stage is practical with advances in tether materials and may be achievable within the next ten years. The single stage is preferable over a two-stage system due to the complexity of the capture and release events between the first and second stages of the two-stage system. The costs are very competitive with existing systems even when the tether system is required to incorporate the development costs.

In summary, the tether system appears to be feasible and worth additional investigation. It is clear that the market is going to continue to expand over the next 10 years with a projected increase in traffic to GEO locations. The sizes of the payloads are increasing due to the desire to extend lifetimes and functionality and due to the very large cost of the slots that are now being auctioned. While there are clear disadvantages in the complexity of the Rendezvous & Capture (R&C) events, there are potential workarounds and engineering solutions to manage this complexity.

From the mission analysis results obtained in this study, the tether system from LEO to GEO appears to be highly competitive from a mass standpoint vs. the present chemical upper stages. Additional studies are required, however, to examine the sensitivities of orbit perturbations and to validate the R&C events for a two stage system. A single stage system reduces the complexity of the R&C events considerably and is the preferred solution.

The majority of the required system hardware and software is available with today's technology. The propulsion system design analysis presented in Section 4.6 was performed using thrust levels, specific impulse, and power consumption values that exist in commercial off-the-shelf (COTS) hardware from a number of vendors. Lifetime (or number of cycles) of the ion thrusters is the main area where advances (or just demonstrations) in performance need to occur. Table 9-1 presents the technology readiness levels of the critical technology areas. The technology readiness levels used to assess the technology maturity are similar to those standards being used throughout the industry with a range of 1 to 9. The lower the Technology Readiness level indicates a lower readiness level. Technology Readiness TR levels of 4 and 5 indicate that the technology is being demonstrated in laboratory environments but not in actual flight applications. A TR of six indicates that similar applications have been developed and demonstrated in appropriate environments. TRs of 7 indicate that the technology is in current use on spacecraft with similar applications. Higher TRs are not presented since they indicate a robust production line with numerous applications in similar environments.

From the engineering analysis results, tether facility rendezvous, and capture of the payload is complex, requiring extrapolations from present technologies for the Attitude Determination and Control System. Additional studies are required to examine the sensor accuracy requirements. The next generation of tether material will likely enable a single-stage system, which, though larger, allows much simpler operations.

TABLE 9-1. TECHNOLOGY READINESS LEVELS FOR CRITICAL HARDWARE ELEMENTS EXCLUDING TETHER SYSTEMS

Technology Area	Technology Readiness Level	Comment
Propulsion – Electrical	6	Scale factors for larger systems require additional development as well as demonstrating the life times / number of cycles.
Power - Storage	7	Technologies exist today with considerable development effort underway to improve the systems
Power - Generation	7 / 4	If current technology is used the costs will be as estimated but new technologies such as AMTEC show a great deal of promise to reduce size and provide some portion of the energy storage needs. These systems have only been demonstrated in the laboratory
Space Differential GPS	5	Technology is matured for application on the earth surface in aircraft but applications to space have not been demonstrated
Attitude determination and control - tether system	5	Only limited demonstrations of a tether system have been conducted. Additional data is required to validate the control and attitude determination approach.
Automated Rendezvous and Capture (AR&C)	5	Similar technology are being developed but not for the approach velocities required here. Additional development is required to support the approach velocities

9.2 RECOMMENDATIONS

This report addresses the system level assessments of a single and two-stage tether momentum transfer system. While conclusive evidence of the success of such of a system can not be ascertained, the study did indicate that the approach has significant merit. This tether system is worthy of further detailed analyses including:

- Verifying the influence of environmental perturbations over time and the necessary adjustments to the orbital design
- Developing an approach for the guidance and control during rendezvous and docking
- Assessing the flow of angular momentum and the use of return traffic to restore the momentum
- Determine the feasibility of using the spinning tethers for storing electrical energy, which would reduce the requirement for batteries
- Perform an investigation of alternative orbital scenarios which enable the second stage to provide the circularization ΔV at apogee

- Perform a detailed analysis of the system architecture and the identification of the most favorable configuration
- Determine concepts or issues for ground testing
- Determine concepts or issues for flight testing.

9.3 FLIGHT EXPERIMENT

Obviously, an excellent first step would be to demonstrate some of these concepts with a flight experiment. While several flight concepts were discussed, we elected to divide the need for flight experiments and flight demonstrations into two categories. The first category is the subsystem enhancements that include systems such as the power generation and storage, and electrical propulsion. These systems are common with most of the spacecraft being developed and extensive development work is on going in both commercial and the government arenas. These areas are not being suggested as flight experiments due to the development work already underway and the fact that most of these technologies are considered enhancing and not enabling.

The second category is the tether-related efforts. These areas are receiving limited attention in projects being developed by the Naval Research Laboratory. The Canadian Space Agency is proposing a mission called BOLAS which will support some of the orbital motions and dynamics issues but we see the need for an additional flight which would demonstrate many of the issues identified here. The experiment is called Spinning Tether Orbit Transfer System (STOTS) and would demonstrate the spinning tether technologies for LEO to GEO payload transfers. The experiment could be flown as a Delta secondary payload using an MSFC developed deployer and the Canadian reel system from BOLAS. The mission would be six months long with a launch date in 2000. Figure 9-1 presents the Delta deployment sequence for this mission. The initial cost estimate for this mission is less than $5 million.
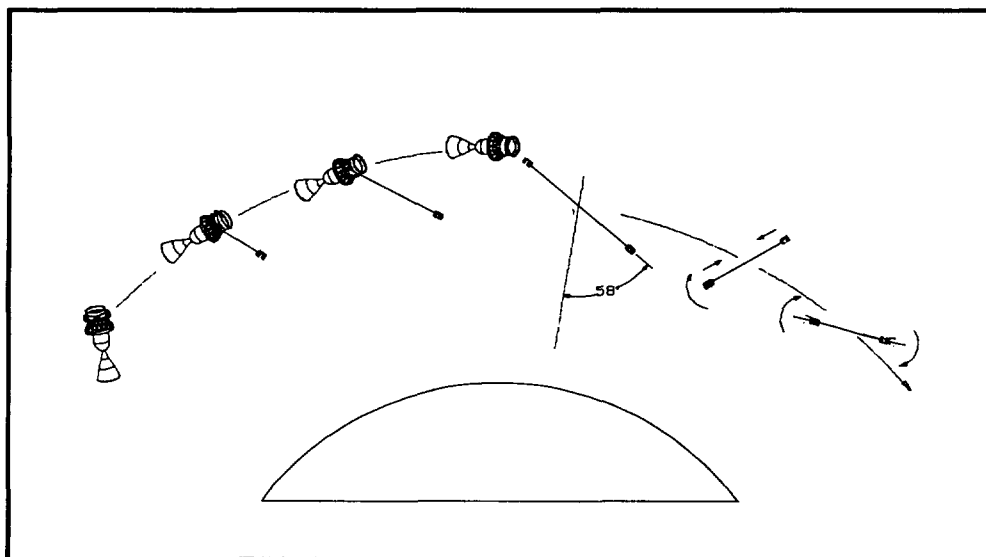

FIGURE 9-1. DELTA DEPLOYMENT SEQUENCE FOR SPINNING TETHER ORBIT TRANSFER SYSTEM (STOTS)

Appendix A

FOOTNOTES

[1]   I. Bekey and P. Penzo, "Tether Propulsion." *Aerospace America,* Vol. 24, No. 7, 40-43, 1986.

[2]   P. N. Fuller, "Commercial Spacecraft Mission Model Update." Report of the COMSTAC Technology & Innovation Working Group, US Department of Transportation, July 1995.

[3]   H. Moravec, "A Non-Synchronous Orbital Skyhook." *The Journal of the Astronautical Sciences,* Vol. 25, No. 4, 307-322, 1977.

[4]   J. Puig-Suari, J. M. Longuski and S.G. Tragesser, "A Tether Sling for Lunar and Interplanetary Exploration." Proceedings of the IAA International Conference on Low-Cost Planetary Missions, Paper IAA-L-0701P, Laurel, MD, April 1994.

[5]   B. I. Yakobson and R. E. Smalley, "Fullerene Nanotubes: $C_{1,000,000}$ and Beyond." American Scientist, Vol. 85, 324-337, July-August 1997.

[6]   R. P. Hoyt and R. L. Forward, "LEO-Lunar Tether Transport System Study." Final Report to Smithsonian Astrophysical Observatory, April 1997.

[7]   D. Vonderwell, Unpublished Report, Boeing, Huntsville, AL, August 1997.

[8]   J. R. Wertz and W. J. Larson, "Space Mission Analysis and Design." p. 614, Kluwer Academic Publishers, 1991.

[9]   L. Johnson, M. Bangham and E. C. Lorenzini, "LEO to GEO Tether Transportation System Study." Interim Review Presentation to NASA/MSFC, May 16th, 1997.

[10]   H. Dionne, Unpublished Report, Boeing, Huntsville, AL, July 1997.

[11]   R. I. Baumgartner, "X-33 Phase II Program Overview." AIAA 96-4314, presented at Space Programs & Technologies Conference, Huntsville, AL, Sept. 24-26, 1997.

[12]   T. Upadhyay, S. Cotterill, A. Deaton, "Autonomous Reconfigurable GPS/INS Navigation and Pointing System for Rendezvous and Docking." AIAA 92-1390, 1992.

FOOTNOTES

[13] W.J. Larson, J. R. Wertz, *Space Mission Analysis and Design*, 2nd Ed., Kluwer Academic Publishers & Microcosm Inc., 1992.

[14] J. A. Carroll, "Preliminary Design of a 1 km/sec Tether Transport Facility." Final Report to NASA Headquarters, prepared under NASW-4461, March 1991.

REPORT DOCUMENTATION PAGE

Public reporting burden for this collection of information is estimated to average 1 hour per response, including the time for reviewing instructions, searching existing data sources, gathering and maintaining the data needed, and completing and reviewing the collection of information. Send comments regarding this burden estimate or any other aspect of this collection of information, including suggestions for reducing this burden, to Washington Headquarters Services, Directorate for Information Operation and Reports, 1215 Jefferson Davis Highway, Suite 1204, Arlington, VA 22202-4302, and to the Office of Management and Budget, Paperwork Reduction Project (0704-0188), Washington, DC 20503

1. AGENCY USE ONLY (Leave Blank)	2. REPORT DATE March 1998	3. REPORT TYPE AND DATES COVERED Technical Publication

4. TITLE AND SUBTITLE Tether Transportation System Study	5. FUNDING NUMBERS NAS8-39400
6. AUTHORS M.E. Bangham*, E. Lorenzini**, and L. Vestal	

7. PERFORMING ORGANIZATION NAMES(S) AND ADDRESS(ES) George C. Marshall Space Flight Center Marshall Space Flight Center, Alabama 35812	8. PERFORMING ORGANIZATION REPORT NUMBER M–853

9. SPONSORING/MONITORING AGENCY NAME(S) AND ADDRESS(ES) National Aeronautics and Space Administration Washington, DC 20546–0001	10. SPONSORING/MONITORING AGENCY REPORT NUMBER NASA/TP—1998–206959

11. SUPPLEMENTARY NOTES
Prepared by the Program Development Directorate
*Boeing, Huntsville, Alabama   **Smithsonian Astrophysical, Cambridge, Massachusetts

12a. DISTRIBUTION/AVAILABILITY STATEMENT Unclassified–Unlimited Subject Category 12 Standard Distribution	12b. DISTRIBUTION CODE

13. ABSTRACT *(Maximum 200 words)*

The projected traffic to geostationary earth orbit (GEO) is expected to increase over the next few decades. At the same time, the cost of delivering payloads from the Earth's surface to low earth orbit (LEO) is projected to decrease, thanks in part to the Reusable Launch Vehicle (RLV). A comparable reduction in the cost of delivering payloads from LEO to GEO is sought. The use of in-space tethers, eliminating the requirement for traditional chemical upper stages and thereby reducing the launch mass, has been identified as such an alternative.

Spinning tethers are excellent kinetic energy storage devices for providing the large delta vee's required for LEO to GEO transfer. A single-stage system for transferring payloads from LEO to GEO was proposed some years ago. The study results presented here contain the first detailed analyses of this proposal, its extension to a two-stage system, and the likely implementation of the operational system.

14. SUBJECT TERMS tethers, orbit transfer, momentum transfer, in-space transportation, upper stages	15. NUMBER OF PAGES 98
	16. PRICE CODE AO5

17. SECURITY CLASSIFICATION OF REPORT Unclassified	18. SECURITY CLASSIFICATION OF THIS PAGE Unclassified	19. SECURITY CLASSIFICATION OF ABSTRACT Unclassified	20. LIMITATION OF ABSTRACT Unlimited